Dual- and triple-targeting of the HER-family members using combinations of mono- and bispecific antibodies

Von der Fakultät Energie-, Verfahrens- und Biotechnik
der Universität Stuttgart zur Erlangung der Würde eines Doktors der
Naturwissenschaften (Dr. rer. nat.) genehmigte Abhandlung

Vorgelegt von

Alexander Rau

aus Almaty

Hauptberichterin: Prof. Dr. Monilola A. Olayioye

Mitberichter: Prof. Dr. Jörn Lausen

Prüfungsvorsitzender: Prof. Dr. Roland E. Kontermann

Tag der mündlichen Prüfung: 21. April 2023

Institut für Zellbiologie und Immunologie der Universität Stuttgart

2023

Table of Contents

Abbreviations

ADCC	antibody-dependent cellular cytotoxicity
Akt	protein kinase B
Amp	ampicillin
APS	ammonium persulfate
AUC	area under the curve
BEAT	Bispecific Engagement by Antibodies based on the T cell receptor
BLAST	basic local alignment search tool
BSA	bovine serum albumin
CD3	cluster of differentiation 3
CDC	complement-dependent cytotoxicity
CH	constant domain of the heavy chain
CNS	central nervous system
Cys	cysteine
d	days
Da	Dalton (g/mol)
ddH_20	double destilled water
DNA	deoxyribonucleic acid
DTT	dithiotreitol
E.coli	*Escherichia coli*
EC_{50}	half maximal effective concentration
ECD	extracellular domain
ECL	enhanced chemiluminescence
EDTA	ethylenediaminetetraacetate
EGF	epidermal growth factor
EGFR	epidermal growth factor receptor
ELISA	enzyme-linked immunosorbent assay
ErbB	erythroblastic leukemia viral oncogene homolog
Erk	extracellular signal-regulated kinase
Fc	fragment crystallizable
FcRn	neonatal Fc receptor
FCS	fetal calf serum
FDA	U.S. Food and Drug administration
FOLFOX	leucovorin calcium (folinic acid), fluorouracil and oxaliplatin

FPLC	fast performance liquid chromatography
GDP	guanosine diphosphat
glc	glucose
GTP	guanosine triphosphat
h	Hour
HB-EGF	heparin-binding EGF-like growth factor
HER	human epidermal growth factor receptor
His	histidine
His_6	hexahistidyl
HPLC	high performance liquid chromatography
HRG	heregulin
HRP	horseradish peroxidase
hu	human
IC_{50}	half maximal inhibitory concentration
IgG	immunoglobulin G
IMAC	immobilized metal ion affinity chromatography
IPTG	isopropyl-β-D-thiogalactopyranoside
LB	lysogeny broth
LL	longer linker
mAb	monoclonal antibody
MAPK	mitogen-activated protein kinase
MEK	MAPK/Erk kinase
MFI	mean fluorescence intensity
min	Minute
MPBS	skim milk on PBS basis
NRG	neuregulin
NTA	nitrilotriacetic acid
OD	optical density
ORR	objective response rate
OS	overall survival
PAGE	polyacrylamide gel electrophoresis
PBA	PBS containing sodium azide
PBS	phosphate buffered saline
PBST	PBS with TWEEN 20

PCR	polymerase chain reaction
PD-1	Programmed cell death protein 1
PE	phycoerythrin
PEI	polyetylenimine
PFS	progression free survival
PI3K	phosphatidylinositol 3-kinase
PIP2	phosphatidylinositol 4,5-bisphosphate
PIP3	phosphatidylinositol 3,4,5-triphosphate
PNS	peripheral nervous system
Raf	Rapidly Accelerated Fibrosarcoma
Ras	rat sarcoma
RIPA	radioimmunoprecipitation assay buffer
rpm	rotation per minute
RT	room temperature
RTK	receptor tyrosine kinase
scDb	single-chain diabody
scFv	single-chain fragment variable
SD	standard deviation
SDS	sodium dodecyl sulfate
SEC	size exclusion chromatography
TAE	tris-acetate-EDTA
taFv	tandem scFv
TGF-α	transforming growth factor alpha
TKI	tyrosine kinase inhibitor
TMB	tetramethylbenzidine
TN1	trypton N1
TRAIL	TNF-related apoptosis-inducing ligand
TY	trypton-yeast medium
UV	ultraviolet
v/v	volume by volume
VH	variable domain of the heavy chain
VL	variable domain of the light chain
w/	with
w/o	without

Abstract

Epidermal growth factor receptor (EGFR)-targeted cancer treatments with antibodies like Cetuximab are successfully used in the clinic for about 20 years. However, intrinsic, as well as newly developed resistance mechanisms to EGFR-targeted therapies, are the main reason for their failure. Activation of human epidermal growth factor receptor 3 (HER3)-signaling upon EGFR-targeted therapies is frequently observed and has motivated the development of combination therapies that simultaneously block EGFR and HER3. In this study, bispecific and bivalent, or tetravalent, respectively, single-chain diabody (scDb) and scDb-Fc molecules were developed comprising the antigen-binding sites of a humanized version of Cetuximab (hu225) as well as a recently developed anti-HER3 antibody (3-43). In total, eight molecules (two scDb and six scDb-Fc) with varying linkers were engineered. The scDb hu225x3-43-Fc showed the most favorable properties regarding production yield, purity, homogeneity and linker setup. Binding of the scDb-Fc to recombinant receptors, as well as to HER-family receptor expressing cell lines revealed retained binding properties, compared to parental antibodies. Furthermore, the scDb hu225x3-43-Fc showed strong and long-lasting inhibition of downstream signaling by EGF, HRG or combination of both ligands. Proliferation studies on head and neck squamous cell carcinoma (HNSCC), triple negative breast cancer (TNBC), and colorectal cancer (CRC) cell lines revealed either similar, or stronger inhibition, compared to parental antibodies as single or combination treatment, which translated into to long-lasting growth suppression in a s.c. xenograft tumor model. Treatment with the bispecific antibody inhibited *in vitro* HRG-stimulated oncosphere formation of two TNBC cell lines. In an orthotopic MDA-MB-468 tumor model, superior antitumor effects were observed compared to those obtained by the parental antibodies alone or in combination. Furthermore, this was associated with a reduced number of cells with stem-like properties demonstrating that the bispecific antibody not only efficiently blocks TNBC proliferation but also the survival and expansion of the cancer stem cell population. The high degree of plasticity and compensatory signaling within the HER-family not only leads to compensatory crosstalk by HER3 but also HER2 giving the rational to combine the EGFR- and HER3-targeting scDb-Fc with a HER2-targeting antibody like Trastuzumab. The triple-targeting approach with the scDb-Fc and Trastuzumab was superior in inhibition of HRG-stimulated proliferation of the CRC cell line LIM1215 compared to the combination of IgG hu225, Trastuzumab and IgG 3-43. This was also observed in primary and secondary CRC oncosphere formation assays. Finally, in CRC patient derived organoids (PDOs) grown in HRG-supplemented medium the triple-targeting of EGFR, HER2 and HER3 provided broader efficacy than dual- or mono-targeting of receptors of the HER-family. In contrast to Afatinib (anti-EGFR, -HER2, -HER4), the triple-targeted antibody approach showed efficient inhibition in all tested

PDOs. Thus, the bispecific scDb-Fc alone or in combination with Trastuzumab represents a superior strategy to deal with primary and acquired resistances compared to targeting a single receptor with different antibodies or any combination of antibodies targeting two receptors of the HER-family.

Zusammenfassung

Epidermal growth factor receptor (EGFR)-gezielte Krebsbehandlungen mit Antikörpern wie Cetuximab werden seit etwa 20 Jahren erfolgreich in der Klinik eingesetzt. Allerdings führen sowohl intrinsische als auch neu entwickelte Resistenzmechanismen gegen EGFR-gerichtete Therapien zu ihrem Versagen. Die Aktivierung des human epidermal growth factor receptor 3 (HER3)-Signals bei EGFR-gerichteten Therapien wird häufig beobachtet und hat zur Entwicklung von Kombinationstherapien geführt, die gleichzeitig EGFR und HER3 blockieren. In dieser Studie wurden bispezifische und bivalente bzw. tetravalente single-chain diabody (scDb)- und scDb-Fc-Moleküle entwickelt, die die Antigen-Bindestellen einer humanisierten Version von Cetuximab (hu225) sowie eines kürzlich entwickelten Anti-HER3-Antikörpers (3-43) integrieren. Insgesamt wurden acht Moleküle (zwei scDb- und sechs scDb-Fc-Moleküle) mit unterschiedlichen Linkern entwickelt. Der scDb hu225x3-43-Fc erwies sich aufgrund von Produktionsausbeute, Reinheit, Homogenität und Linker-Setup als der Favorit. Die Bindung des scDb-Fc an rekombinante Rezeptoren sowie an Zelllinien, die Rezeptoren der HER-Familie exprimieren, zeigte, dass die Bindungseigenschaften im Vergleich zu den parentalen Antikörpern erhalten wurden. Darüber hinaus zeigte der scDb hu225x3-43-Fc eine starke und langanhaltende Hemmung von durch EGF, HRG oder der Kombination dieser Liganden induzierten nachgeschalteten (downstream)-Signalwegen. Proliferationsstudien an Zelllinien des Plattenepithelkarzinom im Kopf- und Halsbereich (head and neck squamous cell carcinoma: HNSCC), des dreifach negativen Mammakarzinoms (triple negative breast cancer: TNBC) und des kolorektalen Karzinoms (colorectal cancer: CRC) zeigten entweder eine ähnliche oder eine stärkere Hemmung im Vergleich zu den parentalen Antikörpern als Einzel- oder Kombinationsbehandlung, was in einem s.c.-Xenograft-Tumormodell zu einer langanhaltenden Unterdrückung des Tumorwachstums führte. Die Behandlung mit dem bispezifischen Antikörper hemmte die HRG-stimulierte Entstehung von Oncospheres zweier TNBC-Zelllinien. In einem orthotopen MDA-MB-468-Tumormodell wurden überlegene Antitumoreffekte im Vergleich zu denen beobachtet, die durch die parentalen Antikörper allein oder in Kombination erzielt wurden. Darüber hinaus war dies mit einer reduzierten Anzahl von Zellen mit Stammzell-ähnlichen Eigenschaften verbunden, was zeigte, dass der bispezifische Antikörper nicht nur die TNBC-Proliferation, sondern auch das Überleben und die Expansion der Krebsstammzellpopulation effizient blockiert. Der hohe Grad an Plastizität und kompensatorischen Signalen innerhalb der HER-Familie führt nicht nur zu einem kompensatorischen Crosstalk durch HER3, sondern auch durch HER2, so dass es sinnvoll ist, den EGFR- und HER3-bindenden scDb-Fc mit einem HER2-bindenden Antikörper wie Trastuzumab zu kombinieren. Der Triple-Targeting Ansatz mit der Kombination aus dem

scDb-Fc und Trastuzumab war bei der Hemmung der HRG-stimulierten Proliferation der CRC-Zelllinie LIM1215 im Vergleich zur Kombination von IgG hu225, Trastuzumab und IgG 3-43 überlegen. Dies wurde auch in primären und sekundären CRC-Oncophere-Assays beobachtet. Bei Organoiden (PDOs) aus CRC-Patienten, die in HRG-supplementärem Medium gezüchtet wurden, führte das Triple-Targeting von EGFR, HER2 und HER3 zu einer breiteren Wirksamkeit als das Dual- oder Mono-Targeting von Rezeptoren der HER-Familie. Darüber hinaus zeigte der Triple-Targeting-Antikörper-Ansatz, anders als der Rezeptortyrosinkinase-Inhibitor Afatinib (anti-EGFR, -HER2, -HER4), eine effiziente Hemmung bei allen getesteten PDOs. Somit stellt der bispezifische scDb-Fc allein oder in Kombination mit Trastuzumab eine vorteilhafte Strategie dar, um primäre und erworbene Resistenzen zu behandeln, als es durch die Blockierung von einzelnen Rezeptoren möglich ist.

1 Introduction

1.1 HER-family receptors

The superfamily of protein kinases consists of more than 500 members. Based on the residues that they phosphorylate they are classified into protein-serine/threonine kinases, protein-tyrosine kinases and tyrosine-kinase like proteins. The ErbB/HER-family belongs to the receptor protein-tyrosine kinases (RTKs), consisting of 58 members which are further divided into 20 subfamilies. RTKs are involved in the regulation of various normal cellular processes like, inter alia, cell proliferation, migration and differentiation (Schlessinger 2000; Roskoski 2019). Dysregulated overexpression and activity of the four HER-family members, EGFR/ErbB1/HER1, ErbB2/HER2, ErbB3/HER3 and ErbB4/HER4, is one of the most recognized pathobiological mechanisms of solid tumors (Yarden and Pines 2012). EGFR, the first described HER-family member, is widely upregulated and/or hyperactivated in epithelial tumors, as a result of gene amplification, transcription activation, protein overexpression, and/or mutations (Hynes and MacDonald 2009). Similar to EGFR, the second member of the HER-family, HER2, is widely overexpressed, amplified or mutated in many different cancer types (Oh and Bang 2020). Approved targeted cancer therapies like monoclonal antibodies or small molecule inhibitors directed against EGFR or HER2 exhibit substantial improvements in survival of patients. However, disease progression due to innate or acquired resistance is frequently observed (Wang 2017). One of those resistance mechanisms is compensatory signaling by other HER-family members. HER3 plays a significant role in cancer progression, increased invasion, acquired therapeutic resistance, and drug resistance in tumors (Black et al. 2019). HER4, is the least studied and understood HER-family member in the context of cancer and was associated on one hand with tumor promoting activity and on the other hand with tumor inhibiting activity (Lucas et al. 2022). The following chapter focuses on the structure of the HER-family members, their activity and signaling, their role in healthy tissue, and in non-malignant and malignant disease. Furthermore, therapeutic options for HER-family member expressing tumors are described with a focus on antibody-based treatments.

1.1.1 Structure of HER-family receptor members

The ErbB/HER-family consist of four gene members *EGFR/ERBB1/HER1*, *HER2/ERBB2/NEU*, *ERBB3/HER3* and *ERBB4/HER4*. These genes are translated into one EGFR isoform, two full-length HER2 isoforms as a result of alternative mRNA splicing, as well as two HER3 isoforms, of which one is lacking the amino acid residues 1-59. HER4 takes on a special role. In the process of alternative splicing, four isoforms can be formed, with two different versions of the juxtamembrane segments (JMa, JMb), and two different carboxyterminal tails (Cyt1, Cyt2)

(Roskoski 2019). However, the basic structure of all 4 HER-family members is similar. The extracellular part of the receptor consists of the leucine-rich domains I and III, which bind the ligand (except HER2), and the cysteine-rich domains II and IV, which consist of extended repeats of disulfide-containing modules. Upon ligand binding to domain I and III, the interaction between domain II and IV is disrupted. Domain II now can interact with a different sleeve in domain II of a second ligand-bound receptor molecule, thereby forming homo- and heterodimers. This change from a tethered (closed) to an extended (untethered or open) conformation is essential for dimerization of the receptors. In total, 11 ligands bind to the HER-family, of which some are receptor specific while others bind to two members. The epidermal growth factor (EGF), amphiregulin (AR), epigen (EPG), and transforming growth factor-α (TGFα), are specific for EGFR, and neuregulin (NRG) 3 and 4 bind specifically to HER4. The ligands betacellulin (BTC), epiregulin (EPR), and heparin-binding EGF-like growth factor (HB-EGF) can bind EGFR, as well as HER4. Heregulin (NRG1/HRG) and neuregulin 2 (NRG2) bind to HER3 and HER4. On the contrary, there is no known ligand binding to HER2, as it exists only in an extended and open confirmation. This structural particularity results in a constitutively ready-to-dimerize state of HER2 (Penuel et al. 2002; Garrett et al. 2003). However, under physiological conditions no HER2 homodimers are formed. In contrast, when expression levels are highly elevated, for example in breast cancer, this constrain is violated and HER2 homodimers are formed (Yarden and Sliwkowski 2001). The intracellular part of the HER-family members is linked to the extracellular domains via a single transmembrane segment. Inside the cell the receptors comprise a short juxtamembrane segment, a kinase domain and a long C-terminal tail. When activated, receptors within homo- or heterodimers transphosphorylate the dimerization partner (except HER3). The phosphorylation of tyrosines occurs at specific sites, which allow for the docking of different downstream effectors (Olayioye et al. 2000). HER3 has an impaired kinase domain, which reduces its transphosphorylation activity by approximately 1000-fold when compared to EGFR (Shi et al. 2010). This property of HER3 makes it dependent on heterodimerization to become phosphorylated. In general, the heterodimers show more potent activation of downstream pathways, compared to homodimers, due to the higher variation of docking sites for adapter proteins (Roskoski 2014).

1.1.2 Activation and signaling of HER-family receptors

The kinase domains of HER-family receptor dimers are active and catalyze auto- and transphosphorylation of tyrosine residues in conserved amino acid motifs of the C-terminal tail. Cytoplasmic and transmembrane adapter proteins can bind to these motifs and further activate downstream signaling. The two major signaling pathways are the mitogen-activated protein kinase (MAPK) and the phosphatidylinositol 3-kinase (PI3K) pathway. EGFR and HER2 mainly

activate the MAPK pathway by binding of Src-homology-2-containing (Shc) and growth-factor-receptor-bound protein 2 (Grb2) (Kennedy et al. 2019; Batzer et al. 1994). Grb2 is recruiting son of sevenless (SOS) resulting in a signaling cascade, in which the small GTPase Ras and sequentially kinases are activated (Raf-MEK-MAPK/Erk.). In turn, the mitogen activated protein kinase MAPK/Erk activates transcription factors which promote proliferation and differentiation. Through coupling of the Ras-PI3K-AKT/PKB pathway all four receptors are able to indirectly activate the PI3K pathway (Hynes and Lane 2005; Citri and Yarden 2006). HER3 comprises six docking sites for p85, the regulatory subunit of PI3K, enabling direct and strong activation of the PI3K pathway (Plowman et al. 1990; Carpenter et al. 1990; Hellyer et al. 1998). HER4 comprises one docking site for p85, however, like EGFR and HER2, it mainly activates the MAPK pathway. Binding of p85 to the phosphorylated tyrosine relieves its inhibitory effects on p110, the kinase subunit of PI3K. The activated PI3K leads to conversion of phosphatidylinositol bisphosphate (PIP_2) to phosphatidylinositol trisphosphate (PIP_3), allowing the activation of Akt and further downstream proteins of the pathway, promoting cell growth, proliferation and survival (Citri, Yarden 2006; Ma et al. 2015; Olayioye et al. 2000). Of note, the HER2:HER3 heterodimer has the broadest adaptor binding profile and possesses potent transforming capacity (Cohen et al. 1996; Tzahar et al. 1996). Despite the impaired kinase activity of HER3, both receptors are phosphorylated in the heterodimer. Zhang et al. used a HER3 targeting RNA aptamer (A30) to disrupt formation of homo-heterodimers of two HER2:HER3-dimers (Zhang et al. 2012). HER2 was still able to phosphorylate HER3 upon A30 binding. However, no HER2 phosphorylation was observed, indicating that heterodimerized HER2 trans-phosphorylates HER2 molecules contained in adjacent heterodimers. Further, Choi and coworkers demonstrated that endogenously-formed HER2:HER3 heterodimers can simultaneously interact with multiple downstream effectors and catalyze tyrosine phosphorylation at an unusually high rate (Choi et al. 2020).

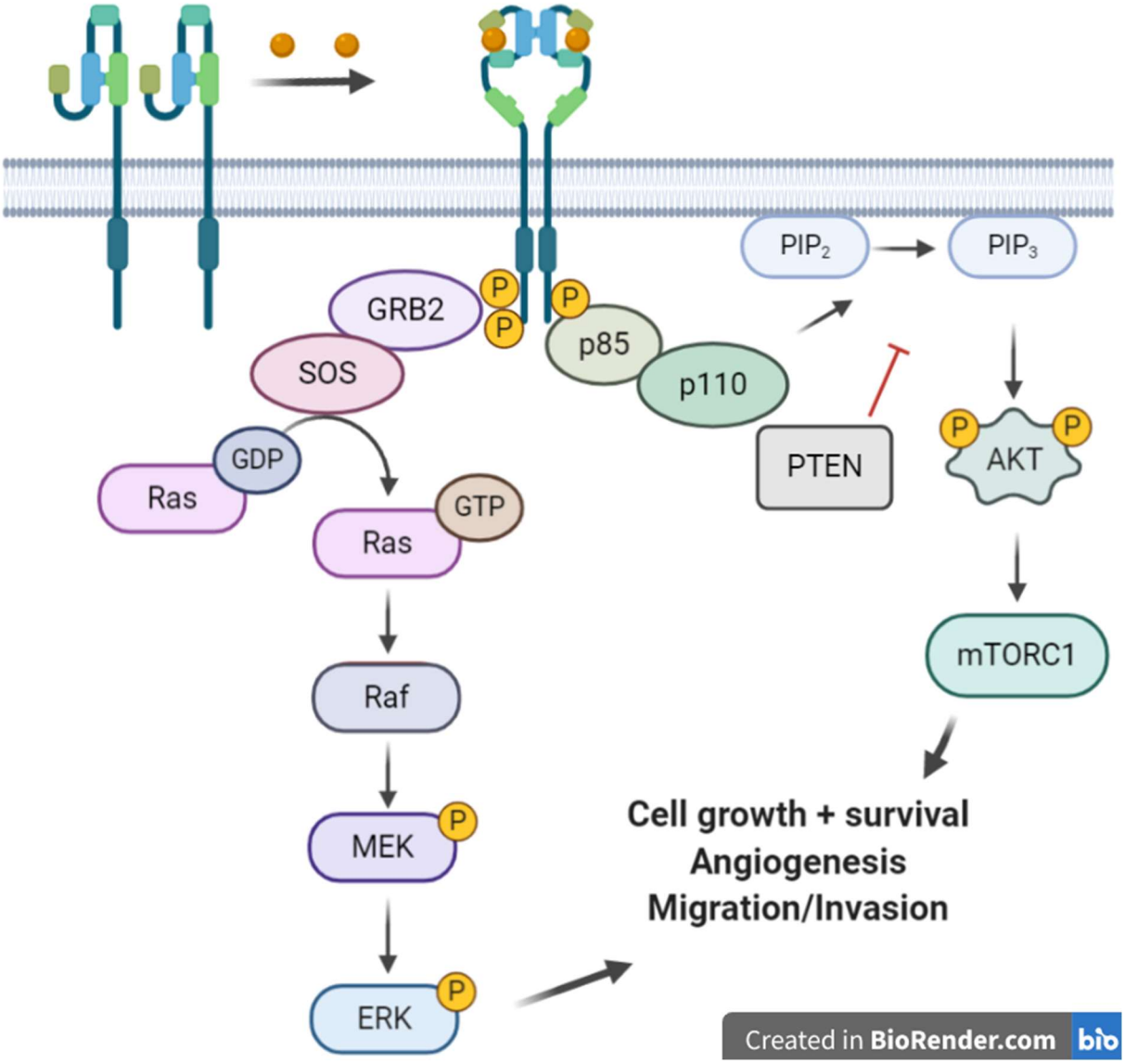

Figure 1: Receptor phosphorylation and downstream signaling of activated HER-family members. The HER-family receptors consist of an extracellular domain, which is subdivided into subdomains I-IV, a single membrane-spanning region, a juxta membrane segment, a cytoplasmic tyrosine kinase-containing domain (PKD) and a C-terminal tail. In the absence of ligand, the receptors are kept in an inactive, tethered form. Ligand binding to subdomain I and III leads to an untethered active state, resulting in the interaction of subdomain II with subdomain II of another receptor, forming homo- or heterodimers. Phosphorylation of the C-terminal tail allows for docking of adapter proteins of the MAPK- and PI3K-pathway, activating a signaling cascade.

1.1.3 Role in healthy tissue and non-malignant diseases

The HER-family receptors and their ligands are involved in many processes during development, as well as in homeostasis of different organs (Britsch 2007; Citri and Yarden 2006). Mice with EGFR knockout show growth retardation, epithelial immaturity and dysfunction, leading to early postnatal lethality (Miettinen et al. 1995). However, knockout of

the EGFR ligands EGF, AR, or TGFα did not lead to lethal phenotype, but abnormalities in the small intestine, and for TGFα knockout, open eyelids at birth, reduced eyeball size and superficial opacity were observed (Luetteke et al. 1993; Troyer et al. 2001). This allows for the conclusion of partial redundancy of the EGFR ligands. HER2 and HER4 knockout in mice lead to severe heart defects and postnatal lethality (Gassmann et al. 1995; Erickson et al. 1997). The knockout of HRG, the ligand of HER3 and HER4, leads to similar heart defects as knockout of HER2 (Erickson et al. 1997). Mice with HER3 knockout suffer from developmental defects of the peripheral and central nerve system, leading to postnatal death (Erickson et al. 1997). In summary, function of the HER-family receptors and their ligands was proposed inter alia, in the peripheral nervous system (PNS), central nervous system (CNS), heart and mammary gland underlining the importance of the HER-family for development and homeostasis (Britsch 2007). The HER-family also plays an important role in non-malignant diseases, mainly cardiovascular associated. HER2-targeted therapies, like Trastuzumab, a monoclonal antibody used for cancer therapy, are well known for their cardiotoxic effects (Babar et al. 2014). Further, elevated serum HER2 levels are associated with coronary artery disease, high triglycerides and insulin resistance (Jian et al. 2020; Fernández-Real et al. 2010). A recent study showed increased EGFR phosphorylation and activity in atherosclerotic lesion development in mice, which could be prevented by EGFR inhibitors (Wang et al. 2017). Taken together, the HER-family is essential for the development and the functional maintenance of several organs.

1.1.4 HER-family receptors in cancer and therapeutic options

In the last release of the GLOBOCAN database Bray and coworkers estimate that worldwide approximately 18 million new cases of cancer will be diagnosed and about 10 million will die from cancer in 2018 (Bray et al. 2018). Thus, cancer is the first or second leading cause for deaths in most countries, next to ischemic heart diseases and stroke. Cancer incidence reflects national socioeconomic development whereby countries with higher human development index (HDI) have a higher incidence. Not only that, but also the type of the cancer reflects this socioeconomic state, with higher incidence for infection-associated cancers, including cervix, stomach and liver in countries with low HDI. The four most common cancer types include lung, breast, prostate and colon, together accounting for approximately one third of all cases, as well as all cancer associated deaths. With global transition to higher prosperity, leading to an increase of population and aging of humans, the prominence of cancer will rise (Arnold et al. 2017; Bray et al. 2018).

1.1.4.1 EGFR in cancer

Dysregulation of the HER-family signaling cascade plays an important role in in many different types of cancer (Hynes and MacDonald 2009). Mutation in the kinase domain, gene amplification, increased biosynthesis, or decreased degradation as well as activation by ligands are the main reasons for overactivity of EGFR (Wang 2017; Roskoski 2014). EGFR overactivity is often observed in patients with inter alia, HNSCC, CRC and TNBC (Rocha-Lima et al. 2007; Wang 2017). Overexpression of EGFR is observed in more than 90 % of HNSCC tumors, in up to 75 % of CRC, and in 20-50 % of all TNBC cases (Xu et al. 2017; Cohen 2003; Nakai et al. 2016; Ueno and Zhang 2011; Sabatier et al. 2019). These observations habe led to the development of EGFR targeted therapies. In 1995 the efficacy of the EGFR targeted monoclonal antibody Cetuximab was described in a preclinical study initiating first clinical trials (Goldstein et al. 1995). Cetuximab was approved by the FDA in 2004 for the treatment of advanced colorectal cancer and later additionally for head and neck and non-small cell lung cancer (Troiani et al. 2016).

Globally approximately 550,000 patients are diagnosed with HNSCC and 380,000 die of this disease every year (McDermott and Bowles 2019). HNSCC is associated with smoking, alcohol abuse as well as human papillomavirus (HPV) infections. Patients treated with Cetuximab in combination with either radiation therapy, or as single agent for refractory, recurrent, or metastatic disease showed strong benefit in overall survival (OS) (Bonner et al. 2006; Vermorken et al. 2007). However, Cetuximab treatment response rates are very low (~10 %) and prediction of responders remains difficult, despite a large number of clinical studies addressing this topic (Hammerman et al. 2015). In a recent study of oropharyngeal cancer (OPC) patients, protein levels of EGFR and its phosphorylated form were quantified using immunohistochemistry (IHC). It was demonstrated that HPV-related samples had significantly lower levels of EGFR, compared to HPV-negative samples. However, levels of phosphorylated EGFR were higher in HPV-positive samples (Taberna et al. 2018). Furthermore HPV-positivity was also associated with high HER3-expression (see also 1.1.4.3 and 1.2.2) (Brand et al. 2017). Reasons for the unsatisfactory EGFR-targeted treatment success is explained by inter alia, frequently occurring mutations of downstream effector genes as *HRAS* and *PI3KCA*, as well as expression of HER3 or its ligand HRG (Chang et al. 2015; Mota et al. 2017). Until now, no other EGFR-targeted therapies have been approved for the treatment of HNSCC. With the approval of Nivolumab and Pembrolizumab, a PD-L1, and a PD-1 targeting antibody, respectively, the recommendation for EGFR-targeted treatments shifted towards second choice after immunotherapy (Cohen et al. 2019).

With 1.8 million new diagnosis in 2018 and 881,000 deaths in the same year CRC accounts for 1 in 10 cancer cases and deaths (Bray et al. 2018). The treatment with Cetuximab for CRC patients is approved for metastatic disease and for patients *KRAS* wildtype disease. K-Ras is a small GTPase which initiates the sequential activation of kinases of the MAPK-pathway (see 1.1.2) and mutations lead to resistance against Cetuximab, as well as to other EGFR-targeted therapeutics, like the human monoclonal antibody Panitumumab (van Cutsem et al. 2009; Lièvre et al. 2006). However, the EGFR-targeted treatment with Cetuximab was described as being ineffective in 40-70 % of patients with *KRAS*-wt disease (Pauw et al. 2019; Leto and Trusolino 2014). Amongst others, the amplification or transcriptional upregulation of HER2, as well as the expression of HRG or its receptor HER3, are primary or acquired resistances which can occur upon Cetuximab treatment (Oliveras-Ferraros et al. 2012; Leto and Trusolino 2014; Leto et al. 2015; Stahler et al. 2017; Kruser and Wheeler 2010; Zhang et al. 2020).

Triple-negative breast cancer (TNBC) is associated with a high mortality rate and characterized by the lack of progesterone receptor (PR), estrogen receptor (ER) and HER2 overexpression (Thakur et al. 2018; Bray et al. 2018; Goldhirsch et al. 2013). TNBC accounts for 15 – 20 % of all breast carcinomas and, compared to ER/PR and HER2 positive breast carcinomas, is associated with increased metastasis risk, early recurrence and worse outcome (Gonçalves et al. 2018; Fremd et al. 2018; Morante et al. 2018; Dent et al. 2007; Liedtke et al. 2008). Despite EGFR abundance in TNBC and numerous clinical trials investigating efficacy of EGFR-targeting antibodies or TKIs, no treatment has been approved until now. Cetuximab treatment reached only a ~10 % overall response rate, and for Lapatinib, an EGFR and HER2 targeting TKI, a negative trend for PFS was observed (Baselga et al. 2013; Carey et al. 2012; Finn et al. 2009). One reason for this lack of efficacy in TNBC is the lack of predictive biomarkers. Mutations in the EGFR gene or its amplification are rarely observed and do not correlate with the expression (Nakajima et al. 2014; Levva et al. 2017). However, recently Cetuximab efficacy was correlated to gene amplification, raising hope for prediction of therapeutic efficacy (Sabatier et al. 2019; Park et al. 2014).

1.1.4.2 HER2 in cancer

In 1984, Schechter and coworkers connected HER2 to its rat ortholog, Neu, which was isolated from carcinogen induced neuroblastomas, and implicated its role in the malignant transformation and the establishment of cancer. They suggested the use of immunological reagents against HER2 to inhibit its growth activating properties (Schechter et al. 1984). Already in 1986, it was described that HER2-transformed NIH-3T3 cells showed reduced tumor growth *in vivo*, when treated with a HER2-targeting antibody (Drebin et al. 1986). Today we know, that HER2 overexpression, amplification or mutation are associated with many different

cancer types, including breast cancer and gastric cancer, as well as biliary tract, colorectal, non-small-cell lung and bladder cancers (Oh and Bang 2020). Breast cancer is the leading cause of cancer death in women, where the expression of HER2 is found in approximately 25 % of all patients (Slamon et al. 1987; Costa and Czerniecki 2020).

The development of Trastuzumab, a humanized HER2-targeting antibody, changed the outcome of HER2 positive breast cancer patients dramatically (Carter et al. 1992; Smith 2001). Trastuzumab binds to the extracellular domain IV of HER2, thereby inhibiting the homodimerization and heterodimerization with other RTKs and further downstream signaling (Shepard et al. 1991; Baselga et al. 1998; Olayioye et al. 2000). Furthermore it allows for interaction with the immune system via binding of the Fc part to immunoglobulin G fragment gamma receptors (FcγR) of natural killer (NK) lymphocytes, thereby activating antibody-dependent cellular cytotoxicity (ADCC) which results in strong antitumor activity (Sliwkowski et al. 1999). Additionally, Trastuzumab was used for the development of antibody drug-conjugates (ADC). Trastuzumab emtansine (T-DM1) is an ADC consisting of Trastuzumab with linked emtansine, a potent microtubule inhibitor (Lewis Phillips et al. 2008). In the KATHERINE trial (NCT01772472), T-DM1 recently showed a 50 % lower risk of recurrence of invasive breast cancer or death, while only minor differences in quality of life were observed, compared to Trastuzumab (Minckwitz et al. 2019; Conte et al. 2020). To improve the treatment efficacy by enhancing ADCC, Margetuximab, a chimeric HER2-targeting antibody sharing the same epitope as Trastuzumab was developed. In contrast to Trastuzumab, Margetuximab has a modified Fc domain allowing for higher affinity to FcγRIIIa leading to a more efficient recruitment of NK cells (Bang et al. 2017). However, in a phase 3 clinical trial for metastatic breast cancer (SOPHIA trial, NCT02492711) the achieved improvement was rather modest in PFS compared to Trastuzumab treatment (median of 6 months vs 5 months; hazard ratio [HR], 0.76; 95 % CI, 0.59–0.98; P = 0.033). Clinical outcomes were improved in FcγRIIIa 158F allele carriers (median PFS, 7 months vs. 5 months; HR, 0.68; 95 % CI, 0.52–0.90; P = 0.005) (Rugo et al. 2019). HER2-targeted therapies played and play a major role in breast cancer, and these promising therapies become more and more used in other cancer types.

Treatments targeting HER2 are also under investigation in CRC patients. In about 20 % of primary rectal cancer HER2 expression was observed, subdivided in ~5 % having overexpression, ~6 % amplification of HER2 and in ~10 % of patients with liver metastasis overexpression was observed (Conradi et al. 2013; Styczen et al. 2015; Seo et al. 2014; El-Deiry et al. 2015; Fernández-Real et al. 2010). Several studies indicate that HER2-targeted therapy with antibodies, or antibodies in combination with HER2-targeting TKIs, are very effective in CRC patients harboring HER2 gene amplification, HER2 mutations, as well as

overexpression of HER2 (Oh and Bang 2020). High objective response rates (ORRs: 33 – 52 %) were observed in metastatic CRC patients with *KRAS*-wt and *HER2*-amplified tumors treated with Trastuzumab and Pertuzumab in the TRIUMPH study (UMIN000027887), or with Trastuzumab in combination with tucatinib in the MOUNTAINEER trial (NCT03043313) (Nakamura et al. 2019; Strickler et al. 2019). These high ORRs were also demonstrated in the HERACLES trial (Trastuzumab + Lapatinib; ORR: 30 %) and the MyPathway basket trial (Trastuzumab + Pertuzumab; ORR: 38 %) (Sartore-Bianchi et al. 2016; Meric-Bernstam et al. 2019). Considering the low ORRs of approved third line therapies for CRC such as the multikinase inhibitor Regorafenib (1–4 %) and trifluridine plus tipiracil (2 %), these results indicate the strong benefit of combinatorial treatments with Trastuzumab (Oh and Bang 2020).

Furthermore, HER2 also plays a major role in resistance formation against Cetuximab treatment (Bertotti et al. 2011; Yonesaka et al. 2011). Yonesaka and coworkers demonstrated the contribution of HER2 to *de novo* and acquired drug resistance in CRC *in vitro*. In this study HER2-activation by either HER2 amplification or through heregulin upregulation, prevented the inhibitory effects of Cetuximab on downstream signaling via the MAPK pathway. Furthermore, in a cohort of 233 Cetuximab-pre-treated CRC patients a dramatically shorter PFS and OS in patients with *HER2* amplification was observed (PFS: 149 vs. 89 days; OS: 515 vs. 307 days) (Yonesaka et al. 2011). Additionally, Bertotti and coworkers identified HER2 as a predictor of resistance to EGFR-targeted therapies in murine CRC PDX models and demonstrated that dual blockade of EGFR and HER2, either with Lapatinib alone or in combination with Cetuximab or Pertuzumab, could overcome this resistance (Bertotti et al. 2011).

1.1.4.3 HER3 in cancer

Although HER3 was already described in 1989, EGFR and HER2 were the main focus in cancer research for a long time (Kraus et al. 1989). Due to its impaired kinase domain, which allows only for limited autophosphorylation activity, but no transphosphorylation of heterodimerized RTKs, the role of HER3 in dimers remained unclear for a long time (Shi et al. 2010). However, HER2 and HER3 were described to form the strongest dimer, considering transformative activity as well as potential of downstream activation (see 1.1.2) (Cohen et al. 1996; Tzahar et al. 1996). HER3 was not found to be a driving oncogene, but an obligate partner in HER family oncogenesis (Amin et al. 2010). Jaiswal and coworkers described several HER3 mutations which transformed colonic and breast epithelial cells in a HRG-dependent manner, however, this was dependent on HER2 expression (Jaiswal et al. 2013). Additionally, the transformation of NIH-3T3 cells was dependent on overexpression of HER3 and EGFR, or HER3 and HER2, whereas HER3 overexpression alone was not transformative (Zhang et al. 1996). Still, HER3 overexpression is associated with poor disease free survival (DFS) in both TNBC and $HER2^{+}$

breast cancer subtypes as well as with poor OS in TNBC (Bae et al. 2013). High HER3 expression was reported in 70-80 % of primary CRC and corresponding metastases in liver and lymph nodes (Conradi et al. 2019; Lédel et al. 2015; Lédel et al. 2014).

Therapeutic approaches targeting HER3 mainly focus on using monoclonal antibodies, but also TKIs, receptor-Fc fusion molecules, alternative scaffolds, bivalent ligands or in combination with immunotherapy are tested in preclinical studies (Black et al. 2019; Malm et al. 2016). Patritumab (U3-1278) is an IgG1 antibody, showing rapid internalization and degradation of HER3 *in vitro* as well as inhibition of HER3 phosphorylation and further downstream signaling (LoRusso et al. 2013). A phase 3 trial of Patritumab in combination with Erlotinib in NSCLC was stopped because no additional benefit and more adverse events (AD) were observed, even in the HRG-high subgroup (Paz-Arez et al. 2017). In October 2016, Daiichi-Sankyo announced, that Patritumab will be part of the I-SPY2 TRIAL, which aims to rapidly screen and identify new treatments for locally-advanced breast cancer (Stage II/III), however the treatment was stopped due to a safety issue with grade 3 hearing loss (Helsten et al. 02152020). Based on Patritumab, the ADC U3-1402 (Patritumab deruxtecan, or HER3-DXd) was developed, composed of Patritumab linked to a novel topoisomerase-I inhibitor (DX-8951 derivative (DXd)) by an enzymatically cleavable peptide-linker (Gly-Gly-Phe-Gly). U3-1402 showed promising results in preclinical studies of HER3 expressing CRC models, independent of *KRAS* mutations, as well as other cancer models, leading to two clinical trials (NCT02980341; NCT03260491) (Koganemaru et al. 2019; Hashimoto et al. 2019; Haratani et al. 2019). At the ASCO Annual Meeting in June 2021 Jänne et al. updated on the NCT03260491 trial that U3-1402 demonstrated antitumor activity in heavily pretreated metastatic/locally advanced EGFR-mutated NSCLC patients (Janne et al. 2021). Based on this promising trial a phase 2 study was initiated for patients with EGFR-mutated NSCLC after failure of EGFR TKI and platinum-based chemotherapy (NCT04619004).

Up to today, none of the monospecific HER3-targeting antibodies that are or were in clinical tests has translated the promising preclinical results to the clinical trials. However, there are still more than two dozen antibodies currently investigated in preclinical studies (Jacob et al. 2018; Malm et al. 2016; Gandullo-Sánchez et al. 2022). One of these preclinical antibodies is IgG 3-43, a fully human IgG1 antibody, targeting an epitope located on subdomain III and IV of the extracellular domains of HER3. IgG 3-43 induces internalization and degradation of the receptor leading to inhibition of downstream signaling. Further, it showed promising results in signaling inhibition of the MAPK pathway and the PI3K pathway *in vitro*, and inhibited tumor growth and prolonged survival in a FaDu xenograft tumor model in SCID mice (Schmitt et al. 2017). Another promising HER3-targeting antibody is KTN3379, which binds to domain III and

locks it in the inactive configuration, thereby blocking ligand dependent and independent signaling (Lee et al. 2015). In a window-of-opportunity study KTN3379 demonstrated activity on phosphorylation of HER3 and a tumor shrinkage in 42 % of the patients was observed (Duvvuri et al. 2019). Of note, all patients with tumor shrinkage expressed both HRG and HER3. These results led to initiation of a phase 2 trial of KTN3379 in combination with Cetuximab in HNSCC (NCT03254927). Better prognostic and predictive biomarkers for HER3-targeting approaches will allow for a more precise selection of patients benefiting from these therapies. Furthermore, multi-target therapy set ups and combinations with classical chemo therapies or radio-therapy show more promising clinical results and raise hope for efficacious HER3-targeting antibody therapies (Gandullo-Sánchez et al. 2022).

1.1.4.4 HER4 in cancer

The fourth member of the HER-family HER4, was discovered in 1993, and was described to activate morphologic differentiation of a breast cancer cell line (Plowman et al. 1993). There are different splicing variants of HER4, which allow for two different juxtamembrane variants (JM-a and JM-b), as well as two cytosolic variants (CYT-1 and CYT-2) (Elenius et al. 1997; Veikkolainen et al. 2011; Määttä et al. 2006). JM-a comprises a cleavage site for tumor necrosis factor-α converting enzyme (TACE), whereas JM-b is lacking this cleavage site. CYT-1, in contrast to CYT-2, comprises an additional site for PI3K recruitment that increases the downstream signaling capacity (Määttä et al. 2006; Erben et al. 2018). Cleavage of JM-a by TACE triggers a second cleavage of HER4 by γ-secretase activity. The resulting fragment HER4 Intracellular Domain (4ICD) accumulates within the nucleus or mitochondria (Hollmén et al. 2009; Rio et al. 2000; Lee et al. 2002; Jones 2008). On one hand, intracellular 4ICD can operate as a transcriptional cofactor promoting the expression of ER target genes such as progesterone receptor (PR), on the other hand, it can induce apoptosis of tumor cells through the activity of the Bcl2 homology 3 (BH3)-like proapoptotic domain (Fujiwara et al. 2014).

The role of HER4 in development of cancer is not clear and seems to be dependent on the expressed isoform (Fujiwara et al. 2014). Some studies correlate HER4 expression with low proliferation or even antiproliferative effects, prolonged event free survival, as well as overall survival (Tovey et al. 2004; Sartor et al. 2001; Machleidt et al. 2013). Other studies associate HER4 expression with poor prognosis in TNBC, breast cancer, CRC, ovarian cancer and meningiomas (Kim et al. 2016; Mota et al. 2017; Arnli et al. 2019; Fuchs et al. 2007; Hollmén et al. 2012). This unclear role of HER4 led to the development of two oppositely working antibodies: mAb 1479 inhibits HER4 phosphorylation as well as ectodomain shedding and stimulates HER4 downregulation and ubiquitination (Hollmén et al. 2009). Further, mAb 1479 has been shown to suppress tumor growth in a breast cancer cell xenograft model (Hollmén

et al. 2012). On the contrary, Lanotte and coworkers developed an agonistic antibody (C6) that mimics the mechanism of HRG-dependent activation of HER4-JMa/CYT1, thereby activating anti-proliferative signaling (Lanotte et al. 2019). C6 enhanced the cleavage of HER4, activated PARP cleavage and lead to an accumulation of 4ICD in the mitochondria. Additionally, C6 showed tumor growth inhibition in two xenograft models of TNBC and ovarian cancer. These two opposing approaches demonstrate that there is still a need for clear evidence on which isoform of HER4 is crucial for tumor promoting or tumor inhibiting activity. Furthermore, the ratio of expressed isoforms and expression of other RTKs must be considered to get a clearer picture of HER4 and its role in cancer.

1.2 Bispecific antibodies

In 1958 Rodney Porter described the basic structure of antibodies isolated from rabbit. He used papain to digest the antibodies and observed three fractions, of which two were able to block antigen precipitation by the parental antibody while one fragment could not (Porter 1958; Riethmüller 2012). Today, we know that the three fractions correspond to two antigen-binding fragments (Fab) and the crystallizable fragment (Fc), mediating effector functions, such as antibody-dependent cell-mediated cytotoxicity (ADCC), antibody-dependent cellular phagocytosis (ADCP), complement fixation and recycling mediated by the neonatal Fc receptor (FcRn) (Brinkmann and Kontermann 2017). In 1960, Alfred Nisonoff speculated about preparation of antibodies with mixed specificity and just four years later demonstrated a hybrid, bivalent antibody with specificity for ovalbumin (EA) and bovine gamma globulin (BGG) (Nisonoff et al. 1960; Fudenberg et al. 1964). This hybrid antibody was produced by reoxidation of pepsin-digested antibodies targeting EA, or BGG, respectively. The bispecific properties were demonstrated using agglutination experiments with human and chicken erythrocytes (Nisonoff et al. 1960; Fudenberg et al. 1964). In 1975, Köhler and Milstein published their work on the hybridoma technology, which allowed for manufacturing of predefined specific antibodies (Köhler and Milstein 1975). The extension of this technology by fusion of two hybridoma cells, called hybrid-hybridoma, allowed to produce bispecific antibodies, called quadromas, without the need of chemical coupling (Milstein and Cuello 1983). However, none of these bispecific antibodies was developed to be used as therapeutic. This changed in 1985, when Staerz, Kanagawa and Bevan demonstrated T-cell retargeting using a hybrid antibody targeting T-cell receptor and the Thy-1 alloantigen. They demonstrated strong cytotoxic effects and described their future use as therapeutic for tumor or virus-infected patients in which their own T-cell response failed (Staerz et al. 1985). From this time point on, numerous bispecific formats were described forming the diverse “zoo” of bispecific antibodies (Brinkmann and Kontermann 2017). Within the past 35 years, more than 110 antibodies were approved by the FDA or EMA, respectively, of which 8 are bispecific antibodies, which are used in the treatment of Oncology, Hematological Disorders, and Ophthalmology (Kaplon et al. 2022). Five of these approved bispecific antibodies target one cancer associated target and retarget T-cells by their CD3 mioety (Catumaxomab, Removab®; Blinatumomab, Blincyto®; Tebentafusp, KIMMTRAK®; Teclistamab, TECVAYLI®; Mosunetuzumab, Lunsumio®) (Chenoweth and Crescioli 2022). Emicizumab (Hemlibra®) is a bispecific antibody that binds to factor IXa and factor X, thereby mimicking the function of coagulation factor VIII, and is approved for the treatment of hemophilia A. Amivantamab (Rybrevant®) is a bispecific antibody targeting EGFR and MET (Vijayaraghavan et al. 2020). Amivantamab was approved for the treatment of NSCLC

patients harboring exon 20 insertion mutations in EGFR and showed tumor progression after platinum-based chemotherapy. Furthermore, Faricimab (Vabysmo®) a vascular endothelial growth factor A (VEGF-A) and angiopoietin-2 (ANG2) targeting antibody, was approved for the treatment of neovascular age-related macular degeneration, and diabetic macular edema (Chenoweth and Crescioli 2022). Besides these approved molecules, there are more than 100 bispecific antibodies in clinical trials (November 2019), and more than 100 formats described, giving hope for more approvals in the near future (Brinkmann and Kontermann 2017; Labrijn et al. 2019; Brinkmann and Kontermann 2021).

1.2.1 Bispecific IgG-like antibody formats

Besides naturally occurring bispecific IgG4 molecules, which are capable of Fab-arm exchanges and thereby formation of random combination of specificities, all bispecific antibodies are artificial (Schuurman et al. 1999; Brinkmann and Kontermann 2017). In the early days of the development of bispecific antibodies either chemical coupling or fusion of two hybridoma cell lines (hybrid-hybridoma) were the standard procedures (Fudenberg et al. 1964; Milstein and Cuello 1983). Today, most of the bispecific antibodies are developed by recombinant methods, allowing for defined structure and composition, as well as biochemical, functional and pharmacological properties (Brinkmann and Kontermann 2017). Bispecific antibodies can be subdivided into two groups, the combinatorial and the obligate (Labrijn et al. 2019; Brinkmann and Kontermann 2021). Combinatorial bispecific antibodies aim to combine the basic properties of two parental antibodies and add potential new functionality. One example is the recently published Db3-43xhu225-C_H1/C_L-Fc, which combines the properties of the parental antibodies, the EGFR-targeting IgG hu225 and the HER3-targeting IgG 3-43. This antibody showed stronger inhibition of proliferation and triggered apoptosis more efficiently when compared to the parental antibodies while retaining the binding characteristics to the recombinant receptors and target-positive cells as well as displaying a similar pharmacokinetic profile (Seifert et al. 2019). Obligate bispecific antibodies are defined by properties, which cannot be achieved by the mixture of two parental antibodies. Six of the approved bispecific antibodies, Catumaxomab, Blinatumomab, Tebentafusp, Teclistamab, Mosunetuzumab, Emicizumab, are obligate bispecific antibodies. Except for Emicizumab, they are all engaging T-cells by binding CD3 and a tumor-associated antigen (TAA) on the tumor cell. This binding allows for close proximity between T-cell and tumor cell, the formation of an immunological synapse, resulting in the activation of the cytotoxic mechanisms of the T-cell (Brandl et al. 2007; Riesenberg et al. 2001). This coupling of two cells cannot be achieved by a mixture of two monospecific antibodies. Emicizumab is approved for the treatment of hemophilia A, a hereditary bleeding disease which is defined by the lack of Factor VIII or expression of an

unfunctional form thereof (Kitazawa and Shima 2020). This bispecific antibody binds Factor IX and Factor X, mimicking the dual binding properties of Factor VIII (Kitazawa et al. 2012; Kitazawa and Shima 2020).

The development of IgG-based bispecifics is subjected to certain requirements and depends on heterodimerization of either the heavy chains (heavy chain problem) or the heavy and the light chains (light chain problem). Chemical coupling or hybrid-hybridoma have low efficiency considering correct pairing of the heterodimer. In the case of the hybrid-hybridoma technology, 16 combinations with 10 different molecules can be formed and among all of these only one is the desired bispecific antibody (Milstein and Cuello 1983). One of the first solutions for the heavy chain problem was the knobs-into-holes (KIH) technology developed by the lab of Paul Carter, leading to correctly formed heterodimers of up to ~92 % (Ridgway et al. 1996). Based on this idea several other approaches were developed, inter alia the strand-exchange engineered domain (SEED), or the bispecific engagement by antibodies based on the T-cell receptor (BEAT) technology. The SEED technology includes an IgG/IgA chimeric CH3 domain, while the BEAT technology uses the heterodimer interface of the α- and β-domains of the T-cell receptor (Davis et al. 2010; Skegro et al. 2017). Besides knobs-into-holes based technologies for the heavy chain problem several formats use individual solutions for the light chain problem. One example is the CrossMab$^{CH1\text{-}CL}$ technology, which solves the light chain problem by swapping the constant domain between light and heavy chain of one Fab-arm (Schaefer et al. 2011b; Klein et al. 2019). Faricimab (Vabysmo®), a bispecific antibody targeting Ang-2 and VEGF-α for the treatment of wet age-related macular degeneration (AMD), was developed based on the CrossMab$^{CH1\text{-}CL}$ technology. For the DuetMab technology F126 in the CH1 and S121 in CL was substituted to cysteine (HC: F126C/LC: S121C), thereby replacing the natural disulfide bond of the Fab and solving the light chain problem (Mazor et al. 2015). Again, this molecule uses the knobs-into-holes technology to solve the heavy chain problem.

Other formats allow for bypassing of the heavy and light chain problem. One is the single-chain diabody Fc (scDb-Fc) format used in this study (Figure 2) (Alt et al. 1999). This format was developed based on mono- or bispecific and bivalent diabodies (Db). These are small antibody fragments, that assemble from two polypeptides in the format of VHA-VLB and VLA-VHB, or VHB-VLA and VLB-VHA, respectively. The short linkers (G_4S) between the VH and VL, prevent formation of a functional single-chain (sc) Fv fragment, leading to assembly into a dimeric molecule (Holliger et al. 1993). Addition of linker between the two polypeptides ($G_4SGGRASG_4S$) resulted in the single-chain diabody (scDb) format (Müller-Brüsselbach et al. 1999). Further, a human γ1 Fc was fused to the C-terminus of the scDb, forming a scDb-Fc (Alt

et al. 1999). Due to the symmetric homodimerization, a tetravalent and mono- or bispecific IgG-like antibody can be formed, bypassing the heavy and light chain problem.

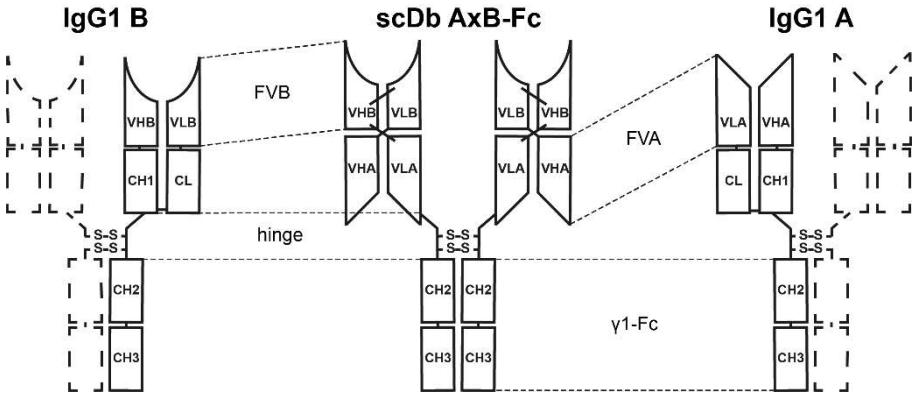

Figure 2: Schematic representation of the scDb-Fc format: To form a scDb-Fc, variable domains of heavy (VH) and light chain (VL) of two distinct antibodies (IgG1 A and IgG1 B, A and B indicating different binding moieties) are connected by a hinge to γ1-Fc (CH2 and CH3). For formation of the diabody between VHA and VLB, as well as between VHB and VLA, a 5 amino acid long linker is introduced. To form a single-chain diabody an additional 15 amino acid long linker connecting VLB and VHB, is added (Alt et al. 1999; Müller-Brüsselbach et al. 1999).

1.2.2 Bispecific antibodies for HER-family associated cancer therapy

As described above, malfunctioning of the HER-family members is highly associated with numerous cancer types. Despite the huge benefits of monospecific HER-family targeting antibodies, there are several limitations like biomarker selected non-responders and development of therapy resistances (Thomas and Weihua 2019; Vernieri et al. 2019; Jacob et al. 2018). Hope is set on bispecific antibody approaches targeting two members of the HER-family receptors at the same time or two different epitopes on one of the members, to improve the survival of cancer patients, which is reflected by numerous bispecific antibodies in preclinical and clinical testing (Table 1). Most of the clinical stage bispecific antibodies are developed for the treatment of cancer (~90 %) (Labrijn et al. 2019). About 45 % of these bispecific antibodies bind to a tumor-associated antigen (TAA) and redirect T-cells to the tumor site via binding to CD3 (Reichert 2020). T-cell retargeting approaches can overcome limitations in TAA-positive tumors due to their mode of action. Presentation of the TAA is sufficient for tumor killing, independent of intracellular mutations or bypassing mechanisms (Lopez-Albaitero et al. 2017; Goebeler and Bargou 2020). Two examples are GBR1302 (now called ISB1302), a HER2 and CD3 targeting antibody based on the BEAT technology, and RG6194, also targeting HER2 and CD3. Both antibodies are currently evaluated in phase I clinical trials (Labrijn et al. 2019). However, mutations of the targeted TAA or downregulation of the

expression can make retargeting antibodies ineffective (Braig et al. 2017; Goebeler and Bargou 2020).

Another approach is biparatopic targeting of the same HER-family receptor. ZW25, or the ADC-conjugated version thereof, ZW49, uses a biparatopic HER2-targeting approach, comprising the Trastuzumab and Pertuzumab binding moieties, thereby increasing avidity (Caruso 2019). Further, the biparatopic binding results in more potent silencing of HER2 signaling and stronger internalization compared to Trastuzumab alone (Caruso 2019; Hamblett et al. 07012018). In a phase I clinical trial of HER2-postive cancer of mixed entity, patients treated with ZW25 showed an objective response rate of 41 %. Another 41 % had stable disease, even in patients who have progressed under Trastuzumab treatment (Caruso 2019).

Other than EGFR and HER2, HER3 is rather associated with primary or acquired resistance to EGFR- and HER2-targeted therapy (Leto and Trusolino 2014; Stahler et al. 2017; Zhang et al. 2020; Kruser and Wheeler 2010; Tao et al. 2014). Bispecific antibodies, like Duligotuzumab (MEHD7945a) or Zenocutuzumab (MCLA-128) target HER3 and EGFR, or HER2, respectively, to overcome the development of resistance. The binding moieties of Duligotuzumab are based on the two-in-one Fab format, where one Fab arm allows binding of two different targets. First, Schäfer and coworker screened for an antibody targeting EGFR, using an antibody library with diversity restricted to the heavy-chain CDRs. In a second step diversity was restricted to the light-chain CDRs, thereby maintaining EGFR binding properties of the heavy chain and acquiring HER3 binding properties (Schaefer et al. 2011a). While preclinical studies accumulated evidence to support the hypothesis that simultaneously targeting EGFR and HER3 with Duligotuzumab will provide better clinical outcomes, no benefit compared to established therapies was observed in two phase 2 studies (Hill et al. 2018; Fayette et al. 2016). Zenocutuzumab (HER2xHER3) comprises a heterodimerizing γ1-Fc and a common light chain. It has a higher affinity for HER2, thereby allows for docking to HER2, and binding of HER3 blocks ligand association (Geuijen et al. 2018). In an early access program for patients with advanced NRG1-fusion positive solid tumors (two with ATP1B1–NRG1 and one with CD74–NRG1 fusion), Zenocutuzumab treatment achieved stable disease in one of three patients and partial response in the other two, even with improvement of brain metastasis (Rose 2019). These data underline the power of dual targeting of two receptors of the HER-family.

Table 1: Bispecific antibodies targeting receptors of the HER-family

Antibody	Format	Target 1 / 2	Most advanced phase	Clinical trial identifier	Company	References
BMX-002	Fab-hinge-IgG	EGFR / HER2	preclinical	-	BIOMUNEX	(Golay et al. 2016)
Db3-43xhu225-CH1/CL-Fc	Diabody-Ig	EGFR / HER3	preclinical	-	University of Stuttgart	(Seifert et al. 2019)
Duligotuzumab	2-in-1	EGFR / HER3	phase II	NCT01652482	Roche	(Hill et al. 2018; Schaefer et al. 2011a)
anti-EGFR/anti-HER2	Antibody-Darpin fusion	EGFR / HER2	preclinical	-	Samsung Electronics Co Ltd	(Cheong et al. 2016)
anti-EGFR/anti-HER3	Zybody	EGFR / HER3	preclinical	-	Zyngenia	(LaFleur et al. 2013)
MCLA-128	Biclonics	HER2 / HER3	phase II	NCT03321981	Merus	(Vries Schultink et al. 2020; Rose 2019)
MM-111	scFv-HSA-scFV	HER2 / HER3	phase II	NCT01774851	Merrimack	(Denlinger et al. 2016)
TAb6	IgG-scFv	HER2 / HER3	preclinical	-	University of Texas Southwestern Medical Center	(Kang et al. 2013)
anti-HER2/anti-HER3	Tandem scFv	HER2 / HER3	preclinical	-	Fox Chase Cancer Center	(Robinson et al. 2008)
ZW25 (Azymetric)	scFv-Fc/Fab-Fc	HER2 ECD2+4	phase II	NCT04224272; NCT03929666	Zymeworks	(Caruso 2019)
ZW49 (Azymetric)	scFv-Fc/Fab-Fc-ADC	HER2 ECD2+4	phase I	NCT03821233	Zymeworks	(Hamblett et al. 07012018)
MEDI4276	scFv-IgG-ADC	HER2 / HER2	phase I/II	NCT02576548	Medimmune	(Hamilton et al. 2016; Pegram et al. 2020)
MBS301	Hetero IgG1	HER2 / HER2	Phase I	NCT03842085	Beijing Mabworks Biotech	(Huang et al. 2018)
KN026	Hetero scFv-Fc	HER2 / HER2	Phase II	NCT03925974; NCT04165993	Alphamab	(Wei et al. 2017)

1.3 Objective of the study

HER-family receptors play an import role in many different cell processes and malfunctioning is highly associated with the development of different cancer types. EGFR overexpression is frequently observed in various cancer entities, where it stimulates survival, proliferation and motility of cancer cells, and shows involvement in tumor initiation and progression (Wieduwilt and Moasser 2008; Roskoski 2019; Olayioye et al. 2000). Hence, several EGFR-targeted treatments e.g. the chimeric monoclonal antibody Cetuximab were developed for the treatment of cancer (Mendelsohn and Baselga 2000; Herbst and Kies 2003; Goldstein et al. 1995). After nearly 20 years of regular clinical use and infinite clinical and preclinical studies, not only the modes of action but also the primary and acquired resistance mechanisms are known. One resistance mechanism that EGFR-targeted approaches exhibit is the primary expression or upregulation of HER3 or its ligand HRG upon treatment (Oliveras-Ferraros et al. 2012; Leto and Trusolino 2014; Leto et al. 2015; Stahler et al. 2017; Kruser and Wheeler 2010; Zhang et al. 2020). In previous studies, the HER3 targeting antibody IgG 3-43 was developed and showed promising results i*n vitro* and *in vivo* (Schmitt et al. 2017). Consequently, dual targeting of EGFR and HER3 was analyzed, either by combining the two monoclonal antibodies targeting HER3 and EGFR or by using a newly developed scDb-Fc combining the EGFR-targeting moiety of a humanized version of Cetuximab (hu225) and the HER3-targeting moiety of IgG 3-43. Here, superior effects of dual EGFR/HER3 inhibition with respect to EGF- and HRG-induced downstream signaling and inhibition of proliferation were observed when compared to the single antibody treatments (Honer 2016). The purpose of this study was to further develop this strategy, by generating new scDb and scDb-Fc molecules optimized in terms of producibility, affinity and target binding, followed by evaluation of *in vitro* and *in vivo* efficacy. Further, the most promising EGFR- and HER3-targeting scDb-Fc was combined with Trastuzumab for the treatment of CRC cell lines and patient derived organoids (PDO), aiming to block bypassing mechanisms activated in response to dual HER-family receptor inhibition.

2 Material

2.1 Instruments

Automated Cell Counter	Countess™ II [Thermo Fisher, Waltham, USA]
Balances	440-39N, 440-333N and ALJ 120-4 [Kern, Balingen, Germany]
Centrifuges	Eppendorf 5415C, 5810R [Eppendorf, Hamburg, Germany] J2-MC with rotors JA14, JA30.5 [Beckman Coulter, Krefeld, Germany] Avanti J-30I [Beckman Coulter, Krefeld, Germany] Optima™ TL with rotor TLA 100.3 [Beckman Coulter, Krefeld, Germany]
Electrophoresis systems	Mini-PROTEAN 3 Electrophoresis Cell System [BioRad, Munich, Germany] Ready Agarose Precast Gel System [BioRad, Munich, Germany] XCell SureLock® Midi-Cell [Thermo Fisher, Waltham, USA]
ELISA plate reader	Tecan SPARK® MULTIMODE MICROPLATE READER [Tecan Austria, Grödig, Austria]
Flow cytometer	MACSQuant®VYB; MACSQuant® Analyzer 10 [Miltenyi Biotec, Bergisch Gladbach, Germany]
FPLC System	ÄKTApurifier [GE Healthcare UK eLimited, Buckinghamshire, UK]
Gel documentation	Transilluminator, gel documentation system Felix [Biostep, Jahnsdorf, Germany]

Heat block	HBT-1-131 [HLC BioTech, Bovenden, Germany]
HPLC systems	Waters 2695 Separation Module, Waters 2489 UV/Visible detector [Waters Cooperation, Milford, USA]
Imager (immunoblots)	FUSION SOLO [Vilber Lourmat Deutschland, Eberhardzell, Germany]
Incubator for bacteria	Multitron II [Infors AG, Bottmingen, Switzerland]
Incubator for cell culture	Varocell 140 [Varolab, Giesen, Germany]
Magnetic stirrer	MR 3001K 800W [Heidolph Instruments, Nürnberg, Germany]
Microscope	CKX31 [Olympus, Hamburg, Germany]
PCR Cycler	Eppendorf Mastercycler [Eppendorf, Hamburg, Germany]
Real-time live cell imager	Incucyte® S3 Live-Cell Analysis System [Essen BioScience, Ann Arbor, USA]
Spectrophotometer	NanoDrop Spectrophotometer ND-1000 [PEQLAB, Erlangen, Germany]
Sterile bench	Variolab Mobilien W90 [Waldner-Laboreinrichtungen, Wangen, Germany]
Western blotting system	iBlot® 2 Dry Blotting System [Thermo Fisher, Waltham, USA]
Wound maker	IncuCyte® Cell Migration Kit [Essen BioScience, Ann Arbor, USA]

2.2 Special Implements

Attana sensor chips	Low nonspecific binding-carboxyl chips [Attana AB, Stockholm, Sweden]

Cell Culture Microplate	F-Bottom (Chimney Well), White, Cellstar® Tc [Greiner Bio-One; Frickenhausen, Germany]
Chromatography columns	Poly-Prep® columns [Bio-Rad, Munich, Germany]
Counting chamber	Neubauer 0.002 mm^2 [Marienfeld, Lauda-Königshofen, Germany]
Dialysis membranes	23 mm (cut-off 12.4 kDa) [Merck KGaA, Darmstadt, Germany]
ELISA plates	Microlon high binding ELISA plate [Greiner Bio-One, Frickenhausen, Germany]
FPLC columns	Superdex 200 Increase 10/300 GL [GE Healthcare UK eLimited, Buckinghamshire, UK]
HPLC columns	TSKgel SuperSW mAb HR cloumn [Merck KGaA, Darmstadt, Germany]
IMAC affinity beads	Protino® Ni-NTA agarose [Machery-Nagel, Düren, Germany]
Collection tubes for organoid culture	Low Protein Binding Collection Tubes (1.5 mL) [Thermo Fisher, Waltham, USA]
SDS-PAGE/western blot supplies	iBlot® NC Regular Stacks [Thermo Fisher, Waltham, USA] NuPAGE™ Novex™ 4-12 % Bis-Tris Midi Gels [Thermo Fisher, Waltham, USA]
Protein A beads	TOYOPEARL® AF rProtein A-650F [Tosoh Bioscience, Stuttgart, Germany]

2.3 Chemicals

All chemicals were purchased from Roth [Karlsruhe, Germany], Merck [Darmstadt, Germany], Roche [Basel, Switzerland] and Sigma-Aldrich [St. Louis, USA]. It is stated when chemicals were purchased from other companies.

2.4 Buffers and solutions

Bradford reagent	BioRad protein assay [BioRad, Krefeld, Germany]
Coomassie staining solution	0.008 % (w/w) Coomassie Brilliant Blue G-250, 35 mM HCl in H_2O
DNA loading buffer (5x)	25 % (v/v) glycerol, 0.02 % (w/v) bromphenol blue in 5x TAE buffer
ECL reagent	SuperSignal™ West Dura [Thermo Fisher, Waltham, USA]
ELISA – developing solution	0.1 mg/ml TMB, 100 mM sodium acetate buffer pH 6.0, 0.006 % (v/v) H_2O_2
ELISA – stopping solution	1 M H_2SO_4
Freezing solution	10 % (v/v) DMSO + 10 % FCS in cell culture medium
IMAC elution buffer	250 mM imidazole in 1x sodium phosphate buffer
IMAC wash buffer	25 mM imidazole in 1x sodium phosphate buffer
Laemmli sample buffer (5x)	Non-reducing: 10 % (w/v) SDS, 25 % (v/v) glycerin, 0.05 % (w/v) bromphenol blue in 312.5 mM Tris-HCl pH 6.8 Reducing: non-reducing buffer, 25 % (v/v) β-mercaptoethanol
MPBS	3 % (m/v) dry milk powder in 1x PBS
PBA	2 % (v/v) FCS, 0.02 % (w/v) NaN_3 in 1x PBS

PBST	0.05 % (v/v) TWEEN 20 in 1x PBS
Phosphate-buffered saline (PBS, 10x)	80.6 mM $Na_2HPO_4 \cdot 2\ H_2O$, 14.7 mM KH_2PO_4, 1.37 M NaCl, 26.7 mM KCl (10x); used as 1x PBS diluted in dH_2O
Protein A – elution buffer	100 mM glycine, pH 2.5 – 3.5
Protein A – neutralization buffer	1 M Tris-HCl, pH 8.0
RIPA buffer	50 mM Tris pH 7.5, 150 mM NaCl, 10 mM NaF, 20 mM β-Glycerophosphate, 1 mM EDTA, 1 % NP-40, 1 mM Na_3VO_4, 0.5 mM PMSF, 0.25 % DOC, 0.1 % SDS in H_2O
SDS running buffer, 10x	1.92 M glycine, 0.25 M Tris, 1 % SDS, pH 6.8
SDS-PAGE buffers and reagents	NuPAGE® MES Running Buffer; NuPAGE® Antioxidant [Thermo Fisher, Waltham, USA]
TAE buffer, 50x	2 M Tris, 0.95 M glacial acetic acid, 50 mM EDTA in H_2O, pH 8

2.5 Media and supplements

2.5.1 Bacterial culture

Ampicillin (Amp)	100 mg/ml in H_2O [Roth, Karlsruhe, Germany]
IPTG	Isopropyl-β-D-thiogalactopyranoside, 1 M in H_2O [Gebru Biochemicals, Gaiberg, Germany]
LB Amp, Glc agar plates	LB-medium, 2.0 % (w/v) agar, after autoclaving added ampicillin (100 µg/ml) and 1 % (w/v) glucose
LB-medium (Amp)	1 % (w/v) peptone, 0.5 % (w/v) yeast extract, 0.5 % (w/v) NaCl in H_2O (for selection 100 µg/ml ampicillin)

2.5.2 Eukaryotic cell culture

Advanced DMEM/F-12	[+] 4,5 g/L D-Glucose, [+] NEAA, [+] Sodium pyruvate, [+] Phenol red [Thermo Fisher, Waltham, USA]
B27 supplement	B-27™ Supplement, serum-free [Thermo Fisher, Waltham, USA]
b-FGF	Recombinant Human FGF-basic (154 a.a.) [Peprotech, Hamburg, Germany]
DMEM (1x)	[+] 4,5 g/L D-Glucose, [+] L-Glutamine [Thermo Fisher, Waltham, USA]
EGF	Animal-Free Recombinant Human EGF [Peprotech, Hamburg, Germany]
Eosin solution	0.4 % (m/v) eosin G, 0.02 % (w/v) NaN_3 in sterile 1x PBS, pH 7.4
GlutaMAX	GlutaMAX™ Supplement [Thermo Fisher, Waltham, USA]

HEPES	Gibco® HEPES (N-2-hydroxyethylpiperazine-N-2-ethane sulfonic acid) [Thermo Fisher, Waltham, USA]
HRG	Recombinant Human Heregulinβ-1 [Peprotech, Hamburg, Germany]
Fetal bovine serum (FBS)	FBS Premium (PAN Biotech, Aidenbach, Germany)
Freestyle F17-medium	Supplemented with 4mM GlutaMAX-I, 0.1 % Kolliphor P188
Lipofectamine	Lipofectamine™ 2000 [Thermo Fisher, Waltham, USA]
N2 supplement	N-2 Supplement (100X) [Thermo Fisher, Waltham, USA]
N-Acetyl-L-Cystein	≥98 % [Roth, Karlsruhe, Germany]
Opti-MEM®	GIBCO® [Thermo Fisher, Waltham, USA]
Polyethylenimine (PEI)	[Polisciences, Inc., Hirschberg an der Bergstrasse, Germany]
Penicillin/streptomycin (100x)	10,000 U/ml / 10,000 µg/ml (100x) GIBCO® [Thermo Fisher, Waltham, USA]
RPMI 1640	+ 2 mM glutamine GIBCO® [Thermo Fisher, Waltham, USA]
TrypLE	TrypLE Express Enzym (1X) [Thermo Fisher, Waltham, USA]
Trypsin/EDTA	0.5 % (w/v) trypsin, 5.3 mM EDTA (10x) [Thermo Fisher, Waltham, USA]
Trypton N1 (TN1)	[Organo Technie, La Courneuve, France]
Mitomycin C	0.5 mg/ml in H_2O [Sigma-Aldrich, St. Louis, USA]

2.6 Detection antibodies

Name	Origin	Dilution
Anti-His_6-HRP	Mouse monoclonal IgG1, 200 µg/ml [Santa Cruz Biotechnology, Santa Cruz, USA]	1:1000 (ELISA)
Anti-human IgG (Fab specific)-HRP	Polyclonal [Sigma-Aldrich, St. Louis, USA]	1:20000 (ELISA)
Anti-human IgG (Fc specific)-HRP	Polyclonal [Sigma-Aldrich, St. Louis, USA]	1:5000 (ELISA)
Anti-human IgG (γ-chain specific)-R-PE	Goat anti-human IgG [Sigma-Aldrich, St. Louis, USA]	1:500 (FACS)
Anti-human IgG (γ-chain specific)-R-PE	Goat IgG anti-Human IgG (Fc)-RPE [Dianova, Hamburg, Germany]	1:500 (FACS)
Anti-mouse IgG (Fc specific)-HRP	Polyclonal [Sigma-Aldrich, St. Louis, USA]	1:4000 (WB)
Anti-mouse IgG (H+L)-HRP	Goat IgG anti-Mouse IgG (H+L)-HRPO [Dianova, Hamburg, Germany, #115-035-062]	1:5000 (WB)
Anti-rabbit-IgG-Peroxidase	Goat polyclonal [Sigma-Aldrich, St. Louis, USA, #A0545]	1:5000 (WB)
Anti-EGFR	Rabbit polyclonal IgG [Santa Cruz Biotechnology, Santa Cruz, USA, #sc-03-G]	1:500 (WB)
Anti-phospho-EGFR (Tyr 1068) XP®	Rabbit mAb [Cell Signaling Technology®, Danvers, USA, #3777]	1:500 (WB)
Anti-HER2 Ab17	Mouse mAb [Thermo Fisher, Waltham, USA, MS-730-PA]	1:500 (WB)
Anti-phospho-HER2 (Tyr1221/1222)	Rabbit mAb [Cell Signaling Technology®, Danvers, USA, #2243]	1:500 (WB)
Anti-HER3 Ab2 (2F12)	Mouse mAb [Thermo Fisher, Waltham, USA, #MA5-12675]	1:500 (WB)

Anti-phospho-HER3 (Tyr1289)	Rabbit mAb [Cell Signaling Technology®, Danvers, USA, #4791]	1:500 (WB)
Anti-Akt	Mouse mAb [Cell Signaling Technology®, Danvers, USA, #2920]	1:500 (WB)
Anti-phospho-Akt (Thr308) XP®	Rabbit mAb [Cell Signaling Technology®, Danvers, USA, #13038]	1:500 (WB)
Anti-phospho-Akt (Ser473) XP®	Rabbit mAb D9E [Cell Signaling Technology®, Danvers, USA, #4060]	1:500 (WB)
Anti-Erk1/2	Mouse mAb [Cell Signaling Technology®, Danvers, USA, #9107]	1:500 (WB)
Anti-phospho-Erk1/2 (Thr202/Tyr204)	Polyclonal [Cell Signaling Technology®, Danvers, USA, #9101]	1:500 (WB)
Anti-Tubulin	Mouse mAb [Sigma-Aldrich, St. Louis, USA, #T6793]	1:500 (WB)

2.7 Enzymes

Fast Digest BamHI	[Thermo Fisher, Waltham, USA]
Fast Digest BshTI (AgeI)	[Thermo Fisher, Waltham, USA]
Fast alkaline phosphatase	1 U/µl [Thermo Fisher, Waltham, USA]
Fast Digest NotI	[Thermo Fisher, Waltham, USA]
***Pfu* DNA polymerase (native)**	2.5 U/µl [Thermo Fisher, Waltham, USA]
Fast Digest SgsI	[Thermo Fisher, Waltham, USA]
T4 DNA ligase	5 U/µl [Thermo Fisher, Waltham, USA]
Fast Digest XbaI	[Thermo Fisher, Waltham, USA]
Fast Digest XhoI	[Thermo Fisher, Waltham, USA]

2.8 Marker

GeneRuler™ DNA ladder mix	[Thermo Fisher, Waltham, USA]

PageRuler™ prestained protein ladder	[Thermo Fisher, Waltham, USA]

2.9 Kits

CellTiter-Glo® 2.0 Assay	[Promega, Fitchburg, WI, USA]
CellTiter-Glo® 3D Assay	[Promega, Fitchburg, WI, USA]
***DC*™ Protein Assay**	[BioRad, Munich, Germany]
NucleoBond® Xtra Midi	[Machery-Nagel, Düren, Germany]
NucleoSpin® Gel and PCR Clean-up	[Machery-Nagel, Düren, Germany]
NucleoSpin® Plasmid	[Machery-Nagel, Düren, Germany]
REDTaq ReadyMix PCR Reaction Mix (1 U/ml)	[Sigma-Aldrich, St. Louis, USA]

2.10 Bacterial Strains

Escherichia coli TG1 strain (Genotype: supE thi-1 Δ(lac-proAB) Δ(mcrB-hsdSM)5 (rK–mK–) [F´ traD36 proAB laclqZΔM15], StrataGen, Kirkland, WA, USA) was used for cloning and periplasmic production.

2.11 Eukaryotic cell lines

Cell line	Origin	Culture medium
DiFi	Colorectal adenocarcinoma (familial adenomatous polyposis; Gardner Syndrom)	RPMI 1640 + 10 % FCS
FaDu	Human squamous cell carcinoma	DMEM + 10 % FCS
HCC1806	Primary acantholytic squamous cell carcinoma	RPMI 1640 + 10 % FCS
HEK293-6E	Human embryonic kidney	F17 Freestyle medium + L-Glutamine + Kolliphor P-188 + G418 (25 µg/ml)
HT-29	Colorectal adenocarcinoma	RPMI 1640 + 10 % FCS

LIM1215	Colorectal carcinoma (Lynch-Syndrom; Derived from metastatic site: Omentum)	RPMI 1640 + 10 % FCS
MCF-7	Human adenocarcinoma, breast	RPMI 1640 + 10 % FCS
MDA-MB-468	Adenocarcinoma (mammary gland/breast; derived from metastatic site: pleural effusion)	RPMI 1640 + 10 % FCS
NCI-N87	Human gastric carcinoma	RPMI 1640 + 10 % FCS
SK-BR-3	Human adenocarcinoma, breast	DMEM + 10 % FCS

2.12 Primary colorectal cancer organoids

Patient-derived organoids (PDOs) were obtained from the biobank of the Institute of Clinical Pharmacology (IKP) – Robert Bosch Hospital (RBK) in Stuttgart. Experiments were approved by the ethics commission of the RBK. For cultivation of CRC PDOs see 3.4.2.

PDO	**Gene**	**Coding variant**	**Amino acid variant**
PDO1	APC	334C>T	P112S
		694>T	R232*
	PI3K	2176G>A	E726K
	TP53	742C>T	R248W
PDO2	CTNNB1	121A>G	T41A
	PI3KCA	1369A>G	N457D
		1634A>G	E545G
	HDAC2	887G>T	G296V
PDO3	APC	4348C>T	R1450*
	TP53	393_395delCAA	131delN
PDO4	TP53	743G>A	R248Q
	SMAD4	115G>A	A39T

2.13 Primer

#	Name	Sequence
89	pET-Seq1/T7-back	5’-TAATACGACTCACTATAGG
91	pSec-Seq2/BGH-Reverse	5’-TAGAAGGCACAGTCGAGG
881	CH1-for	5'-TGGGGGGAAGAGGAAGAC
1457	AAA-back	5’-AAAAGCGGCCGCAGACAAAACTCACACATGC
1469	NotI-AAA-(GGSGG)2-Fc-back	5’-AAAAGCGGCCGCAGGTGGCAGCGGAGGCGGGGGAAGCGGCGGT
1685	(GGRAS_GGGGS)-back	5’-CGGTGGGGGCGGATCGGGCGGAGGTGGCTCACAAG
1686	(GGRAS_GGGGS)-for	5’-CGATCCGCCCCCACCGCTGCCACCGCCTCCCAG

2.14 Plasmids

#	Name	Cloned by
805	pSecTagA-EGFR-Fc	Sina Fellermeier
806	pSecTagA-HER2-Fc	Sina Fellermeier
807	pSecTagA-HER3-Fc	Sina Fellermeier
952	pecTagHis-scDb4D5hu225	Aline Plappert
1719	pSecTagAHis-scDbhu225HER3-43-LL	Jonas Honer
1766	pSecTagAHis-EGFR	Jonas Honer
1767	pSecTagAHis-HER2	Jonas Honer
1768	pSecTagAHis-HER3	Nadine Heidel
1707	pSecTagAL1-scDbhu225HER3-43-Fc	Jonas Honer
1716	pSecTagAL1-scDbHER3-43-Fc	Jonas Honer
1822	pSecTagAL1-scDb 3-43xhu225-Fc	Alexander Rau
1824	pSecTagAL1-scDb hu225x3-43-LL-Fc	Alexander Rau
1925	pSecTagAL1-scDb 4D5x3-43-LL-FLL(7aa)-Fc	Alexander Rau
2105	pSecTagAL1-scDb hu225x3-43-Fc-$(GGSGG)_0$	Alexander Rau
2106	pSecTagAL1-scDb hu225x3-43-Fc-$(GGSGG)_2$	Alexander Rau
2109	pSecTagAL1-scDb hu225x3-43-LL-FLL(7a)-Fc	Alexander Rau
2111	pSecTagAL1-scDb hu225x3-43-Fc (GGRAS_GGGGS)	Alexander Rau
2296	pSecTagAL1-scFv hu9G5	Alexander Rau
2689	pSecTagAL1-scDb hu225x3-43 (GGRAS_GGGGS)	Alexander Rau
2690	pSecTagAL1-scDb hu225x3-43-LL	Alexander Rau

2.15 Proteins

Cetuximab	Merck, Darmstadt, Germany
Rituximab	Roche, Basel, Switzerland
Trastuzumab	Roche, Basel, Switzerland

2.16 Small molecules

Afatinib	MedChemExpress, Monmouth Junction, USA

2.17 Software

ExPASy ProtParam	[http://web.expasy.org/protparam/]
FlowJo Version 10.6.1	[Treestar, Ashland, USA]
GraphPad Prism 7	[GraphPad Software, La Jolla, USA]
MACSQuantify™ Software	[Miltenyi Biotec, Bergisch Gladbach, Germany]
Serial Cloner 2.6	

3 Methods

3.1 Cloning

3.1.1 Cloning strategy of scDb and scDb-Fc antibodies

For pSecTagAL1-scDb hu225x3-43-Fc (GGRAS_GGGGS) (scDb-Fc-1, #2111) the amino acids RA of linker 2 (Figure 3) were exchanged by GG. Using the combination of primer #1685 and #881, or #1686 and #89 two DNA fragments were amplified from pSecTagAL1-scDb hu225x3-43-Fc (#1707). The amplified fragments were fused by Fusion-PCR (see 3.1.3), digested with BshTI/NotI and ligated with BshTI/NotI pre-digested pSecTagAL1-scDb hu225x3-43-Fc (#1707).

The elongated intermediate linker between the V_H and V_L of 3-43 in pSecTagAL1-scDb hu225x3-43-LL-Fc (scDb-Fc-2, #1824) was cloned by exchanging this domain in pSecTagAL1 scDb hu225x3-43-Fc (#1707), against the 3-43-LL domain of pSecTagAHis scDbhu225x3-43-LL (#1719). Vector and insert were digested by XhoI/SgsI.

For pSecTagAL1-scDb hu225x3-43-Fc-$(GGSGG)_0$ (scDb-Fc-3, #2105) the linker 3 (Figure 3) was removed. Using primer #1457 and #91 a DNA fragment was amplified by PCR (see 3.1.2), digested with NotI/XbaI and ligated with pre-digested pSecTagAL1-scDb hu225x3-43-Fc (#1707).

pSecTagAL1-scDb 3-43xhu225-Fc (scDb-Fc-4, #1822) was cloned by inserting the V_H and V_L domains of scFv hu225 into the vector pSecTagAL1-scDbHER3-43-Fc (#1716), exchanging the inner variable fragments of 3-43. For this, pSecTagHis scDb4D5hu225(#952) was digested with XhoI/SgsI and cloned into pre-digested (XhoI/SgsI) pSecTagAL1 scDbHER3-43-Fc.

For pSecTagAL1-scDb hu225x3-43-Fc-$(GGSGG)_2$ (scDb-Fc-5, #2106) 5 amino acids (GGSGG) were added to linker 3 (Figure 3). Using primer #1469 and #91 a DNA fragment was amplified by PCR (see 3.1.2), digested with NotI/XbaI and ligated with pre-digested pSecTagAL1-scDb hu225x3-43-Fc (#1707).

pSecTagAL1-scDb hu225x3-43-LL-FLL(7aa)-Fc (#2109) was cloned by inserting the sequence of linker 2-VL3-43-linker 3-VH3-43-linker 4 domain from pSecTagAL1-scDb 4D5x3-43-LL-FLL(7aa)-Fc (#1925) into pSecTagAL1-scDb hu225x3-43-Fc (#1707). For this, plasmid #1925 and #1707 were digested with XhoI/BamHI. The smaller fragment of #1925 was ligated with the predigested #1707.

pSecTagAL1-scDb hu225x3-43 (GGRAS_GGGGS) (scDb-1, #2689) was cloned by inserting the scDb sequence of pSecTagAL1-scDb hu225x3-43-Fc (GGRAS_GGGGS) (scDb-Fc-1, #2111) into pSecTagAL1 scFv-hu9G5 (#2296). Both plasmids were digested using BshTI/NotI. The shorter fragment of the digested #2111 was ligated with pre-digested #2296.

pSecTagAL1-scDb hu225x3-43-LL (scDb-1, #2690) was cloned by inserting the scDb sequence of pSecTagAL1-scDb hu225x3-43-LL-Fc (scDb-Fc-2, #1824) into pSecTagAL1 scFv-hu9G5 (#2296). Both plasmids were digested using BshTI/NotI. The shorter fragment of the digested #1824 was ligated with pre-digested #2296.

3.1.2 Polymerase chain reaction (PCR)

DNA was amplified using *Pfu* DNA polymerase. A typical PCR mixture for four reactions contained 200 µl.

Table 2: Composition of PCR mixture.

Components	**Volume [µl]**	
	1x	**4x**
10 x *Pfu* polymerase buffer + $MgSO_4$	5	20
forward primer (10 pmol/µl)	1	4
reverse primer (10 pmol/µl)	1	4
Template	~0.25	1
dNTPs	2,5	10
Pfu DNA polymerase (2.5 U/µl)	1	4
ddH_2O	39,25	157

The *Pfu* DNA polymerase has a replication fidelity of 500 nt/min, hence the elongation time depends on length of the amplified DNA sequence. The PCR was performed using the PCR program as described in Table 3. The PCR products were loaded onto a 1 % agarose gel and separated from template DNA and primers.

Table 3: PCR program

PCR step	Temperature [°C]	Time [min]	No. of cycles
Initial denaturation	94	5	1x
Denaturation	94	1	30x
Annealing	50	1	
Elongation	72	Dependent on PCR product	
Final elongation	72	5	

3.1.3 Fusion-PCR

For fusion-PCR overlapping primers were designed in silico. DNA fragments were amplified using standard PCR conditions, using overlapping primers, as well as sequencing primers. After PCR DNA was extracted and eluted in 41 µl ddH_2O into one reaction tube (see 3.1.2 and 3.1.5). Further 5 µl pfu-buffer, 3 µl dNTPs and 1 µl pfu DNA-Polymerase were added and PCR was performed as described in Table 4.

Table 4: Fusion-PCR program

PCR step	Temperature [°C]	Time [min]	No. of cycles
Initial denaturation	95	5	1x
Denaturation	95	0.5	5x
Annealing	Tm	0.5	
Elongation	71	Dependent on PCR product	
Final denaturation	95	Holding	

After PCR, tube was put on ice for 3 min and 2.5 µl of sequencing primer were added. Now PCR was performed as described in Table 3 (see 3.1.2).

3.1.4 Restriction digestion

For restriction digestion 10 µg vector DNA or complete extract from PCR products was used. Restriction enzymes (1 µl each) and the corresponding 10x buffer were added and incubated according to manufacturer's protocol. Vector DNA was additionally dephosphorylated with 1 U fast alkaline phosphatase. ddH_2O was added up to a total volume of 50 µl. Digestions were performed for 1 h at enzyme specific temperature. Exchange of buffer was conducted using

NucleoSpin® Gel and PCR Clean-up kit. Digested insert DNA was separated from vector DNA using agarose gel electrophoresis.

3.1.5 Agarose gel electrophoresis and DNA gel extraction

PCR-amplified and digested DNA fragments were analyzed by agarose gel electrophoresis (1 % (w/v) agarose in 1x TAE buffer). DNA was mixed with 5x DNA loading buffer and loaded onto an agarose gel containing 1 µg/ml ethidium bromide. Electrophoresis run was performed in 1x TAE buffer at 80 V for 35 min and DNA was visualized using ultraviolet light. The relevant bands were cut out and purified with a NucleoSpin® Gel and PCR Clean-up kit according to the manufacturer's protocol. DNA was eluted in 30 µl ddH_2O.

3.1.6 Ligation of DNA

Vector DNA (2 µl) and insert (15 µl) were mixed at 1:6 molar ratio and T4 DNA ligase (1 µl) and appropriate buffer (2 µl) were added. Incubation was conducted for 1 h at RT.

3.1.7 Transformation of competent *E.coli* TG1 cells

Chemical competent *E.coli* TG1 cells were gently thawed on ice. 100 µl of cells were added to the ligation mixture and incubated on ice for 10 min. Next, heat shock was performed for 1 min at 42°C and cells were placed back on ice for 1 min. 1 ml of pre-warmed LB medium was added and cells were incubated for 30 min at 37°C. After centrifugation for 1 min at 16,000g, supernatant was discarded and cells were plated on agar plates containing glucose (1 %) and ampicillin (100 µg/ml). Plates were then incubated at 37°C overnight.

3.1.8 Colony screen

Insertion of DNA into vector plasmid was verified using RED*Taq*® ReadyMix™ according to the manufacturer's protocol with the appropriate primers. Individual clones were picked and pipette tip was immersed into 100 µl of pre-warmed (RT) LB-medium in PCR tubes, then mixed with 20 µl of the PCR mixture. Colony PCR was performed as described in Table 3 considering a *Taq*-polymerase replication fidelity of 1000 nt/min. Positive clones were identified by agarose gel electrophoresis.

3.1.9 Plasmid DNA isolation

Overnight cultures of *E.coli* bearing transformed plasmid, were inoculated in 6 ml (Mini-preparation) or 100-200 ml (Midi-preparation) LB-medium containing ampicillin (100 µg/ml). For purification of the plasmid DNA the NucleoSpin® Plasmid kit for the Mini-preparation was used, or the NucleoBond® Xtra Midi kit for the Midi-preparation according to the manufacturer's protocol. DNA pellets were resolved in 30 µl (Mini-preparation) or 150 µl (Midi-

preparation) ddH2O. Resolved DNA incubated for 5 min at 65°C, then stored at -20°C. DNA concentration was measured at 260 nm using NanoDrop 1000. Identity of plasmid was confirmed by sequencing.

3.1.10 DNA sequence analysis

DNA sequencing was performed either by GATC Biotech AG (Constance, Germany), or Microsynth Seqlab (Göttingen, Germany). Sequenced DNA was analyzed using a nucleotide BLAST against the corresponding sequence (Serial Cloner 2.6.1).

3.2 Expression and purification of recombinant protein

3.2.1 Transient expression of recombinant proteins in HEK293-6E cells

Recombinant proteins were produced in HEK293-6E cells, cultured in orbital shaker at 37°C, 5 % CO_2 and 70 % humidity. At day of transfection cells were at exponential phase and density was adjusted to $1.7 \cdot 10^6$ cells/ml. For 100 ml cell suspension, 100 µg plasmid DNA were mixed with 5 ml F17-medium, and 200 µl of PEI (1 mg/ml) were mixed with 5 ml of F17-medium. After 2 minutes, both solutions were mixed and incubated for 15 min at RT, before added to the cell suspension. Cells were cultured as described above during production. 24 h later trypton N1 (TN1) to a final concentration of 0.5 % was added to the cells. After additional 96 h the cell suspension was collected and centrifuged (2000x g, 10 min, 4 °C). The supernatant was sterile filtrated and proteins were purified as described in 3.2.2 and 3.2.3, respectively.

3.2.2 Purification by immobilized metal affinity chromatography (IMAC)

His6-tag containing recombinant proteins were purified by Ni-NTA-IMAC. Supernatant of HE293-E6 culture was dialyzed against 1x PBS at 4°C overnight. The next day, dialyzed supernatant was incubated with Ni^{2+}-NTA-agarose beads at 4 °C for three to four hours, respectively. Next, beads were loaded on a column and washed with IMAC wash buffer (25 mM imidazole) until no undesired protein was detectable in the wash fractions. For determination of protein 10 µl of flow-through were mixed with 90 µl Bradford reagent. Protein was eluted using IMAC elution buffer (250 mM imidazole) and collected in 100 µl – 300 µl fractions. Protein containing fractions were pooled and dialyzed against 1x PBS at 4°C overnight.

3.2.3 Purification by protein A affinity chromatography

Recombinant proteins comprising a human γ1-Fc region were purified by protein A affinity chromatography. Supernatant was incubated with protein A beads at 4 °C for 4 hours, and then was loaded on a column. Beads were washed with 1x PBS until no undesired protein was

detectable. For determination of protein 10 µl of flow-through were mixed with 90 µl Bradford reagent. After washing, proteins were eluted using protein A elution buffer (100 mM glycin, pH 3.5). Protein containing fractions were pooled and dialyzed against 1x PBS at 4°C overnight.

3.2.4 Gel filtration by fast protein liquid chromatography (FPLC)

Fast protein liquid chromatography gel filtration was performed with column Superdex® Increase 10/300 GL. Prior to preparative size exclusion chromatography, the column was washed with five column volumes of ddH_2O (100 ml) and equilibrated with five column volumes of PBS (100 ml). Chromatography was performed at a flow rate of 600 µl/min at pressure of 1.5 mPa, thereby 600 – 1000 µl of Protein were manually applied. 150 µl fraction were automatically collected. Column was stored at RT in 20 % EtOH.

3.3 Protein characterization

3.3.1 Determination of protein concentration

Concentration of proteins was determined at 280 nm using the NanoDrop spectrophotometer 1000. Molecular mass and extinction coefficient was determined using the online tool ProtParam (ExPASy; https://web.expasy.org/protparam/).

3.3.2 SDS polyacrylamide gel electrophoresis (SDS-PAGE)

For protein purity and integrity analysis SDS-PAGE was performed. Depending on expected molecular mass of proteins, acrylamide concentration of gel was prepared as described in Table 5. Before loading, protein samples were mixed with reducing or non-reducing 5x Laemmli sample buffer and incubated at 95 °C for 5 min. Protein samples and prestained protein ladder (PageRuler™) were loaded onto the gel. Electrophoresis was performed in SDS running buffer at 40 mA for approximately 55 min. Gel was washed three times in boiling water and then was stained with Coomassie staining solution overnight. For de-staining tap-water was used.

Table 5: Composition of polyacrylamide gels

	Resolving gel		
Substances	**10 %**	**12 %**	**Stacking gel**
H_2O	3 ml	2.5 ml	2.1 ml
30 % acrylamide mix	2.5 ml	3 ml	500 µl
1.5 M Tris (pH 8.8)	1.9 ml	1.9 ml	-
1.0 M Tris (pH 6.8)	-	-	375 µl
10 % SDS	75 µl	75 µl	30 µl
10 % APS	75 µl	75 µl	30 µl
TEMED	3 µl	3 µl	3 µl

3.3.3 Size exclusion by high performance liquid chromatography (HPLC)

HPLC was performed using Waters 2695 HPLC in combination with a TSKgel SuperSW mAb HR column (Sigma Aldrich, 822854) at a flow rate of 0.5 ml/min. Protein were adjusted to a concentration of 0.2–0.5 mg/ml. 0.1 M Na_2HPO_4/NaH_2PO_4, 0.1 M Na_2SO_4, pH 6.7 was used as mobile phase. Standard proteins: thyroglobulin (669 kDa, R_S 8.5 nm), β-amylase (200 kDa, R_S 5.4 nm), bovine serum albumin (66 kDa, R_S 3.55 nm), carbonic anhydrase (29 kDa, R_S 2.35 nm).

3.4 Mammalian cell culture

3.4.1 General cultivation of cancer cells

Mammalian cells were cultivated in tissue culture flasks and incubated at 37°C with 95 % humidity and 5 % CO_2. Cells were cultured in appropriate culture medium (see 2.11) and split every two to three days, using 1x Trypsin-EDTA for detachment. For long-term storage, cells were detached, harvested (1500 rpm, 5 min) and the cell pellet was resuspended in freeze cell culture medium (cell culture medium + 10 % FCS + 10 % DMSO). Cryo vials with cells were frozen at - 80°C in a cryobox filled with isopropanol. For defrosting, cells were thawed at 37°C and resuspended in appropriate medium. After harvesting by centrifugation (1500 rpm, 5 min), cells were cultured under normal conditions.

3.4.2 CRC organoids

Patient-derived organoids (PDOs) were obtained from the biobank of the Institute of Clinical Pharmacology (IKP) – Robert Bosch Hospital (RBK) in Stuttgart. Experiments were approved by the ethics commission of the RBK. PDOs, embedded in 15 µl Matrigel, were grown in 12-well tissue culture plates with surrounding 400 µl complete medium (Table 6). Every two or three days cells were split. To that end, supernatant was removed by gentle aspiration. All pipette tips were coated with BSA, by pipetting up and down BSA before use for any step at PDO culture. To recover cells from Matrigel 1 ml of ice-cold PBS was used, while a maximum of 6 wells per ml PBS was recovered. PBS-cell mixture was then transferred into BSA coated Eppendorf tubes (low-binding). For harvesting, the cells were centrifuged (16,100 g until maximum speed is reached; total time: approximately 10 s). Then, supernatant was removed gently with a pipette, avoiding contact to cell pellet. To remove remaining Matrigel cells were resuspended in 1 ml of ice-cold PBS and gently pipetted up and down. After additional centrifugation (16,100 g until maximum speed is reached; total time: approximately 10 s) supernatant was discarded and cell pellet was resuspended in 100 µl of TrypLE. Pellet was incubated for a maximum of 5 minutes and resuspended every 1-2 minutes during the incubation. As soon PDO break up and small clumps are visible, 1 ml of P/S medium (Table 6) was added and cells were stored for 10 min on ice, allowing organoids to sink and debris staying in upper volume. Next, the debris were carefully removed by discarding upper 500 µl of supernatant. After additional centrifugation (16,100 g until maximum speed is reached; total time: approximately 10 s), supernatant was discarded and cells were resuspended in a mixture of complete medium and Matrigel (for 10 wells: 30 µl of complete medium + 100 µl of Matrigel). For seeding the number of wells was doubled compared to initial number of wells and 15 µl aliquots were seeded per well. For polymerization of the Matrigel-cell droplets, the cell culture plate was incubated upside-down for 15 min in an incubator at 37°C with 95 % humidity and 5 % CO_2. After incubation Matrigel-cell droplet was overlaid with 400 µl of complete medium. For cryopreservation, PDOs are recovered from Matrigel with 1 ml of ice-cold PBS as described above. Then, cells were centrifuged (16,100 g till maximum speed is reached; total time: approximately 10 s) and washed with 1 ml of ice-cold PBS, thereby removing remaining Matrigel. After additional centrifugation (16,100 g till maximum speed is reached; total time: approximately 10 s) PDO pellets were resuspended in 1 ml of P/S medium (Table 6) supplemented with 20 % FCS and 10 % DMSO. Cryovials with cells were frozen at -80°C in a cryobox filled with isopropanol.

Table 6: Composition of media used for CRC organoid culture

Medium	Substance	Final concentration
P/S Medium	Advanced DMEM/F12	
	1x P/S	1x
Basal medium	Advanced DMEM/12	
	GlutaMAX	1x
	1xP/S	1x
	Hepes	10 mM
	N-Acetylcysteine	1 mM
N2/N27	**Basal medium**	
	1x N2 supplement	1x
	1x B27 supplement	1x
Complete Medium (CM)	**N2/B27 Medium**	
	bFGF	20 ng/ml
	EGF	50 ng/ml
Complete Medium (CM) HRG	**N2/B27 Medium**	
	HRG	50 ng/ml

3.5 Functional characterization of proteins

3.5.1 Enzyme-linked immunosorbent assay (ELISA)

Binding of antibodies to recombinant antigens was determined by ELISA. Antigens were coated with 0.3 µg/well in 100 µl PBS at 4 °C overnight. Residual binding sites were blocked using 3 % MPBS (2 % (w/v) dry milk in 1x PBS) at RT for 2 h. Before antibodies were added, plates were washed with 0.05 % PBST (0.05 % (v/v) TWEEN 20 in 1x PBS) twice and with 1x PBS once. Antibodies were added in serial dilutions in 2 % MPBS and incubated at RT for 1 h. After washing, bound proteins were detected by HRP-conjugated anti-His6-tag mouse antibody or by HRP-conjugated anti-human IgG (Fc specific) antibody. After an additional washing step, ELISA was developed using 100 µl/well of ELISA developing solution (0.1 mg/ml TMB, 100 mM sodium acetate buffer pH 6.0, 0.006 % H_2O_2). Reaction was stopped by adding 50 µl of 1 M H_2SO_4 and absorbance at 450 nm was measured in an ELISA reader.

3.5.2 Flow cytometric binding studies

Binding of antibodies to cell lines and organoids was analyzed by flow cytometry. Detached cells were diluted in growth medium to a concentration of $1x10^6$ cells/ml, or $1x10^5$ organoids/ml,

respectively. Next, 100 µl of diluted cell suspension per well was transferred in a 96-well U-bottom plate. After centrifugation (1500 rpm, 5 min, 4 °C), supernatant was discarded and antibodies were serial diluted in PBA, added to the cells and incubated for 1 h at 4 °C. After incubation cells/organoids were washed with PBA twice. Cells were then incubated with PE-conjugated anti-human IgG antibodies for 1 h at 4 °C. Finally, cells were washed twice, and resuspended in 100 µl PBA. Emitted fluorescence was detected using the Y1 channel (586/15 nm) in a MACSQuant® VYB, or equivalent laser in the MACSQuant Analyzer 10, respectively. Data analysis was performed using FlowJo (V10.6, Tree Star), Microsoft Excel and GraphPad Prism® 7. Calculation of relative MFI was performed with following formula:

$$relative\ MFI = \frac{MFIsample - (MFIdetection - MFIcells)}{MFIcells}$$

The half-maximal binding (EC_{50}) was calculated from the relative MFI using GraphPad Prism 7 according to Benedict et al. (Benedict et al. 1997).

3.5.3 Surface Receptor Expression Analysis

For quantitative surface receptor expression analysis, cells were trypsinized and singularized. $1x10^5$ cells per sample were incubated with primary antibodies against EGFR, HER2 or HER3. For quantification QIFIKIT® was used according to manufacturer's instructions (Agilent, K007811-8). Flow cytometry was performed using a MACSQuant Analyzer 10 (Miltenyi Biotec). For flow cytometry data evaluation FlowJo (V10.6; Tree Star), Microsoft Excel and GraphPad Prism® 7 was used. Relative mean fluorescence intensities (rel. MFI) were calculated as follows:

$$relative\ MFI = \frac{MFIsample - (MFIdetection - MFIcells)}{MFIcells}$$

3.5.4 Signaling inhibition assay: Immunoblotting

Receptor signaling was assessed by immunoblotting. Cells were seeded in 6- or 12-well plates, respectively, at a concentration of $2\text{-}3.5x10^5$ cells/well and incubated overnight. The next day, medium was exchanged to starvation medium (0.2 % FBS). After 24 h of starvation, fresh medium with antibodies at indicated concentrations, were added. After indicated time of incubation at 37°C cells were stimulated with 50 ng/ml of ligands (EGF or HRG, respectively) for indicated time. Lysis was performed using 120 µl RIPA buffer on ice. Lysates were centrifuged (13,200 rpm, 30 min, 4°C). Protein concentration was assessed using the Bio-Rad DC™ Protein Assay. All samples were set to concentration of lysate with lowest protein content using RIPA buffer for dilution. Next, SDS-PAGE fractionated lysates were transferred onto nitrocellulose membranes using the iBlot® 2 Dry Blotting System. After blocking with Roche

blocking solution for 30 min at RT membranes were incubated with primary antibodies (see 2.6) at 4°C overnight, or RT for 1 h, respectively. Next, membranes were washed 3 times with 0.5 % PBST for at least 5 min, before being incubated with HRP-conjugated secondary antibody for 1 h at RT. After incubation, membranes were washed 3 times for at least 5 min. Activity of HRP was detected with ECL substrate and visualized by the FUSION SOLO Imager.

3.5.5 Proliferation assay

Viability analysis of cell lines was performed using CellTiter-Glo (2D assay: Promega, G9242; 3D assay: Promega, G9683). For 3D assay white 96-well plates were precoated with Matrigel:Collagen mixture (1:2, Corning, 354230; Advanced BioMatrix, 5015-20ML). Next, cells ($2x10^3$ cells/well) were seeded into 96-well plates, for 3D assay cells were additionally overlaid with Matrigel (2 %). After 24 h medium was exchanged for starvation medium (0.2 % FBS). Another 24 h later, cells were pretreated with indicated antibodies (50 nM) for 60 min, prior to ligand stimulation with 30 ng/ml recombinant human heregulin β-1 (HRG) (Peprotech, 100-03). After 5 days (2D), or 4 days (3D) medium was gently aspirated and 50 µl of pre-warmed detection reagent (1:2, RPMI-1640:CellTiter-Glo) was added. Cell lysates were incubated for 12 min at RT and luminescence was measured using the Spark® microplate reader (Tecan).

PDO cells (1 - $4x10^3$ cells/well) were seeded as described above for 3D assay. 24 h later PDOs were treated with indicated antibodies (50 nM) or Afatinib (500 nM). After 3 days, medium was aspirated and viability was analyzed using CellTiter-Glo 3D.

3.5.6 Sphere Formation Assays

Singularized cells were seeded onto Poly(2-hydroxyethyl methacrylate)-(pHEMA)-treated (Merck, P3932) 12-well plates ($3x10^3$ cells per well) in sphere formation medium (DMEM/F12 GlutaMAX (Thermo Fisher Scientific, 31331028); 20 ng/ml HRG (Peprotech, 100-03), 1x B27 (Thermo Fisher Scientific, 17504044)) and immediately treated with antibodies. After 5 days, spheres were imaged, counted and the sphere area was analyzed using ImageJ. For extreme limiting dilution assays (ELDA), $1x10^5$ cells per 10 cm plate were seeded and grown as primary oncospheres as described above. After 5 days, primary oncospheres were harvested, singularized, and 1, 10 or 100 cells/well were seeded onto pHEMA-treated 96-well plates, respectively. Cells were cultured for 9, or 10 days, respectively, in 300 µl sphere formation medium (20 technical replicates per condition). Only wells positive for spheres were counted and the relative estimated stem cell frequency was determined by ELDA software (http://bioinf.wehi.edu.au/software/elda/index.html), provided by the Walter and Eliza Hall Institute (Hu and Smyth 2009).

3.5.7 Animal experiments

All animal studies were approved by state authorities and performed in accordance to federal guidelines (reference number 35-9185.81/0456 & 35-9185.81/0456).

3.5.7.1 Pharmacokinetics of scDb hu225x2-43-Fc

Proteins (25 mg of IgG 3-43, or scDb hu225x3-43-Fc, respectively diluted in 100 mL PBS) were injected into the tail vein of CD-1 mice (Charles River, three animals per molecule). After 3 minutes, 1, 6, 24, 72 and 169 h blood samples were taken and immediately incubated on ice. Serum samples were centrifuged (16,000x g, 4°C, 20 min) and stored at -20°C until analysis. Antibody serum concentrations were determined by ELISA using EGFR-His and HER3-His as antigen, and HRP-conjugated anti-human Fc antibody for detection. Initial and terminal half-lives (t1/2α, t1/2β) and AUC were calculated using Excel. Initial half-lives were calculated over the time interval of 3 min to 24 h. Terminal half-lives were calculated with the last three serum concentrations (1h-72h or 24h -169h).

3.5.7.2 Pharmacodynamics of scDb hu225x3-43-Fc

Eight-week-old female SCID beige mice (Charles River, CB17.Cg-PrkdcscidLystbg-J/Crl) were anesthetized with isoflurane during the injection of cancer cells. $5x10^6$ FaDu cells (100 µL PBS) were subcutaneously injected in the left and right flanks, whereas $5x10^6$ MDA-MB-468 cells (100 µL PBS) were orthotopically injected into the right and left 4th mammary fat pads. Tumor growth was monitored with a caliper and tumor volume was calculated as follows:

$$tumor\ volume = \frac{(a \times b^2)}{2}$$

$$\mathrm{a, longitudinal\ diameter\ of\ tumor;\ b, transverse\ diameter\ of\ tumor}$$

Mice were randomly assigned to control and four treatment groups after the tumors had reached ~100 mm^3 (n=7 mice per group). Mice received six intravenous antibody injections (FaDu xenograft model: 300 µg antibody per injection in 100 µL PBS; MDA-MB-468: 300 µg antibody in 100 µL PBS for the first injection, the dose was then adjusted to 200 µg (IgG hu225) and 240 µg (IgG 3-43 or scDb-Fc), respectively) twice weekly for three consecutive weeks. Tumors of MDA-MB-468 xenograft mice were further dissociated for oncosphere formation assays and ALDEFLUOR analysis. Tumor dissociation was performed according to manufacturer's instructions (Miltenyi Biotec, 130-096-730).

3.6 Statistical analysis

All values are presented as mean ± SD. Significance between multiple groups was determined by one-way ANOVA and Tukey’s test for multiple comparison. Significance between two

groups was determined by t-test. Total group effects were analyzed by two-way ANOVA and results at a specific time point were compared via one-way ANOVA followed by Tukey's multiple comparison test (post-test). Data was analyzed, using GraphPad Prism 7. P-values: P ≤ 0.05 (*), P ≤ 0.01 (**), P ≤ 0.001 (***), P ≤ 0.0001 (****), n.s. (not significant).

4 Results

Parts of the studies in chapter 4.1, 4.2 and 4.3 were published in 2020 in Molecular Cancer Therapeutics (Rau et al. 2020) and parts of the studies in 4.4 were published in 2022 in Molecular Cancer Therapeutics (Rau et al. 2022).

4.1 Bispecific, bi- or tetravalent EGFR- and HER3-targeting molecules

Previous studies have described that the expression of heregulin/neuregulin 1 (HRG) or its receptor HER3 are the cause of primary or acquired resistance occurring upon EGFR-targeted treatments, for example with Cetuximab (Oliveras-Ferraros et al. 2012; Leto and Trusolino 2014; Leto et al. 2015; Stahler et al. 2017; Kruser and Wheeler 2010; Zhang et al. 2020). It is therefore plausible that the combination of an EGFR antagonist with a HER3-targeting antibody, like IgG 3-43, a HER3 targeting antibody developed in-house, might overcome these resistance mechanisms. Compared to the treatment with Cetuximab, or IgG 3-43 alone, the combination and the use of a newly developed EGFR- and HER3-targeting bispecific scDb-Fc antibody demonstrated superior inhibition of EGF- and HRG-induced downstream signaling, and proliferation of FaDu cells (Honer 2016). Based on these observations, in this thesis, the bispecific EGFR- and HER3-targeting scDb and scDb-Fc molecules were developed with the aim to improve purity, integrity, and yield.

4.1.1 Structure and biochemical analysis of EGFR- and HER3-targeting single chain Diabody (scDb) and scDb-Fc antibodies

The assembly of the scDb antigen-binding sites can be affected by the length of the connecting linkers within the scDb moieties, hence, new variants of EGFR- and HER3-targeting scDb and scDb-Fc molecules were generated using the variable domains of the EGFR binding humanized Cetuximab (IgG hu225) and the fully human HER3-binding antibody IgG 3-43 (Figure 3A) (Völkel et al. 2001; Schmitt et al. 2017). The scDb moiety was arranged in the VH-VL orientation with three linkers connecting the variable domains (VH(3-43)-linker1-VL(hu225)-linker2-VH(hu225)-linker3-VL(3-43)) (Figure 3B). Two derivates of the scDb were generated with different lengths of linker 2 (Figure 3C). ScDb-1 comprises a linker 2 with 15 amino acids and scDb-2 a linker 2 with 20 amino acids, respectively. Furthermore, the scDb molecules were fused to the hinge region of a Fcγ1 chain using a five amino acid long linker 4 (GGSGG). The Fc region allows the scDb-Fc to form a homodimer, leading to the formation of a bispecific and tetravalent antibody. Both antibody formats, scDb and scDb-Fc, were produced in transiently transfected HEK293-6E suspension cells. The scDb molecules, comprising a hexahistidine-

tag (H6), were purified by IMAC, and scDb-Fc molecules by Protein A chromatography, respectively.

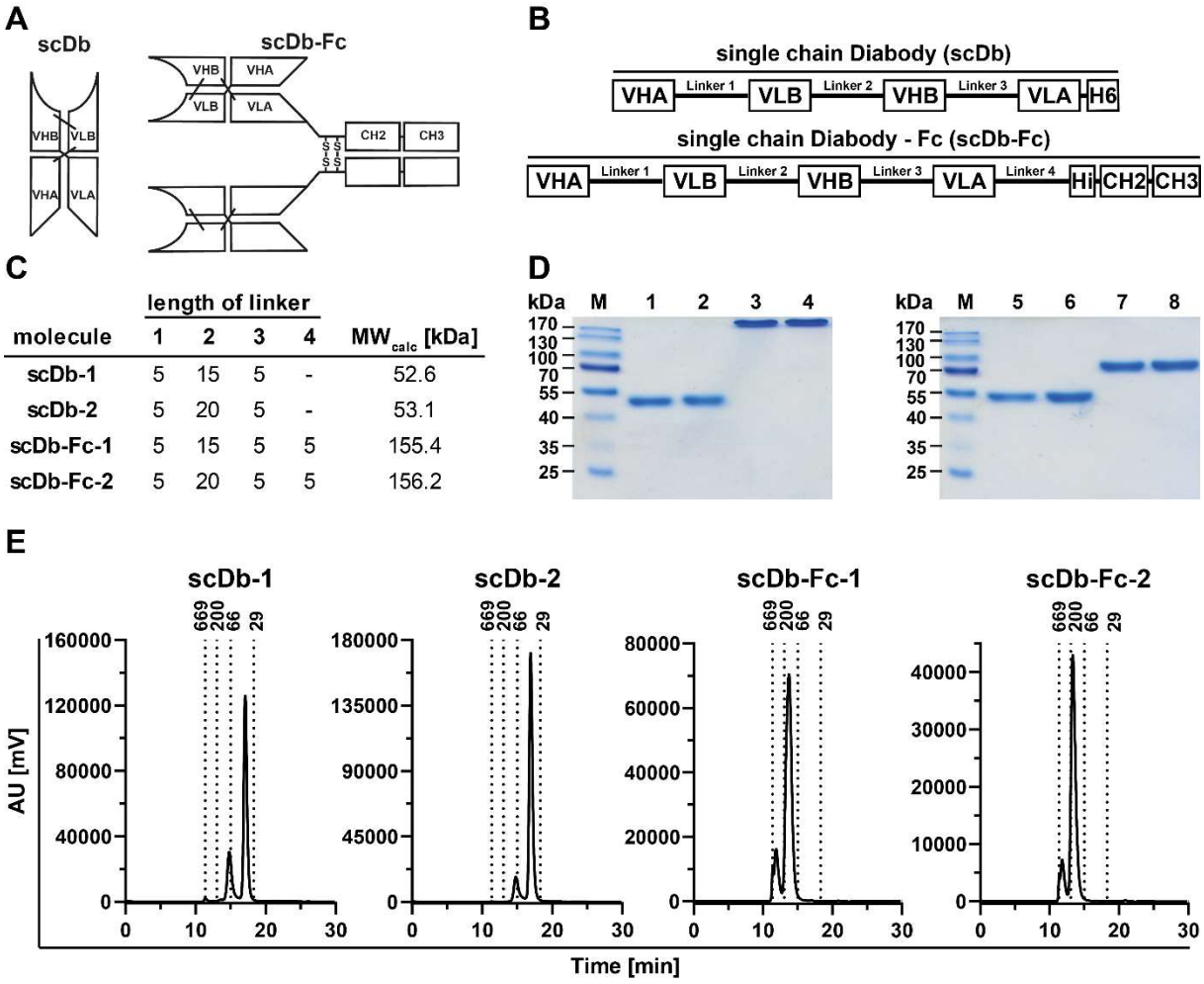

Figure 3: Biochemical characterization of protein integrity and purity of scDb and scDb-Fc molecules targeting EGFR and HER3. A Schematic illustration of the scDb-Fc format and its building blocks. (moiety A: hu225; moiety B: 3-43) **B** Schematic illustration of scDb and scDb-Fc domains and linkers. (moiety A: hu225; moiety B: 3-43; H6: Hexahistidine-Tag; Hi: Hinge) **C** Length of linkers and MW_{calc} (calculated MW, based on amino acid sequence) of scDb and scDb-Fc variants. **D** SDS-PAGE analysis of 3 µg of scDb-1 (1, 4), scDb-2 (2, 5), scDb Fc-1 (3, 6) and scDb-Fc-2 under non-reducing (1-4) and reducing (5-8) conditions (12 % PAA). Proteins were stained with Coomassie brilliant blue. **E** Size-exclusion chromatography (SEC) under native conditions of scDb and scDb-Fc antibodies with varying linker length. Elution times and molecular mass [kDa] of standard proteins are indicated by dotted lines.

Purity of the scDb and scDb-Fc molecules was confirmed by SDS-PAGE analysis under non-reducing and reducing conditions (Figure 3D). Apparent molecular masses under non-reducing conditions were 52.4 kDa (scDb-1), 53.0 kDa (scDb-2), 193.0 kDa (scDb-Fc-1) and 204.0 kDa (scDb-Fc-2), respectively. Under reducing conditions observed apparent molecular masses were 57.0 kDa (scDb-1 and 2), and 85.0 kDa (scDb-Fc-1 and 2), respectively. In HPLC-SEC analysis of the scDb molecules, a major peak with 41.0 kDa (scDb-1), and 43.2 kDa (scDb-2) was observed, respectively (Figure 3D). For both scDb molecules a small fraction with

an apparent mass of 81.0 kDa was observed, indicating formation of non-covalently linked dimers (Völkel et al. 2001). In SEC analysis of the scDb-Fc molecules a major peak was observed, with an apparent mass of 152.0 kDa and Stoke's radius (R_S) of 4.7 nm (scDb-Fc-1), 178.0 kDa and R_S of 5.2 nm (scDb-Fc-2), respectively (Figure 3E, Figure 4B). Furthermore, a small fraction was observed at an apparent mass of 349.1 kDa and R_S of 6.64 nm (scDb-Fc-1), and 384.9 kDa and R_S of 6.8 nm (scDb-Fc-2), respectively (Figure 3E, Figure 4B), here too, indicating non-covalently linked dimers.

For further analysis of the effects of the linker length on the integrity and yield of scDb-Fc antibodies, four additional molecules (scDb-Fc-3 - 6) were generated (total of six scDb-Fc molecules) (Figure 4). For comparison, the SEC profile and yields of the scDb-Fc molecules were analyzed. Compared to scDb-Fc-1, in scDb-Fc-3 and -5 the linker between the scDb and the hinge region of the Fcγ1 chain (linker 4) was either removed (scDb-Fc-3), or 5 amino acids (GGSGG) were added (scDb-Fc-5). While SEC revealed comparable homogeneity of scDb-Fc-1, -3 and -5, respectively, changes of linker 4 resulted in reduced yields. In particular, the addition of 5 amino acids in linker 4 of scDb-Fc-5 resulted in dramatically reduced yields (scDb-Fc-5: 0.7 mg/L vs. scDb-Fc-3: 31.1 mg/L vs. scDb-Fc-1: 40.6 mg/L) (Figure 4A, B). No major differences in SEC or yield were observed for scDb-Fc-6 with two additional amino acids (GG) in linker 1 and 3 compared to scDb-Fc-2 (scDb-Fc-6: 45.5 mg/L vs. scDb-Fc-2: 46.8 mg/L). Compared to scDb-Fc-1, in scDb-Fc-4 the orientation of the binding moieties was changed from VHhu225-linker1-VL3-43-linker2-VH3-43-linker3-VLhu225 to VH3-43-linker1-VLhu225-linker2-VHhu255-linker3-VL3-43. This exchange dramatically reduced the yield (scDb-Fc-4: 3.6 mg/L vs. scDb-Fc-1: 40.6 mg/L), without changes in the SEC profile. Taken together, the modifications of the linkers had no beneficial effect, neither on purity and integrity, nor on homogeneity, compared to scDb-Fc-1 (Figure 3D, E; Figure 4A). Major differences were observed in the yields, ranging from 0.7 mg to 46.8 mg/L of HEK293-6E supernatant. As a result, all further studies were performed with the scDb-Fc-1, named scDb hu225x3-43-Fc.

A

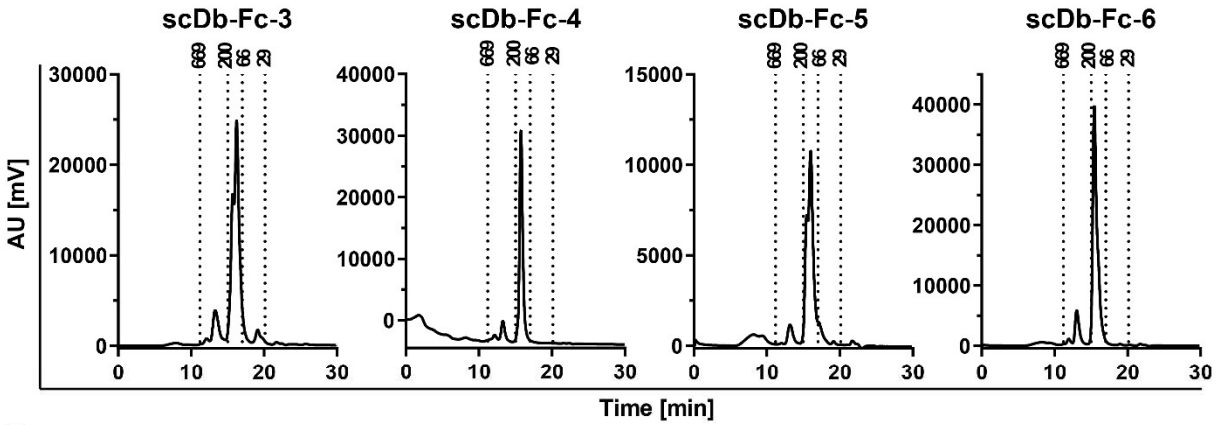

B

	length of linker						HPLC-SEC	
scDb-Fc molecule	1	2	3	4	MW_{calc} [kDa]	Yield [mg/L]	MW [kDa]	R_S [nm]
scDb-Fc-1	5	15	5	5	155.4	40.6	137.0	4.5
scDb-Fc-2	5	20	5	5	156.2	46.8	169.7	4.9
scDb-Fc-3	5	15	5	-	155.0	31.1	133.6	4.4
scDb-Fc-4	5	15	5	5	155.4	3.6	154.9	4.7
scDb-Fc-5	5	15	5	10	156.2	0.7	143.5	4.6
scDb-Fc-6	7	20	7	5	156.6	45.5	170.7	4.9

Figure 4: Protein integrity and purity analysis by SEC-HPLC of variants of scDb hu225x3-43-Fc with different linker lengths. A Size-exclusion chromatography under native conditions of six scDb-Fc molecules, varying in the length of linker 1, 2, 3, or 4, respectively. Elution times and molecular mass [kDa] of standard proteins are indicated by dotted lines. **B** Length of linkers, MW_{calc} (calculated MW, based on amino acid sequence), yield (amount of protein per liter of HEK293-6E supernatant), apparent MW and R_s determined by SEC-HPLC of six scDb-Fc variants, respectively.

4.1.2 Binding of recombinant receptor and affinity measurement of scDb hu225x3-43-Fc

For further analysis scDb hu225x3-43-Fc was purified by an additional preparative SEC-FPLC step, removing the small fraction observed in analytical SEC-HPLC (Figure 5B). For comparison, the parental antibodies IgG hu225 and IgG 3-43 were produced in transiently transfected HEK293-6E suspension cells. Purity and integrity of the scDb-Fc and the parental antibodies were demonstrated by SDS-PAGE analysis, where only one band under non-reducing conditions was observed. Under reducing conditions, the parental antibodies revealed two bands, indicating heavy and light chains and one band was observed for the scDb-Fc (Figure 5A). SEC-HPLC revealed an apparent molecular mass of 163.0 kDa and an R_S of 4.8 nm for IgG hu225, and 149.0 kDa and 5.2 nm for IgG 3-43, respectively (Figure 4B, Figure 5B). Furthermore, binding of scDb-Fc to recombinant receptors (immobilized EGFR or HER3) was analyzed by ELISA and dual binding by sandwich ELISA (immobilized EGFR and

soluble HER3) (Figure 5C). EC_{50} values of scDb-Fc were similar to the parental antibodies, and simultaneous binding to EGFR and HER3 was shown (EGFR: 213 pM vs. 204 pM for IgG hu225; HER3: 221 pM vs. 166 pM for IgG 3-43; EGFR and HER3: 310 pM). Furthermore, affinity measurement by quartz crystal microbalance (QCM) revealed K_D values of 21 nM for EGFR and 19 nM for HER3 for scDb-Fc, and a K_D of 8 nM for IgG hu225 for EGFR (Figure 5D, E). In a previously published study, a K_D of 11 nM for HER3 of IgG 3-43 was observed (Schmitt et al. 2017). In conclusion, the scDb-Fc was produced with high purity, integrity, and homogeneity, with a high protein yield. Furthermore, binding to recombinant receptors in ELISA, as well as affinities determined by QCM were similar to the parental antibodies IgG hu225 and IgG 3-43.

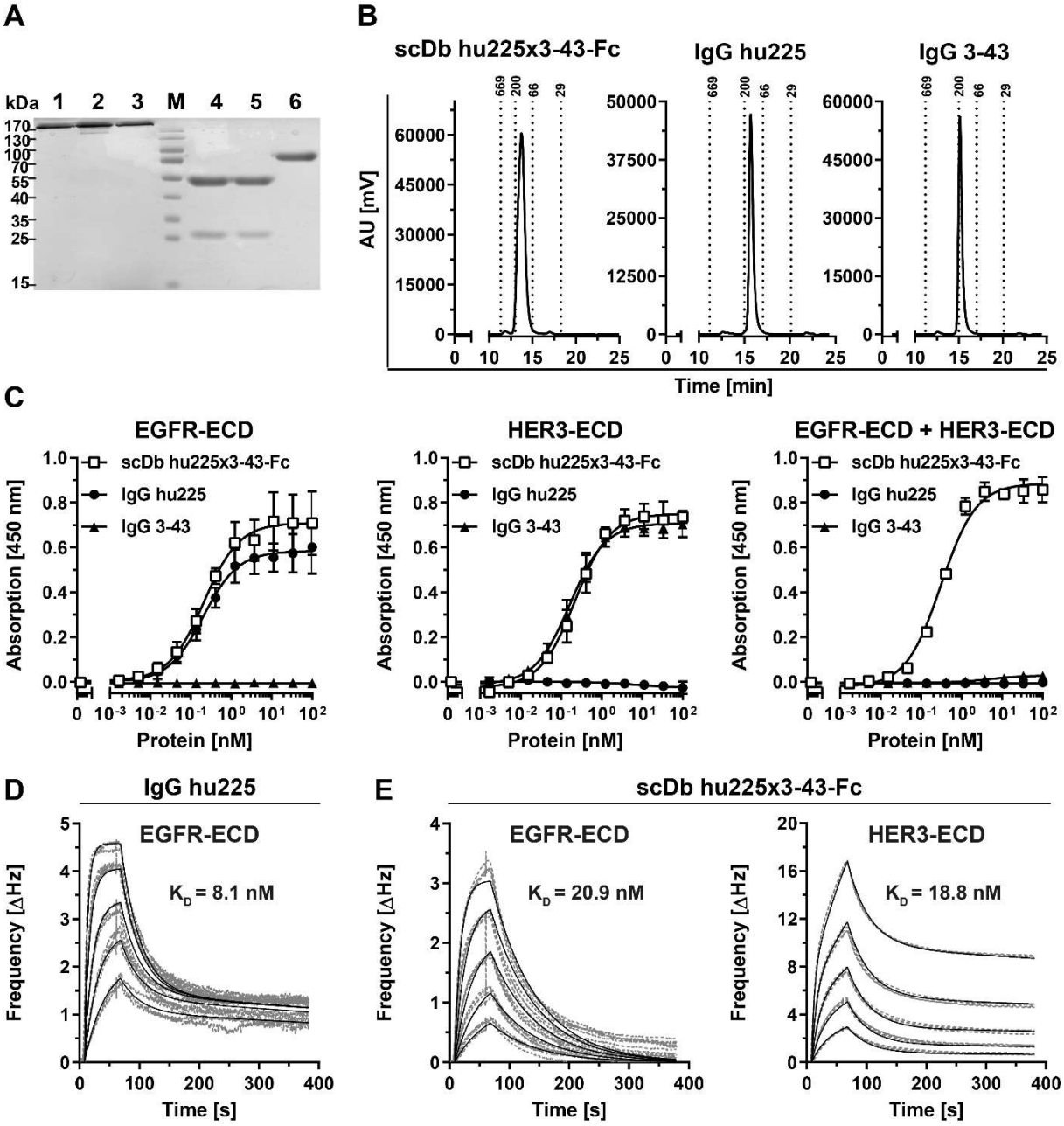

Figure 5: Binding analysis by ELISA, and affinity measurement by QCM of scDb hu225x3-43-Fc. **A** SDS-PAGE analysis of parental antibodies IgG hu225 (1, 4) and IgG-3-43 (2, 5) and scDb hu225x3-43-Fc (3, 6) under non-reducing (1-3) and reducing conditions (4-6). For non-reducing 3 µg of protein were loaded and for reducing conditions 6 µg. Proteins were stained with Coomassie brilliant blue. **B** Size-exclusion chromatography (SEC) under native conditions of IgG hu225, IgG 3-43 and scDb hu225x3-43-Fc. Elution times and molecular mass [kDa] of standard proteins are indicated by dotted lines. **C** Binding analysis by ELISA of IgG hu225, IgG 3-43 and scDb hu225x3-43-Fc to recombinant EGFR, HER3, or simultaneous binding to both receptors. (n=3, mean ± SD) **D, E** Affinity measurement of IgG hu225 (**D**) and scDb hu225x3-43-Fc (**E**) by QCM. QCM chip was coated with either EGFR(D3)-His (**D**), EGFR-His, or HER3-His (**E**), using concentrations between 16 nM and 1 nM of IgG hu225, and between 128 nM and 8 nM for scDb hu225x3-43-Fc. Measurements (grey, dotted line) and fit (black, solid) are shown.

4.2 Activity of scDb hu225x3-43-Fc on receptor signaling, proliferation, migration and tumor growth

Combining the binding properties of the parental antibodies, IgG hu225 and IgG 3-43, scDb hu225x3-43-Fc might elicit synergistic effects regarding the inhibition of receptor signaling and associated cellular responses such as proliferation and migration. In the following experiments, binding to seven cancer cell lines, which express receptors of the HER-family, was investigated. Furthermore, inhibitory effects on receptor phosphorylation and downstream signaling upon stimulation with EGF and/or HRG were determined. In *in vitro* studies of the HNSCC cancer cell line FaDu, effects of the scDb-Fc on proliferation, long-term downstream signaling and migration were compared to the parental antibodies or their combination. Additionally, the tumor growth inhibition by the scDb-Fc in a HNSCC xenograft tumor model was investigated.

4.2.1 Binding to EGFR- and HER3-expressing cancer cell lines and downstream signaling inhibition

Binding of scDb hu225x3-43-Fc to EGFR- and HER3-expressing cancer cell lines (3 breast cancer, 1 HNSCC, and 3 CRC cell lines) was analyzed by flow cytometry (Figure 6). As a control, binding of the parental antibodies IgG hu225 and IgG 3-43 was determined. Strong binding of scDb-Fc was observed, with EC_{50} values ranging from 98 to 594 pM (Figure 6B). Binding to cells expressing high levels of EGFR (FaDu, MDA-MB-468 and DiFi) was similar to the binding of the parental IgG hu225, and binding to cells expressing high levels of HER3 (MCF7, SK-BR-3 and LIM1215) was similar to that of IgG 3-43. Additionally, binding of the HER2-targeting antibody Trastuzumab, used in experiments described in 4.4, to LIM1215 and DiFi cells was shown. In summary, strong binding to EGFR- and HER3-expressing cancer cell lines with similar maximum binding and EC_{50} values to the parental antibodies was demonstrated.

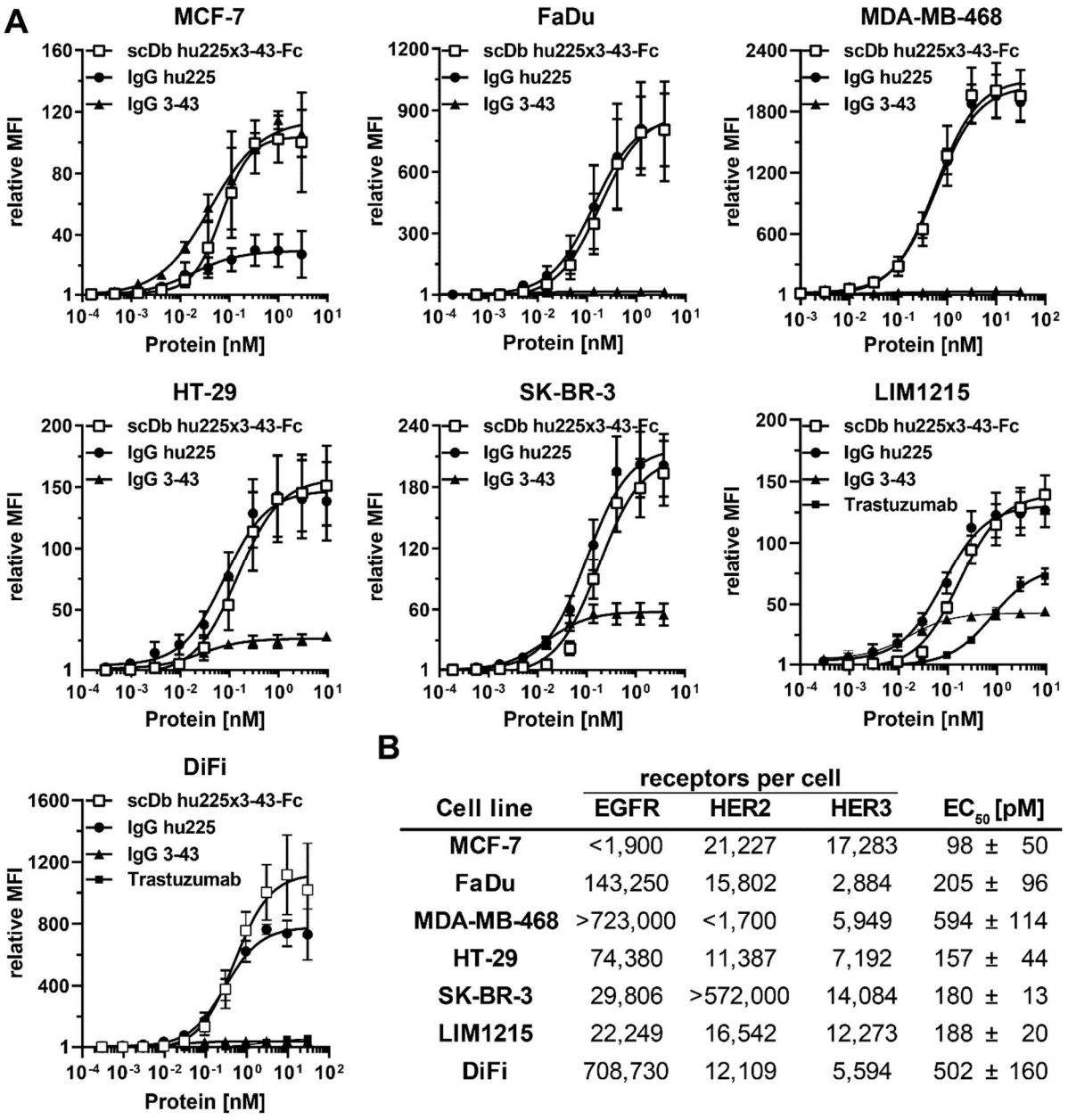

B

Cell line	receptors per cell EGFR	HER2	HER3	EC_{50} [pM]
MCF-7	<1,900	21,227	17,283	98 ± 50
FaDu	143,250	15,802	2,884	205 ± 96
MDA-MB-468	>723,000	<1,700	5,949	594 ± 114
HT-29	74,380	11,387	7,192	157 ± 44
SK-BR-3	29,806	>572,000	14,084	180 ± 13
LIM1215	22,249	16,542	12,273	188 ± 20
DiFi	708,730	12,109	5,594	502 ± 160

Figure 6: Flow cytometry binding analysis of scDb hu225x3-43-Fc for seven cancer cell lines and quantified surface receptor expression levels. A Flow cytometry analysis of binding of scDb hu225x3-43-Fc to seven cancer cell lines (breast: MCF-7, SK-BR-3; HNSCC: FaDu; TNBC: MDA-MB-468, CRC: HT-29, LIM1215, DiFi). Parental antibodies IgG hu225 and IgG 3-43, were included as controls. Additionally, binding of Trastuzumab was analyzed on LIM1215 and DiFi cells. (n=3, mean ± SD, except SK-BR-3: n=2, mean ± SD). **B** Number of surface expressed receptors per cell of EGFR, HER2 and HER3, respectively, and EC_{50} values of scDb hu225x3-43-Fc on above-described cancer cell lines.

The high level of HER3 expressing MCF-7 cells were used to analyze the effects of scDb hu225x3-43-Fc on EGFR and HER3 receptor phosphorylation as well as downstream signaling by western blot analysis (Figure 7). MCF-7 cells were starved overnight, prior to treatment with 50 nM of antibodies for 1 hour (IgG hu225, IgG 3-43, combination of IgG hu225 and IgG 3-43, or scDb hu225x3-43-Fc). MCF-7 cells were then stimulated with 50 ng/ml of

either EGF, HRG or both ligands, respectively. The phosphorylation state of EGFR, HER3, Akt and Erk, as well as total protein levels were detected. Under unstimulated conditions, no phosphorylation of HER3 (Y1289), or pAkt (T308) was detected. Phosphorylation of EGFR (Y1068) and Erk (T202/Y204) was only detectable after long exposure (LE). Total levels of HER3 were decreased upon treatment with IgG 3-43, the combination of IgG hu225 and IgG 3-43, or scDb hu225x3-43-Fc, respectively. This indicates fast internalization and partial degradation of HER3 within one hour. Stimulation with EGF effected phosphorylation of EGFR (Y1068), Akt(T308), Erk (T202/Y204), but not of HER3 (Y1289). Of note, although phosphorylation of EGFR (Y1068) was inhibited by IgG hu225 and the combination of IgG hu225 and IgG 3-43, downstream phosphorylation of Akt (T308) and Erk (T202/Y204) were increased, compared to the untreated control. Treatment with scDb hu225x3-43-Fc showed strongest inhibition of EGFR (Y1068) phosphorylation and did not activate downstream signaling via Akt (T308) and Erk (T202/Y204). Upon stimulation with HRG, strong phosphorylation of EGFR (Y1068), HER3 (Y1289), Akt (T308) and Erk (T202/Y204) was observed, which was inhibited by IgG 3-43, the combination of IgG hu225 and IgG 3-43, and scDb-Fc, but not IgG hu225. Interestingly, HRG induced stronger EGFR (Y1068) phosphorylation compared to EGF. Additionally, HRG stimulation induced internalization and degradation of HER3, which was not further enhanced by any of the antibody treatments. Stimulation with the combination of EGF and HRG was similar to HRG only. Here, the combination of IgG hu225 and IgG 3-43, and the scDb-Fc inhibited phosphorylation of EGFR (Y1068) and HER3 (Y1289). Long-exposure revealed stronger inhibition of HER3 (Y1289) phosphorylation by scDb hu225x3-43-Fc. However, neither for the combination of the parental antibodies, nor for the scDb-Fc treated cells inhibition of downstream signaling was observed. In summary, maximum binding and EC_{50} values on seven cancer cell lines was similar for scDb hu225x3-43-Fc and the parental antibodies IgG hu225 and IgG 3-43. Furthermore, upon binding to MCF-7 cells, scDb hu225x3-43-Fc showed comparable inhibition of receptor phosphorylation and downstream signaling as the combination of IgG hu225 and IgG 3-43 did, and scDb-Fc was even superior in inhibiting the phosphorylation of HER3 (Y1289) and Akt (T308) under ligand-stimulated conditions.

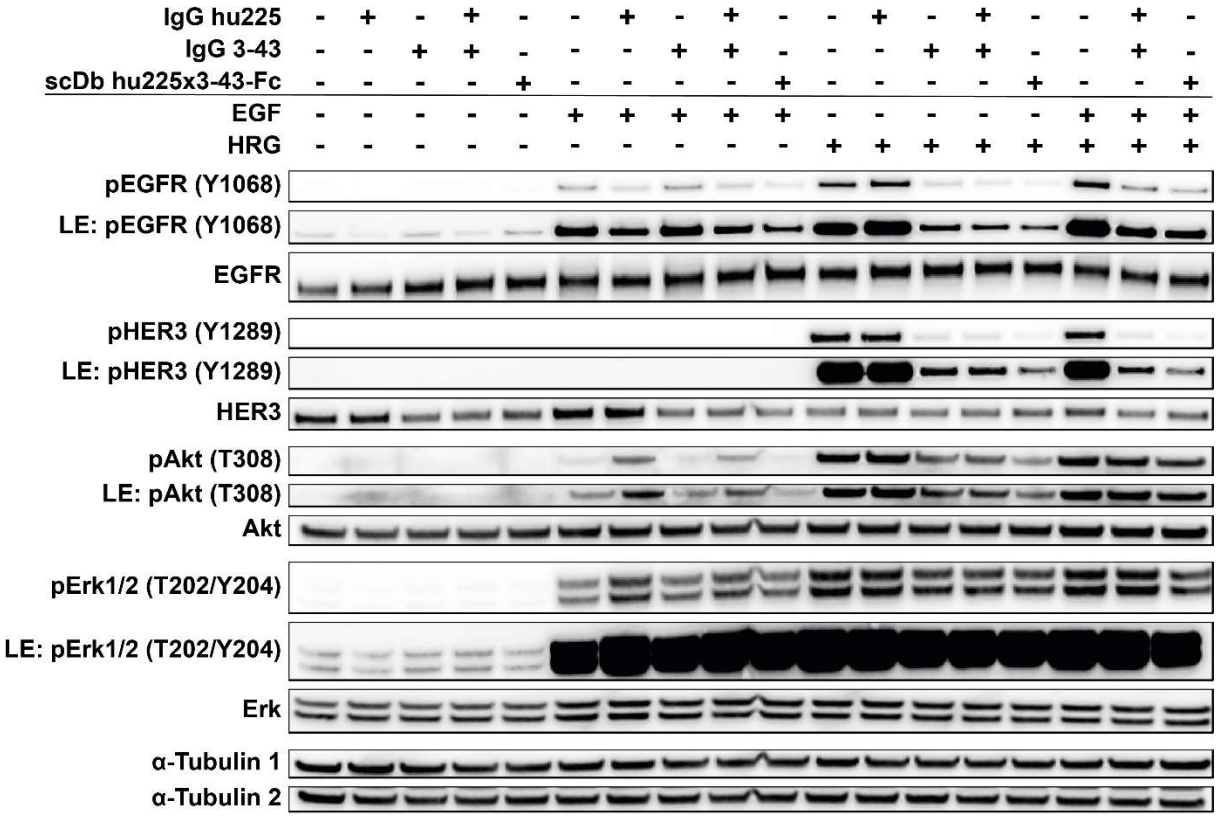

Figure 7: Downstream signaling analysis in MCF-7 cells by western blot. Inhibition of receptor phosphorylation and downstream signaling in MCF-7 cells by scDb hu225x3-43-Fc. Cells were serum-starved overnight before incubation with 50 nM antibodies (IgG hu225, IgG 3-43, combination of IgG hu225 and IgG 3-43, or scDb hu225x3-43-Fc). After 1 h cells were stimulated for 15 min either with 50 ng/ml of EGF, HRG, or both ligands, respectively. Subsequently, cell lysates were analyzed by western blot. Representative western blot of two independent experiments is shown. LE: long-exposure.

4.2.2 Inhibition of proliferation and migration of a HNSCC cell line by scDb hu225x3-43-Fc

To analyze whether downstream signaling inhibition translates into inhibition of proliferation and migration the HNSCC cell line FaDu was used. FaDu cells have an autocrine HRG-loop, which translates into basal activation of the MAPK- and PI3K-pathways driving cell proliferation (Wilson et al. 2011). This basal activity allows to analyze inhibitory effects of the scDb-Fc on receptor activation, downstream signaling, proliferation and migration under basal conditions and after addition of exogenous HRG. In a 2D proliferation assay with FaDu cells in low serum (0.2 % FCS) the addition of exogenous HRG stimulated proliferation (w/o stimulus: 100 % vs. + HRG: 109 %) (Figure 8A). Without HRG-stimulation, the treatment with 50 nM of the parental antibodies (IgG hu225 or IgG 3-43) inhibited proliferation, whereas the combination of the latter and the scDb-Fc showed strongest inhibition (w/o antibody: 100 % vs. IgG hu225: 68.3 % vs. IgG 3-43: 82.0 % vs. IgG hu225 + IgG 3-43: 50.9 % vs. scDb hu225x3-43-Fc: 47.6 %). Under

HRG conditions no benefit of the dual EGFR and HER3 blockade was observed (w/o antibody: 109 % vs. IgG hu225: 95.9 % vs. IgG 3-43: 82.3 % vs. IgG hu225 + IgG 3-43: 84.2 % vs. scDb hu225x3-43-Fc: 85.6 %). Titration of the combination of the parental antibodies and the scDb-Fc revealed superior activity of the scDb-Fc at lower concentrations under unstimulated (IC_{50}: 10 pM vs 71 pM) and HRG-stimulated conditions (IC_{50}: 48 pM vs 462 pM) (Figure 8B).

To further analyze the underlying effects, western blot analysis was performed (Figure 8C). The FaDu cells were grown under the same conditions as described for the proliferation assays (0.2 % FCS, ± HRG). In the absence of HRG, phosphorylation of HER3 (Y1289) and Akt (T308/S473) was inhibited by IgG 3-43, the combination of IgG hu225 and IgG 3-43, and the scDb-Fc. Phosphorylation of Erk (T202/Y204) was inhibited by IgG hu225, the combination of IgG hu225 and IgG 3-43, or the scDb-Fc, but not by IgG 3-43. Of note, phosphorylation of EGFR (Y1068) was increased upon treatment with the scDb-Fc, however this did not translate into activation of the MAPK or PI3K pathways. HER3 signals were reduced upon treatment with IgG 3-43, the combination of IgG hu225 and IgG 3-43 or the scDb-Fc, indicating internalization and degradation of the receptor. In the presence of HRG, phosphorylation of EGFR (Y1068), HER2 (Y1221/1222), HER3 (Y1289), Akt (T308/S473) and Erk (T202/Y204) was observed. Furthermore, total HER3 and HER2 signals were reduced under HRG conditions. Of note, the dual inhibition of EGFR and HER3 mitigated the degradation of HER2. While IgG hu225 and the combination of the parental antibodies efficiently blocked the phosphorylation of EGFR (Y1068), the scDb-Fc did not. However, again this did not activate downstream signaling. Instead, Akt (T308/S473) and Erk (T202/Y204) phosphorylation were inhibited most potently by scDb-Fc, compared to other treatments.

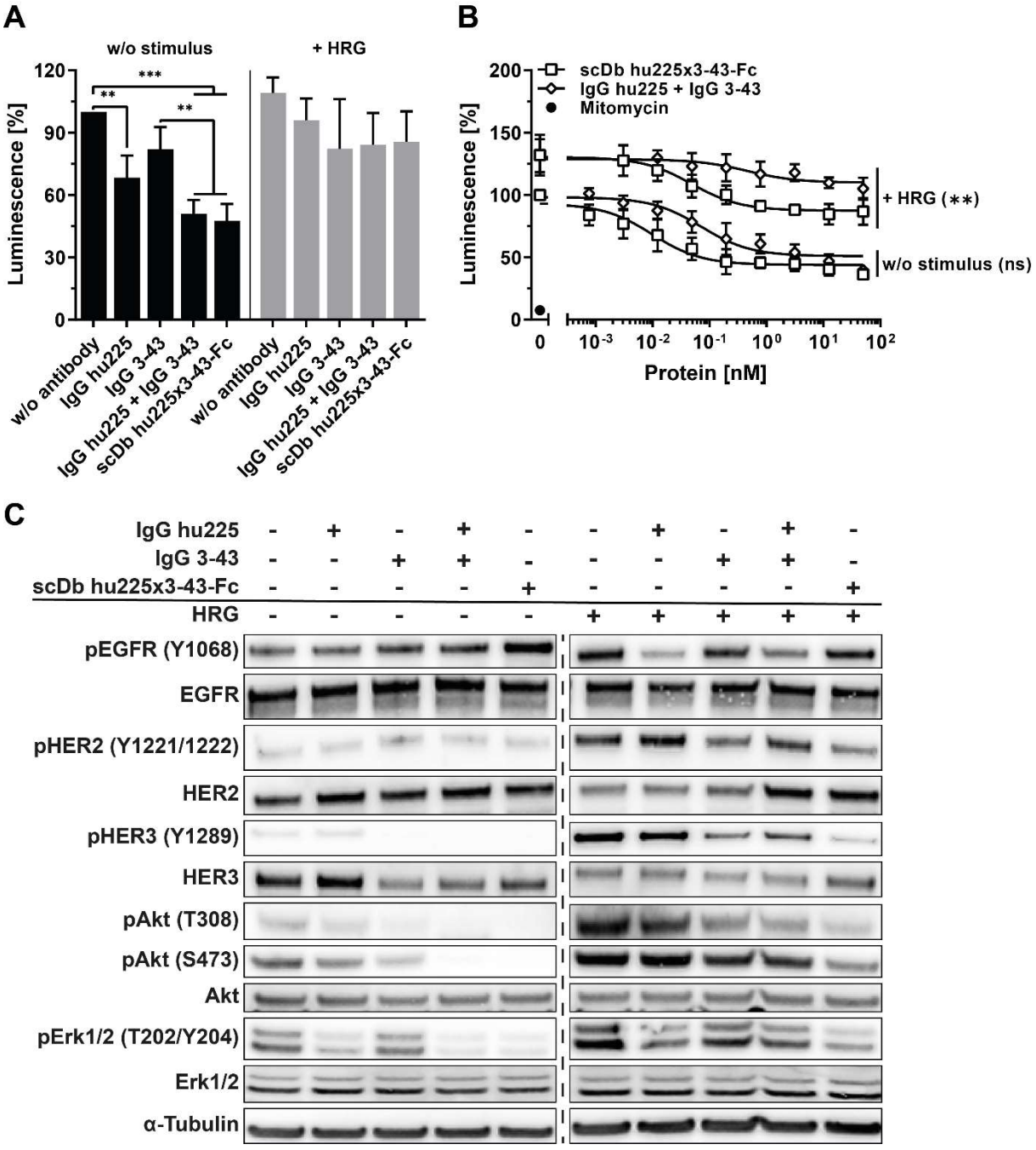

Figure 8: Proliferation of FaDu cells upon HRG stimulation and treatment with scDb hu225x3-43-Fc. **A** Analysis of 2D proliferation of FaDu cells after one week of incubation in low serum (0.2 % FCS). Cells were treated with 50 nM antibodies (IgG hu225, IgG 3-43, combination of IgG hu225 and IgG 3-43, or scDb hu225x3-43-Fc). After 1 h, indicated wells were stimulated with 30 ng/ml of HRG. On day 5 after treatment viability was analyzed using the CellTiterGlo 2.0 Kit (n=3, mean ± SD). Data was analyzed by one-way ANOVA and Tukey's test for multiple comparison. P ≤ 0.05 (*), P ≤ 0.01 (**), P ≤ 0.001 (***), P ≤ 0.0001 (****), n.s. (not significant). **B** Proliferation assay was performed according to **A**, but cells were treated with indicated concentrations of the combination of IgG hu225 and IgG 3-43, or scDb hu225x3-43-Fc (n=3, mean ± SD). Data was analyzed by unpaired t-Test. P ≤ 0.05 (*), P ≤ 0.01 (**), P ≤ 0.001 (***), P ≤ 0.0001 (****), n.s. (not significant). **C** Inhibition of receptor phosphorylation and downstream signaling analysis by western blot for FaDu cells grown and treated under the same conditions as described in **A**. Lysates were loaded and blotted together, dashed line indicates marker lane.

Migration is a prerequisite for invasion and therefore for metastasis (Kramer et al. 2013). To analyze the ability of the scDb-Fc to inhibit migration of FaDu cells a scratch-wound assay was performed (Figure 9). Despite the autocrine HRG-loop, the addition of exogenous HRG increased the motility (relative wound density at 24 h: w/o stimulus: 34.3 ± 3.5 % vs. + HRG: 47.3 ± 1.5 %). No significant inhibition of migration was achieved by single blockade of EGFR or HER3 by the parental antibodies, IgG hu225 or IgG 3-43 (relative wound density at 24 h without stimulus: IgG hu225: 29.8 ± 6.6 %, IgG 3-43: 27.8 ± 1.7 %; + HRG: IgG hu225: 41.1 ± 3.8 %, IgG 3-43: 45.3 ± 2.1 %). Of note, dual blockade of EGFR and HER3 with either the combination of IgG hu225 and IgG 3-43, or scDb-Fc significantly blocked cell migration in the absence or presence of HRG (relative wound density at 24 h without stimulus: IgG hu225 + IgG 3-43: 16.3 ± 4.6 %, scDb hu225x3-43-Fc: 15.5 ± 2.4 %; + HRG: IgG hu225 + IgG 3-43: 30.5 ± 2.6 %, scDb hu225x3-43-Fc: 30.0 ± 4.8 %). Taken together, scDb hu225x3-43-Fc efficiently inhibited proliferation and migration of FaDu cells. Compared to the combination of the parental antibodies, the scDb-Fc was more efficient in inhibition of cell proliferation.

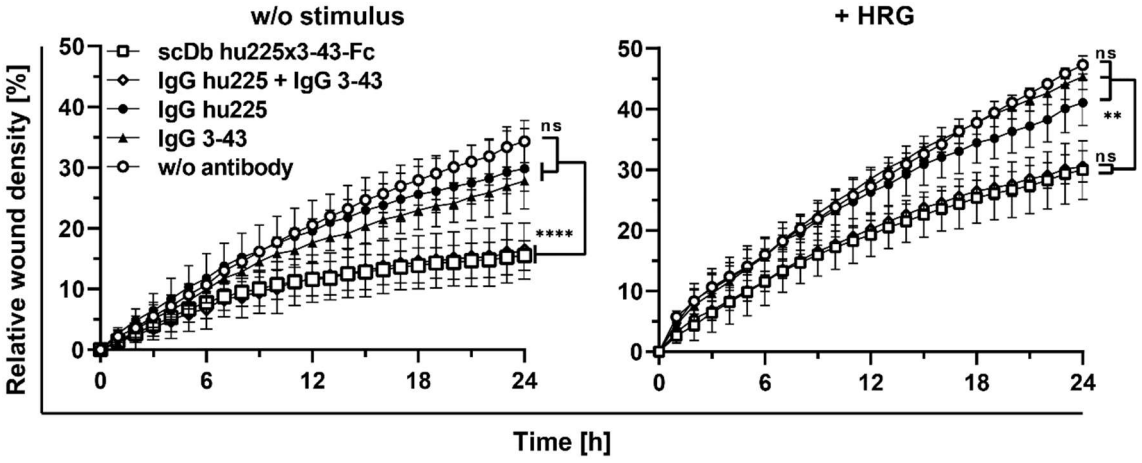

Figure 9: Migration of FaDu cells upon EGFR- and HER3-targeted antibody treatment. Scratch wound assay of FaDu cells in low serum (0.2 % FCS) in the absence or presence of HRG (30 ng/ml). Cells were treated with 50 nM antibodies (IgG hu225, IgG 3-43, combination of IgG hu225 and IgG 3-43, or scDb hu225x3-43-Fc). Migration into the scratched wound was observed and analyzed using the Incucyte® S3 live-cell analysis system (n=3, mean ± SD). Data were analyzed by two-way ANOVA. P ≤ 0.05 (*), P ≤ 0.01 (**), P ≤ 0.001 (***), P ≤ 0.0001 (****), n.s. (not significant).

4.2.3 Antitumor activity of scDb hu225x3-43-Fc in FaDu 3D and xenograft model

Next, the activity of scDb hu225x3-43-Fc on the proliferation of FaDu cells embedded into a 3D matrix was analyzed, recapitulating the conditions found *in vivo* more closely (Langhans 2018) (Figure 10A). The effects of the antibodies were observed in the presence or absence

of HRG. Proliferation was strongly increased upon addition of HRG (w/o stimulus: 100 % vs. + HRG: 170.1 %). Treatment with IgG hu225 resulted in strong inhibition of proliferation under both conditions (w/o stimulus: 39.7 % vs. + HRG: 101.1 %). Even stronger inhibitory effects were observed after scDb-Fc treatment (w/o stimulus: 31.8 % vs. + HRG: 88.9 %). The combination of IgG hu225 and IgG 3-43 (w/o stimulus: 49.5 % vs. + HRG: 137.2 %), as well as IgG 3-43 alone (w/o stimulus: 66.5 % vs. + HRG: 158.5 %) also led to a decreased proliferation, however, to a lesser extent.

Further, the anti-tumor activity of scDb hu225x3-43-Fc in a subcutaneous FaDu xenograft model was analyzed. The scDb-Fc as well as the parental antibodies (300 µg per injection) were injected twice weekly for 3 subsequent weeks (Figure 10B). All four treatments (IgG hu225, IgG 3-43, IgG hu225 + IgG 3-43, or scDb hu225x3-43-Fc) induced almost complete tumor remission during the treatment phase. However, tumors of mice treated with IgG 3-43 showed regrowth after the treatment was terminated, while tumors of mice treated with IgG hu225, IgG hu225 + IgG 3-43, or scDb hu225x3-43-Fc showed stable tumor volume until end of observation (day 90). Comparison of the serum concentration levels after the first and last treatment revealed a ~2– to 3-fold accumulation of the antibodies, whereby the accumulation of IgG hu225 was strongest (Figure 10D). Furthermore, analysis of pharmacokinetics after a single i.v. injection of scDb hu225x3-43-Fc into CD-1 mice revealed a comparable pharmacokinetic profile to IgG 3-43 (Figure 10C). For the scDb-Fc a terminal half-life of approximately 65 h was calculated, when detected with EGFR-His, and of 49 h, when detected with HER3-His (Table 7). The analyzed drug exposure was approximately 601 µg/ml*h when detected with EGFR-His, and 566 µg/ml*h, when detected with HER3-His. Half-life and drug exposure (AUC) of scDb hu225x3-43-Fc were similar to IgG 3-43 (Table 7, Figure 10C). In summary, the scDb-Fc combined the antitumor activities of the parental antibodies and demonstrated IgG-like pharmacokinetic properties.

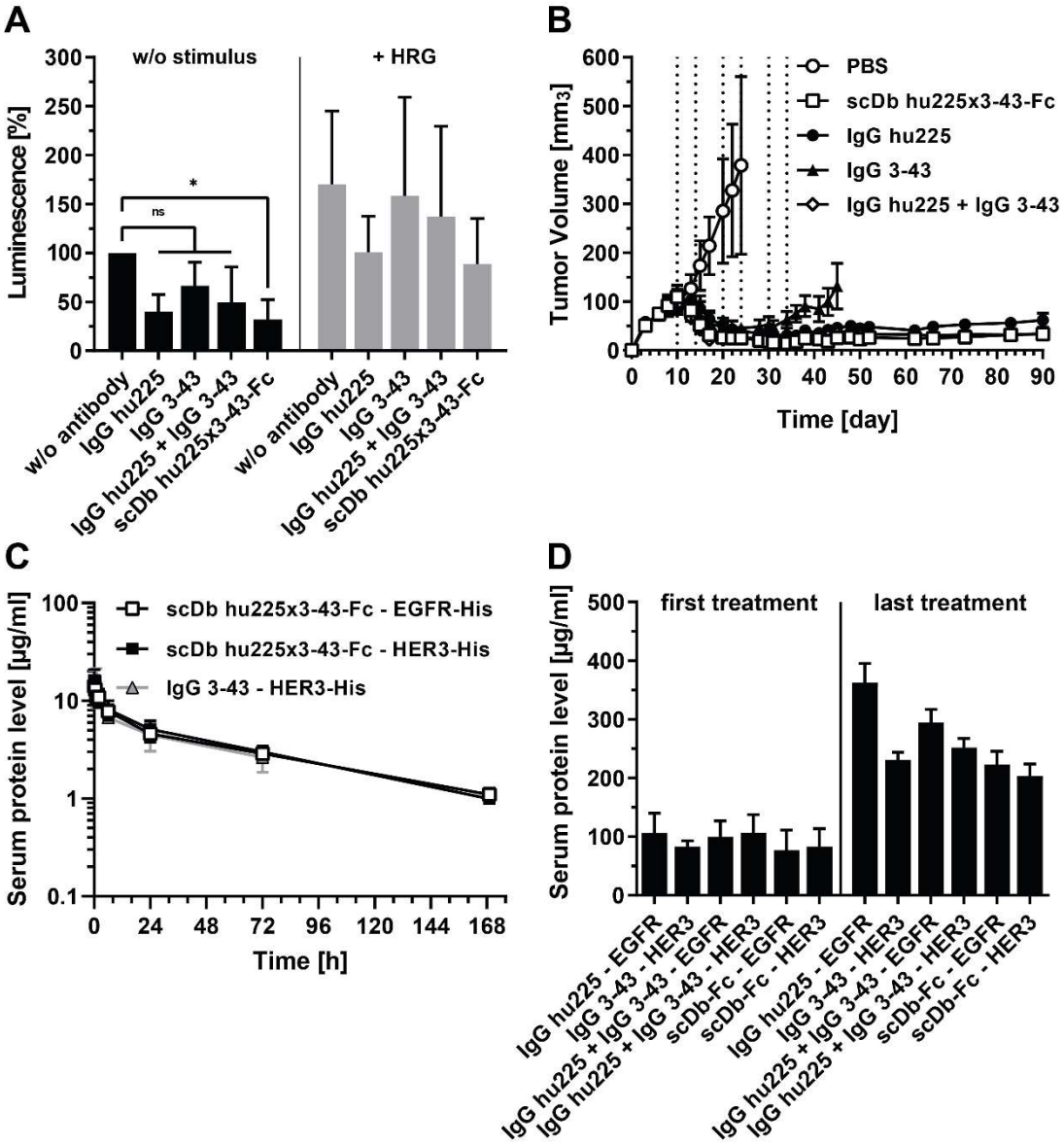

Figure 10: Inhibition of proliferation of FaDu cells in 3D and tumor growth inhibition in a FaDu xenograft model: **A** Analysis of proliferation in 3D of FaDu cells after 6 days of incubation in low serum (0.2 % FCS). Cells were treated with 50 nM antibodies (IgG hu225, IgG 3-43, combination of IgG hu225 and IgG 3-43, or scDb hu225x3-43-Fc). After 1 h cells were stimulated with 30 ng/ml of HRG as indicated. On day 4 after treatment viability was analyzed using the CellTiterGlo 3D Kit (n=3, mean ± SD). Data was analyzed by one-way ANOVA and Tukey's test for multiple comparison. $P \leq 0.05$ (*), $P \leq 0.01$ (**), $P \leq 0.001$ (***), $P \leq 0.0001$ (****), n.s. (not significant). **B** Tumor growth of FaDu cancer cells in a subcutaneous xenograft model in SCID mice. Mice were treated when mean tumor volume of ~100 mm^3 was reached. 300 µg of antibodies (IgG hu225, IgG 3-43, combination of IgG hu225 and IgG 3-43, or scDb hu225x3-43-Fc) in 100 µl PBS were applied i.v. twice weekly, for 3 subsequent weeks. **C** Pharmacokinetic profiles of IgG 3-43 and scDb hu225x3-43-Fc (25 µg; i.v.) were analyzed in female CD1 mice (n=3). Serum protein levels were analyzed by ELISA, using EGFR- and HER3-His. **D** Serum protein concentration after the first and last treatment of the FaDu xenograft described in **B** was analyzed by ELISA using EGFR- and HER3-His. The animal experiment and analysis were conducted by Oliver Seifert.

Table 7: Analysis of initial ($t_{½}\alpha$) and terminal ($t_{½}\beta$) half-lives, as well as drug exposure (area under the curve; AUC) of scDb hu225x3-43-Fc and IgG 3-43 (n=3; mean ± SD; n.d.: not determined).

	Antigen	scDb hu225x3-43-Fc	IgG 3-43
$t_{½}\alpha$ [h]	EGFR	2.8 ± 1.6	n.d.
	HER3	1.2 ± 0.7	1.9 ± 1.5
$t_{½}\beta$ [h]	EGFR	65.4 ± 15.2	n.d.
	HER3	48.9 ± 12.6	59.6 ± 25.7
AUC [µg/ml·h]	EGFR	601.3 ± 25.7	n.d.
	HER3	566.2 ± 66.2	565.2 ± 227.5

4.3 scDb hu225x3-43-Fc supresses TNBC proliferation and oncosphere formation *in vitro* and *in vivo*

Despite high EGFR abundance in tumors of TNBC patients, EGFR-targeted therapies showed only modest to no clinical benefit (Carey et al. 2012; Baselga et al. 2013; Finn et al. 2009). Additionally, tumors that initially respond to EGFR blockade show development of resistances, inter alia, by upregulation of HER3 expression or its ligand HRG (Tao et al. 2014; Wheeler et al. 2008). HRG expression in the mammary gland induces formation of adenocarcinomas in transgenic mice and is sufficient for metastatic spreading of breast cancer cell lines (Atlas et al. 2003; Krane and Leder 1996). Further, comparison between paired samples of TNBC patients treated with Cetuximab or Panitumumab revealed increased HER3 abundance post-treatment (Tao et al. 2014). To analyze, whether the scDb hu225x3-43-Fc could be a suitable option for the treatment of TNBC tumors, in this thesis, the effects on the proliferation and colony formation of 2 TNBC cancer cell lines expressing high EGFR levels (MDA-MB-468 and HCC1806) were tested (Figure 6). HRG was also described to promote sphere formation in serum-free suspension culture of breast cancer cell lines, a characteristic associated with stem cell-like and tumor-initiating properties (Shaw et al. 2012). Therefore, primary and secondary sphere formation assays were performed with MDA-MB-468 and HCC1806 cells and expression of the stem-cell marker ALDH was determined (Hu and Smyth 2009). In the last step tumor growth inhibition of scDb hu225x3-43-Fc in an orthotopic TNBC xenograft model were analyzed.

4.3.1 Inhibition of TNBC cell proliferation

Proliferation of the two TNBC cell lines MDA-MB-468 and HCC1806, upon dual inhibition of EGFR and HER3 was analyzed in low serum (0.2 %) in the presence or absence of HRG (Figure 11A, C). In the absence of HRG, the strongest inhibitory effects were observed for the inhibition of EGFR by IgG hu225 in MDA-MB-468 cells (Figure 11). Additional blockage of HER3 did not led to stronger inhibition of the proliferation. Stimulation with HRG increased the proliferation of MDA-MB-468 cells (w/o stimulus: 100 % vs. + HRG: 132 %) (Figure 11A). Under HRG conditions, dual blockade of EGFR and HER3 showed significantly stronger inhibition of proliferation compared to the parental antibodies alone (IgG hu225: 94 % vs. IgG 3-43: 108 % vs. IgG hu225 + IgG 3-43: 68 % vs. scDb hu225x3-43-Fc: 71.1 %). In HCC1806 cells none of the treatments showed inhibitory effects on proliferation (Figure 11C). However, in colony formation assays, single treatment with IgG hu225, combinatorial treatment with the parental

antibodies and bispecific treatment showed comparable inhibition of proliferation (Figure 11B, D).

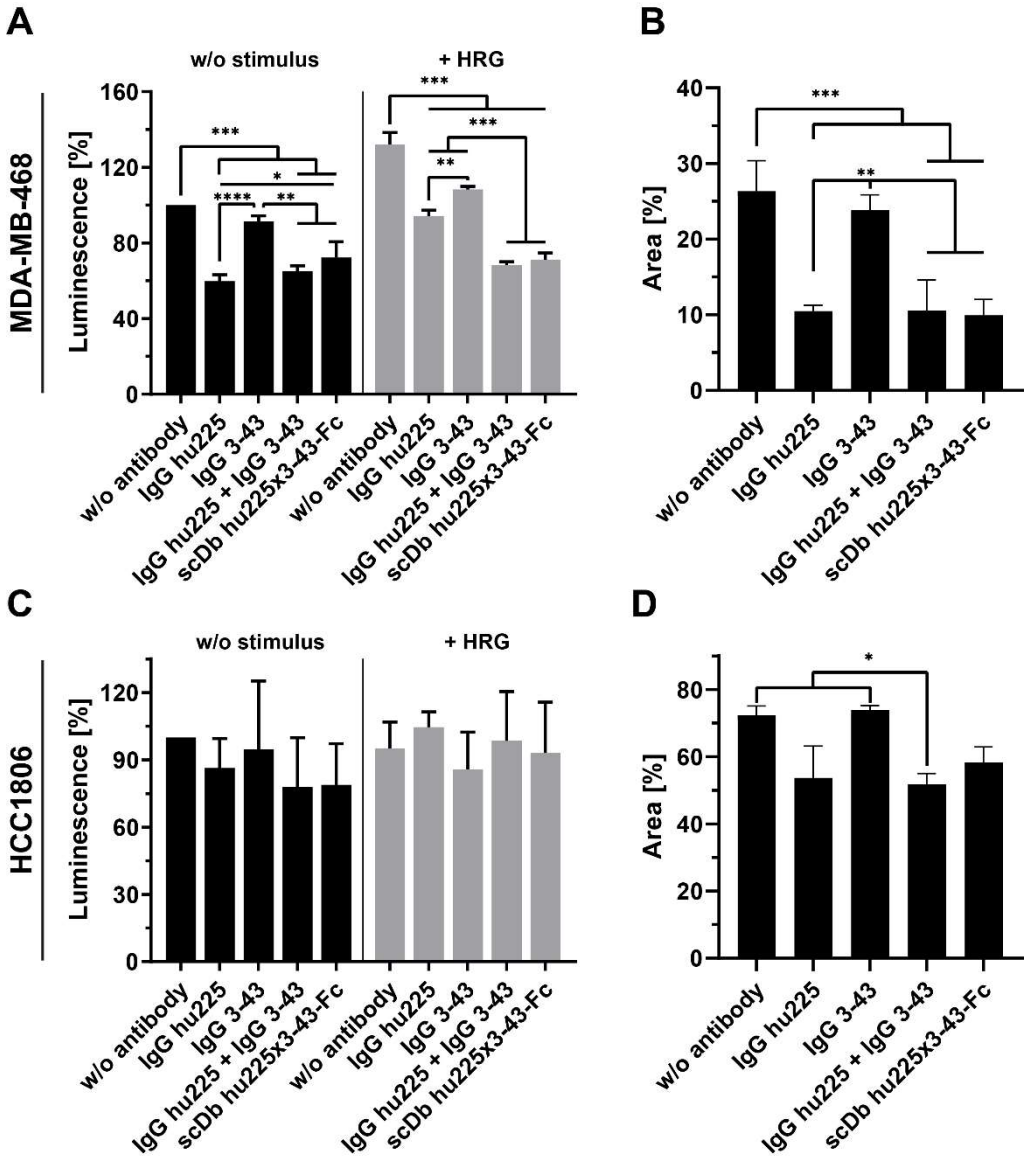

Figure 11: Analysis of inhibition of proliferation upon EGFRxHER3 dual targeting in two TNBC cell lines: A, C Analysis of 2D proliferation of MDA-MB-468 (**A**) and HCC1806 (**C**) cells after one week of incubation in low serum (0.2 % FCS). Cells were treated with 50 nM antibodies (IgG hu225, IgG 3-43, combination of IgG hu225 and IgG 3-43, or scDb hu225x3-43-Fc). After 1 h cells were stimulated with 30 ng/ml of HRG as indicated. On day 5 after treatment viability was analyzed using the CellTiterGlo 2.0 Kit (n=3, mean ± SD). Data was analyzed by one-way ANOVA and Tukey's test for multiple comparison. P ≤ 0.05 (*), P ≤ 0.01 (**), P ≤ 0.001 (***), P ≤ 0.0001 (****), n.s. (not significant). **B, D** For colony formation, MDA-MB-468 (**B**) and HCC1806 (**D**) cells were seeded at low density (5000 cells / 12-well) in 2 % FCS containing RPMI. After 24 h cells were treated with 50 nM antibodies (IgG hu225, IgG 3-43, combination of IgG hu225 and IgG 3-43, or scDb hu225x3-43-Fc). After fixation with paraformaldehyde (PFA, 4 %) and staining with crystal violet, pictures were taken using the Licor Odyssey®. Occupied area by formed colonies was analyzed using ImageJ (plugin: ColonyArea) (MDA-MB-468: n=3, mean ± SD; HCC1806: n=2, mean ± SD). Data was analyzed by one-way ANOVA and Tukey's test for multiple comparison. P ≤ 0.05 (*), P ≤ 0.01 (**), P ≤ 0.001 (***), P ≤ 0.0001 (****), n.s. (not significant).

4.3.2 Reduced number of TNBC cells with stem-cell like properties after treatment with scDb-Fc

Formation of spheres in serum-free suspension culture is characteristic for stem-cell like cells and cells with tumor-initiating properties (Shaw et al. 2012). HRG can drive the formation of breast cancer cell oncospheres (Hinohara et al. 2012; Sachs et al. 2018; Lee et al. 2014). Therefore, the effects of dual targeted inhibition of EGFR and HER3 with the scDb-Fc on stem cell survival and expansion were analyzed (Figure 12). The sphere formation efficiency of MDA-MB-468 cells in serum-free medium supplemented with HRG was significantly reduced by IgG hu225 and strongest inhibition was observed for scDb hu225x3-43-Fc (2.9 ± 0.5 vs. 5.7 ± 1.5 and 11.5 ± 0.8 for IgG hu225 and IgG 3-43, respectively; w/o antibody control: 16.8 ± 6) (Figure 12A). Furthermore, modest reduction of sphere area by all three treatments, IgG hu225, IgG 3-43, or scDb-Fc was observed (0.0043 mm² vs. 0.0042 mm² vs. 0.0034 mm²; w/o antibody control: 0.0049 mm²). Significant inhibitory effects of scDb hu225x3-43-Fc on sphere formation was also observed in HCC1806 cells, again with modest reduction of sphere area (Figure 12C). To confirm the reduction of cells with stem-cell like properties the number of $ALDH^{high}$ cells was analyzed by ALDEFLUOR assay (Figure 12B, D). Interestingly, in both cell lines (MDA-MB-468 and HCC1806) the scDb-Fc reduced the $ALDH^{high}$ population by almost 50 %. Additionally, the stem cell frequency after treatment with scDb-Fc was determined by extreme limited dilution assay (ELDA). TNBC cancer cells were cultured as primary oncospheres, treated with scDb-Fc for 5 days. Developed spheres where collected, singularized and reseeded into the ELDA assay (1, 10, or 100 cells per well) and cultivated for another 10 days (Figure 12E). Notably, the scDb-Fc significantly reduced the stem cell frequency in MDA-MB-468 and HCC1806 cells by 54 % and 74 %, respectively (Figure 12F).

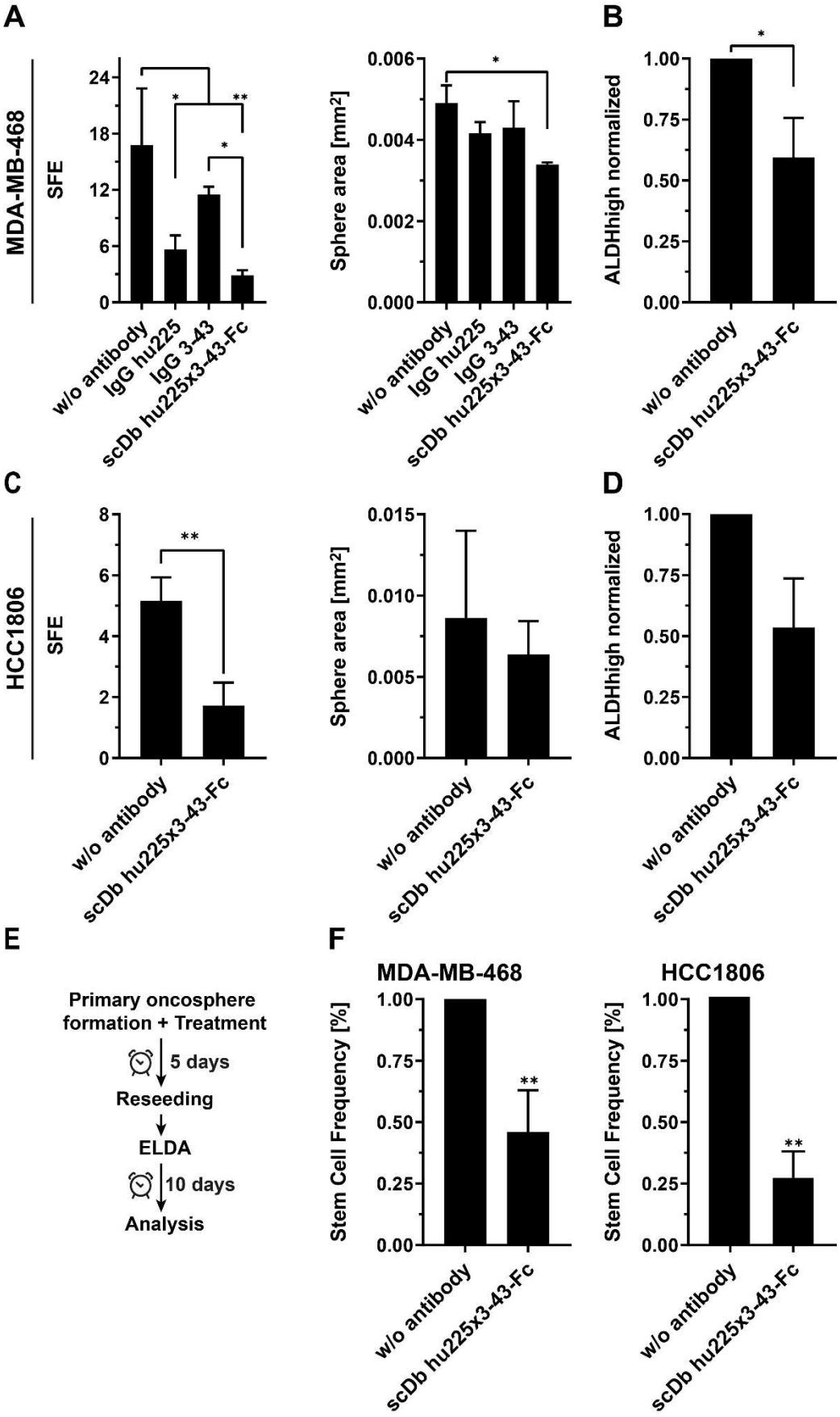

Figure 12: Effects of dual targeting of EGFR and HER3 on TNBC stem cells. A, C MDA-MB-468 (**A**), or HCC1806 (**C**) cells were seeded in pHEMA coated plates and immediately

treated with antibodies (50 nM of IgG hu225, IgG 3-43, combination of both or scDb hu225x3-43-Fc). After 5 days sphere forming efficiency (SFE; spheres formed per 1000 seeded cells) and sphere area were determined from microscope images with ImageJ (n=3, mean ± SD). Data was analyzed by one-way ANOVA. **B, D** The number of $ALDH^{high}$ cells after treatment with scDb hu225x3-43-Fc was analyzed using the ALDEFLUOR Kit. The number of $ALDH^{high}$ cells was normalized to the untreated control (n=3, mean ± SD). Data was analyzed by unpaired t-Test. **E** Schematic illustration of extreme limiting dilution analysis (ELDA). **F** For ELDA assay, cells were seeded into 20 wells per dilution step and the number of wells with spheres were counted manually under the microscope (n=3, mean ± SD). Data was analyzed by unpaired t-Test. $P \leq 0.05$ (*), $P \leq 0.01$ (**), $P \leq 0.001$ (***), $P \leq 0.0001$ (****), n.s. (not significant). Experiments and data analysis were conducted by Sebastian Lieb.

4.3.3 Inhibition of tumor growth and stem cell expansion *in vivo*

Finally, the anti-tumor activity of scDb-Fc in comparison to its parental antibodies in an orthotopic xenograft model using MDA-MB-468 cells was analyzed. Cells were inoculated into the mammary fat pad, thereby better recapitulating the location of the disease. Delay of tumor growth compared to the PBS control was achieved by the treatment with IgG hu225, IgG 3-43 and the combination of both antibodies. However, only the scDb-Fc treatment stopped tumor growth, with effects persisting until the end of observation (day 82) (Figure 13A, B). After mice were sacrificed, tumors were removed, dissociated, and the percentage of $ALDH^{high}$ cells as well as sphere formation was analyzed (Figure 13C, D). IgG 3-43 and scDb-Fc treated tumors contained the lowest number of $ALDH^{high}$ cells compared to PBS control (Figure 13C). Reduction of sphere forming efficiency was achieved by all treatments, yielding the lowest SFE for the cells derived from scDb-Fc-treated tumors (SFE of PBS: 13.5 ± 10.7, IgG hu225: 6.63 ± 2.3, IgG 3-43: 7.5 ± 3.7, IgG hu225 + IgG 3-43: 6.1 ± 1.5, scDb hu225x3-43-Fc: 3.5 ± 0.6). Of note, none of the antibody treatments led to changes in sphere size, indicating, in accordance with the *in vitro* results, that the number of cells with stem-cell like properties was reduced by the antibodies *in vivo* (Figure 12). In summary, the scDb-Fc not only reduced the proliferation of TNBC cell lines, but also reduced the number of oncospheres formed, the number of $ALDH^{high}$ cells and the stem cell frequency *in vitro* and *in vivo*.

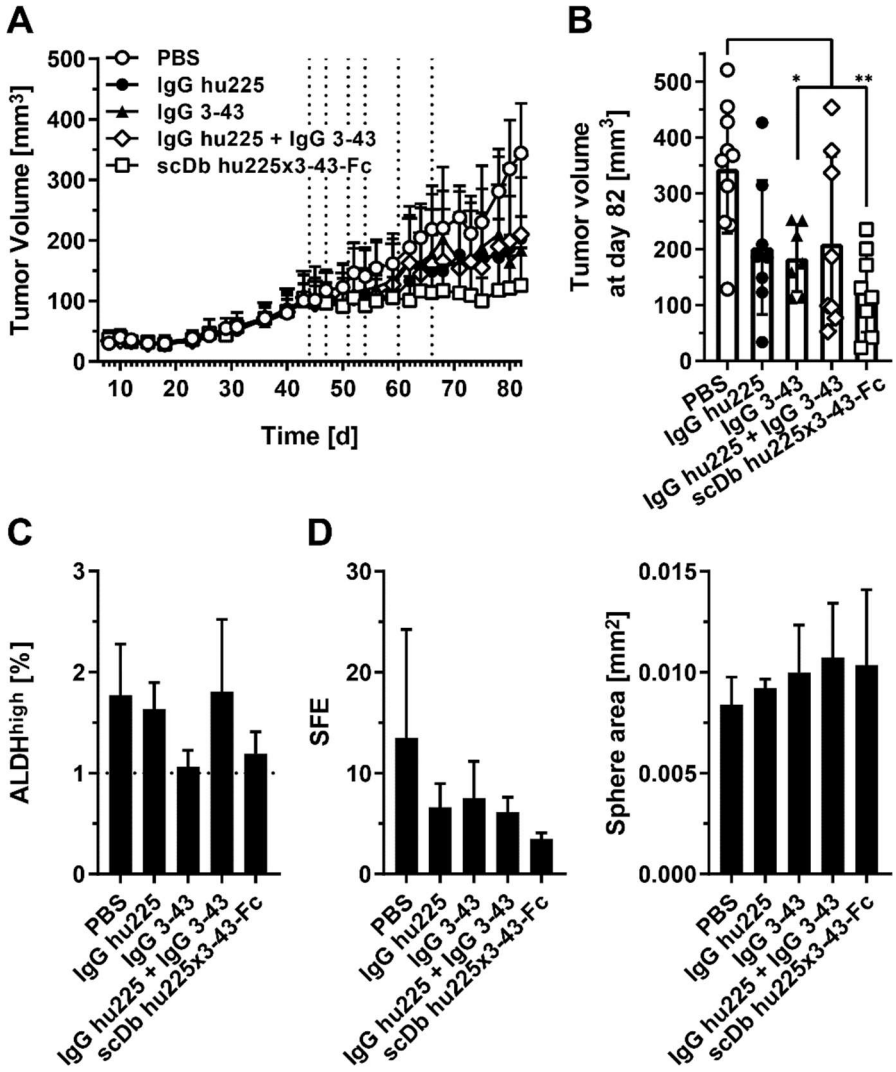

Figure 13: EGFRxHER3 dual targeting is superior to single treatment *in vivo*. A MDA-MB-468 cells were inoculated orthotopically into the mammary fat pad of SCID-beige mice. After tumors reached a mean tumor volume of 100 mm³ mice were treated with antibodies intravenously (IgG hu225, IgG 3-43, combination of both or scDb hu225x3-43-Fc). **B** Mean tumor volume before mice were sacrificed. Data presented as mean ± SD. Statistical comparison by one-way ANOVA. P ≤ 0.05 (*), P ≤ 0.01 (**), P ≤ 0.001 (***), P ≤ 0.0001 (****), n.s. (not significant). **C** ALDEFLUOR assay. ALDH activity of tumor cells was analyzed by flow cytometry. **D** Oncosphere formation assay. Dissociated tumor cells were seeded into pHEMA coated plates. SFE was analyzed by manual counting under the microscope. Sphere areas were analyzed using ImageJ**.** Experiments and analyses were conducted in cooperation with Sebastian Lieb.

4.4 Combination of scDb hu225x3-43-Fc with Trastuzumab shows consistent inhibition of proliferation in CRC cell lines and patient derived organoids

Cetuximab was described to be ineffective in 40-70 % of patients with wildtype KRAS (Pauw et al. 2019; Leto and Trusolino 2014). HER2 amplification or transcriptional upregulation as well as expression of heregulin/neuregulin1 (HRG) or its receptor HER3, are primary or acquired resistance mechanisms occurring upon Cetuximab treatment (Oliveras-Ferraros et al. 2012; Leto and Trusolino 2014; Leto et al. 2015; Stahler et al. 2017; Kruser and Wheeler 2010; Zhang et al. 2020). About 20 % of primary rectal cancer express HER2 and in ~10 % of patients with liver metastasis overexpression of HER2 was observed (Conradi et al. 2013; Styczen et al. 2015). High HER3 expression was reported in 70-80 % of primary CRC and corresponding metastases in liver and lymph nodes (Conradi et al. 2019; Lédel et al. 2015; Lédel et al. 2014). Based on these findings, the additional combination of scDb hu225x3-43-Fc with a HER2-targeting antibody, here Trastuzumab, could be beneficial. Therefore, the effects of this triple targeted approach on the proliferation, downstream signaling and oncosphere formation of CRC cell lines was analyzed. Further anti-proliferative effects on PDOs, embedded in a 3D matrix, which resemble the conditions found *in vivo* more closely compared to 2D cell culture were analyzed.

4.4.1 Inhibitory effects of scDb-Fc on proliferation benefit from combination with Trastuzumab

Binding of IgG hu225, Trastuzumab, IgG 3-43 and scDb hu225x3-43-Fc to DiFi and LIM1215 cells was demonstrated by flow cytometry analysis (see 4.2.1, Figure 6). DiFi cells have high expression levels of EGFR (708,730 surface expressed receptors (SER)), intermediate HER2 (12,109 SER) and HER3 (5,594 SER) expression. LIM1215 have comparable expression levels of all three receptors (EGFR: 25,140 SER; HER2: 15,102 SER; HER3: 10,822 SER) (Figure 6B).

Expression of HER3 or its ligand HRG is described as initial and acquired resistance mechanisms in CRC patients treated with Cetuximab (Yonesaka et al. 2011; Bon et al. 2016). Hence, the inhibitory effects on the proliferation of DiFi and LIM1215 cells by the scDb-Fc was analyzed in presence or absence of exogenous HRG. In the absence of HRG, the inhibitory effects of scDb Fc were comparable to those of IgG hu225 and the combination of IgG hu225 with IgG 3-43 in 2D and 3D, respectively (Figure 14A-D). ScDb-Fc inhibited proliferation in 2D by approximately 75 % in DiFi cells and 50 % in LIM1215 cells, respectively. In 3D, maximum inhibition was approximately 70 % in DiFi cells and 50 % in LIM1215 cells (Figure 14A-D). In

the presence of HRG, the scDb-Fc inhibited the proliferation of DiFi cells in 2D and 3D most potently compared to the combination of IgG hu225 and IgG 3-43, or the parental antibodies alone (2D: 63.2 % vs. 82.3 % vs. 117.9 % vs. 147.8 %; w/o antibody control: 168.9 %; 3D: 45.1 % vs. 77.5 % vs. 124.6 % vs. 77.4 %; w/o antibody control: 157.8 %). Interestingly, in the presence of HRG no inhibition of proliferation of LIM1215 cells by any treatment was observed in 2D or 3D (Figure 14B, D).

A high degree of plasticity in the HER-family allows for compensatory signaling, causing resistance upon partial targeting of the family members (Jacobsen et al. 2015; Kennedy et al. 2019). Therefore, the EGFR- and HER3-targeting approaches were combined with additional HER2-targeting by Trastuzumab in 2D in the presence of HRG. Trastuzumab alone had no effect on the proliferation of DiFi and LIM1215 cells (Figure 14E, F). Furthermore, the strong inhibitory effects on proliferation, achieved by targeting EGFR and HER3, were not enhanced by Trastuzumab in DiFi cells. However, combination of scDb-Fc and Trastuzumab, but not combination of the three parental antibodies, showed significant inhibition of proliferation of LIM1215 cells (84.3 % vs. 113.8 %; w/o antibody control: 127.8 %) (Figure 14F). In summary, the scDb-Fc, especially in combination with Trastuzumab, showed strong inhibition of proliferation of two CRC cell lines in the presence or absence of exogenous HRG.

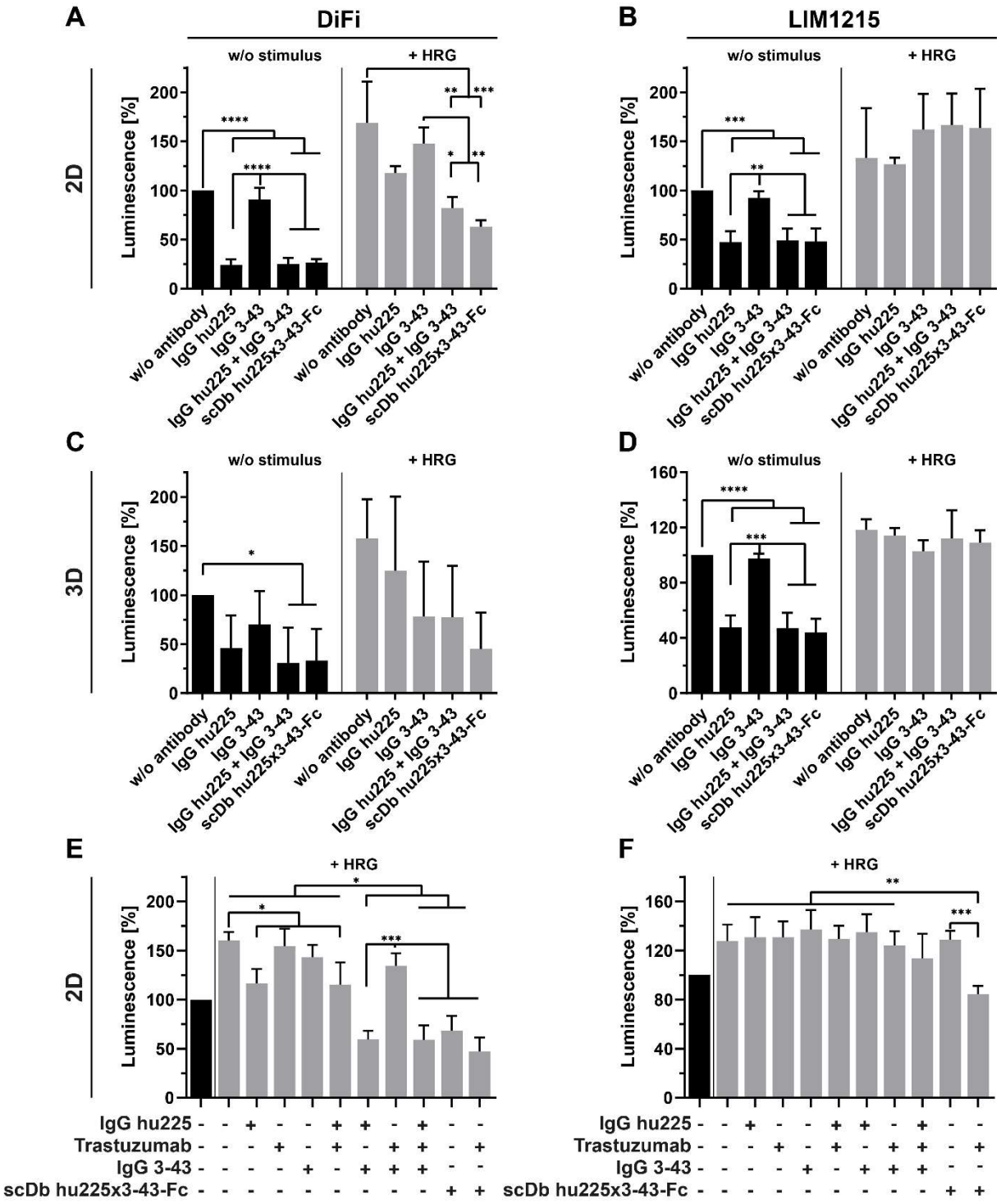

Figure 14: Inhibition of proliferation in 2D and 3D after EGFR, HER2 and/or HER3 targeted antibody treatment of colorectal cancer cell lines: A, B Inhibition of proliferation of DiFi and LIM1215 cells after one week of incubation in low serum (0.2 % FCS) in 2D. Cells were treated with 50 nM antibodies (IgG hu225, IgG 3 43, combination of both or scDb hu225x3 43-Fc). Analysis of viable cells was performed using the CellTiterGlo 2.0 Kit (n=3, mean ± SD). Data was analyzed by one-way ANOVA and Tukey's test for multiple comparison. P ≤ 0.05 (*), P ≤ 0.01 (**), P ≤ 0.001 (***), P ≤ 0.0001 (****), n.s. (not significant). **C, D** Inhibition of proliferation of DiFi and LIM1215 cells in 3D. Cells were cultured and treated as described in **A, B.** Analysis of viable cells was performed using the CellTiterGlo 3D Kit (n=3, mean ± SD). Data was analyzed by one-way ANOVA and Tukey's test for multiple comparison. P ≤ 0.05 (*), P ≤ 0.01 (**), P ≤ 0.001 (***), P ≤ 0.0001 (****), n.s. (not significant). **E, F** Inhibition of proliferation of

DiFi and LIM1215 cells in 2D. Cells were cultured as in **A, B,** but treated with 50 nM EGFR, HER2 and HER3 specific antibodies (IgG hu225, Trastuzumab, IgG 3 43, scDb hu225x3 43-Fc, or combination of two or three antibodies). Analysis of viable cells was performed using the CellTiterGlo 2.0 Kit (n=3, mean ± SD). Data was analyzed by one-way ANOVA and Tukey's test for multiple comparison. P ≤ 0.05 (*), P ≤ 0.01 (**), P ≤ 0.001 (***), P ≤ 0.0001 (****), n.s. (not significant).

4.4.2 Analysis of receptor phosphorylation and downstream signaling over time in LIM1215 cells

Homo- and heterodimerization of the HER-family members upon ligand binding leads to activation of the MAPK and PI3K pathway (Roskoski 2014). To analyze the effects of the different antibody treatments on these two pathways, western blot analyses were performed. Prior to stimulation with HRG, serum-starved LIM1215 cells were incubated with antibodies, IgG hu225, Trastuzumab, IgG 3-43, scDb hu225x3-43-Fc or combination of two, or three antibodies, respectively.

Even without stimulation basal phosphorylation of EGFR (Y1068) was observed, which was not significantly affected by any of the treatments (Figure 15A). Of note, in the absence of HRG the treatment with Trastuzumab alone, but also in combination with EGFR- and/or HER3-targeting antibodies, resulted in increased phosphorylation of HER2, but this did not translate into activation of downstream pathways (Figure 15A). No basal phosphorylation of HER3 (Y1289), ERK (T202/Y204) or AKT (T308) was observed. While total protein levels were largely unchanged by the antibody treatments, HER3 protein levels were lower when IgG 3-43 or scDb-Fc was included in the treatment, independently of the stimulation with HRG. After 15 min of HRG stimulation phosphorylation of EGFR (Y1068), HER2 (Y1221/1222) and HER3 (Y1289) was observed, which resulted in strong downstream phosphorylation of ERK (T202/Y204) and Akt (T308) (Figure 15B). In contrast to IgG hu225 and Trastuzumab, IgG 3-43 alone caused maximum inhibition of phosphorylation of EGFR (Y1068), HER2 (Y1221/1222) and HER3 (Y1289). Combinatorial treatment with scDb-Fc and Trastuzumab showed strongest inhibition of phosphorylation of ERK (T202/Y204) and AKT (T308). However, compared to triple treatment with the combination of IgG hu225, Trastuzumab and IgG 3-43, no significant difference was observed.

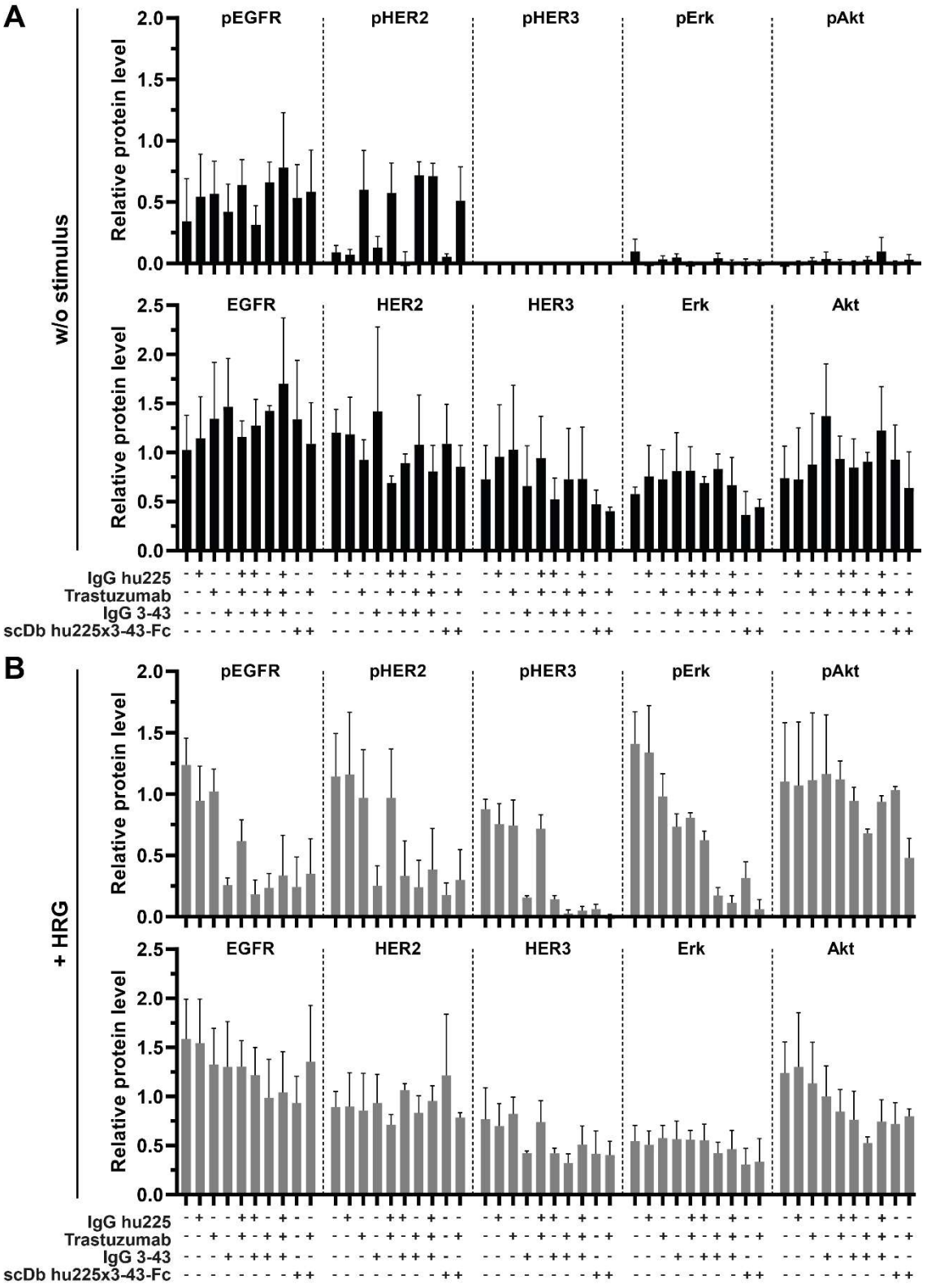

Figure 15: Western blot analysis of receptor phosphorylation and downstream signaling in LIM1215 cells: A, B LIM1215 cells were starved overnight before treatment with antibodies (IgG hu225, Trastuzumab, IgG 3-43, scDb hu225x3 43-Fc, or combination of two or three antibodies) for 1 h. After incubation with the antibodies, cells were left unstimulated (**A**) or were stimulated with 50 ng/ml HRG (**B**). Subsequently, cell lysates were analyzed by western blot. Data shown as mean intensity of signals normalized to α-Tubulin (n=3, mean ± SD).

Because the above-described analysis only allowed for observation of short-term effects, triple targeted treatments (IgG hu225 + Trastuzumab + IgG 3-43 and scDb hu225x3-43-Fc + Trastuzumab) were compared in a kinetic downstream signaling assay and analyzed by western blot. The experiment was performed as described above with LIM1215 cells, but lysates were prepared 1 h, 6 h and 24 h after stimulation with HRG (Figure 16). In the absence of HRG only slight phosphorylation of HER2 (Y1221/1222) was observed for both triple treatments. In the untreated control, after 1 h of stimulation with HRG, strong phosphorylation of HER2 (Y1221/1222), HER3 (Y1289), ERK (T202/Y204) and AKT (T308) was observed. 6 h after ligand stimulation signals of phosphorylated HER2, HER3 and ERK were declining, while reduction of pAKT signals was only observed after 24 h. Of note, both triple-targeted treatments inhibited the phosphorylation of all analyzed proteins over the entire time course, compared to the untreated control. This demonstrates the strong and sustainable inhibitory effects of triple targeted treatments against EGFR, HER2 and HER3 with respect to receptor phosphorylation and downstream signaling in LIM1215 cells.

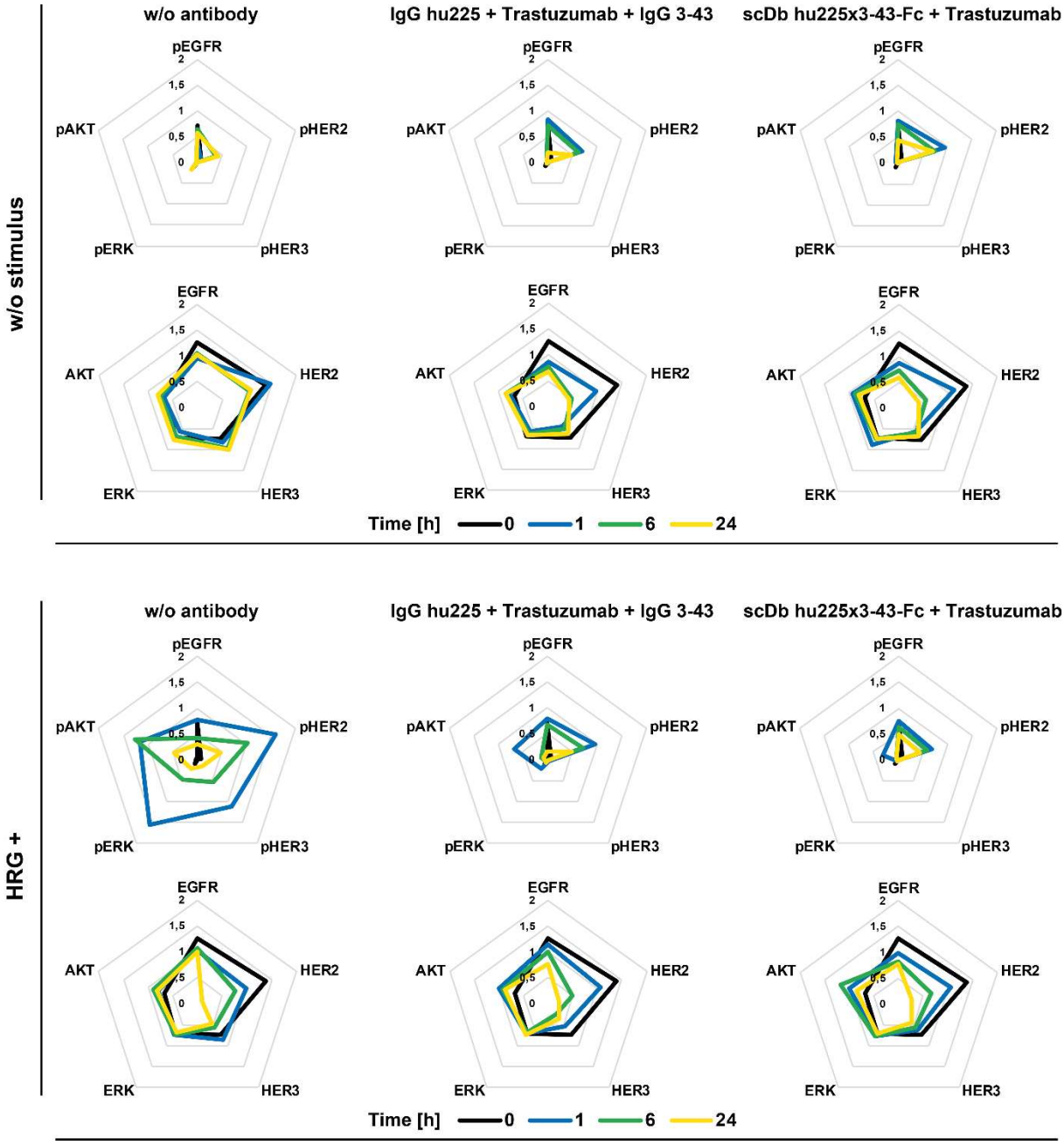

Figure 16: Western blot analysis of receptor phosphorylation and downstream signaling kinetics in LIM1215 cells. LIM1215 cells were starved overnight before treatment with antibodies (combination of scDb hu225x3-43-Fc and Trastuzumab or a combination of IgG hu225, Trastuzumab and IgG 3-43) for 1 h. After incubation with the antibodies for 1 h, cells were stimulated with 50 ng/ml HRG. Cell lysates were prepared after 1 h, 6 h and 24 h, incubation and analyzed by western blot. Data shown as mean intensity of signals normalized to α-Tubulin (n=3).

4.4.3 Combination of scDb-Fc and Trastuzumab blocks sphere formation of CRC cell lines

As described above, cells with stem-cell like characteristics have the ability to form spheres in serum-free suspension culture and they initiate tumor growth *in vivo* (Shaw et al. 2012). HRG

was reported to drive the stemness and growth of spheroids originating from colorectal cancer tissues (Piulats et al. 2018). Hence, the effects of the triple-targeted treatment with scDb-Fc and Trastuzumab on sphere formation of DiFi and LIM1215 cells were investigated (Figure 17).

Sphere formation efficiency (SFE) of DiFi cells grown in serum-free HRG-supplemented medium was significantly reduced by scDb-Fc (SFE: 3.9 ± 1.6) and scDb-Fc + Trastuzumab (SFE: 1.4 ± 1.2), compared to the untreated control (SFE: 16.8 ± 3.7) (Figure 17A). Furthermore, combination of IgG hu225, Trastuzumab and IgG 3-43 (SFE: 4.8 ± 3.7) showed strong inhibition of SFE compared to untreated control, while single antibody treatments (SFE: IgG hu225: 13.0 ± 4.5; Trastuzumab: 17.4 ± 3.1; IgG 3-43: 17.2 ± 6.7) did not inhibit SFE. Dual inhibition of EGFR and HER2 (SFE: 8.2 ± 3.9), as well as EGFR and HER3 (SFE: 9.0 ± 3.5) showed comparable inhibitory effects. On the contrary, targeting of HER2 and HER3 (SFE: 22.4 ± 7.0) showed no inhibition of SFE (Figure 17A). Of note, analysis of the mean area of the counted spheres revealed strong inhibition by IgG hu225, IgG hu225 in combination with Trastuzumab or IgG 3-43, scDb-Fc, scDb-Fc + Trastuzumab and combination of IgG hu225, Trastuzumab and IgG 3-43, respectively, indicating the inhibition of proliferative capacity of sphere forming cells (Figure 17B). In LIM1215 cells, sphere formation was significantly inhibited by the combination of scDb-Fc and Trastuzumab, leading to an almost complete inhibition of sphere formation (SFE: 1.7 ± 0.7 vs. untreated control: 28.0 ± 14.3) (Figure 17D). Triple treatment with the parental antibodies also showed strong inhibitory effects (SFE: 6.6 ± 3.1), albeit to a lesser extent than scDb-Fc + Trastuzumab. Of note, the mean area of LIM1215 spheres was not significantly affected by any of the treatments (Figure 17B, E). Furthermore, comparison of the surface expression of EGFR, HER2 and HER3, for cells grown in 2D under basal cell culture conditions, or in 3D in serum-free HRG-supplemented medium was conducted (Figure 17C, F). For both cell lines, significantly higher surface expression of EGFR in 3D, compared to 2D culture was observed (DiFi 2D vs. 3D: 708,730 vs. >723,000; LIM1215 2D vs. 3D: 25,140 vs. 43,200), suggesting that cells with the ability to form spheres either have the ability to increase the expression of EGFR or the spheres originate from a subpopulation with high expression of EGFR. However, as described above blockade of EGFR with IgG hu225 was not sufficient to inhibit SFE. Further, HER2 surface expression was decreased in spheres (DiFi 2D vs. 3D: 12,109 vs. 6,709; LIM1215 2D vs. 3D: 15,102 vs. 10,019), while HER3 levels did not change (DiFi 2D vs. 3D: 5,808 vs. 5,594; LIM1215 2D vs. 3D: 10,822 vs. 11,026) (Figure 17C, F). In summary, the data obtained from the sphere formation assays underlines that EGFR blockade in combination with inhibition of HER3 and HER2 is superior to single treatment. Furthermore, the HER-family expression profile of the spheres indicates that

a triple targeted combination treatment could prevent rescue mechanisms by incomplete blockade of the HER-family members.

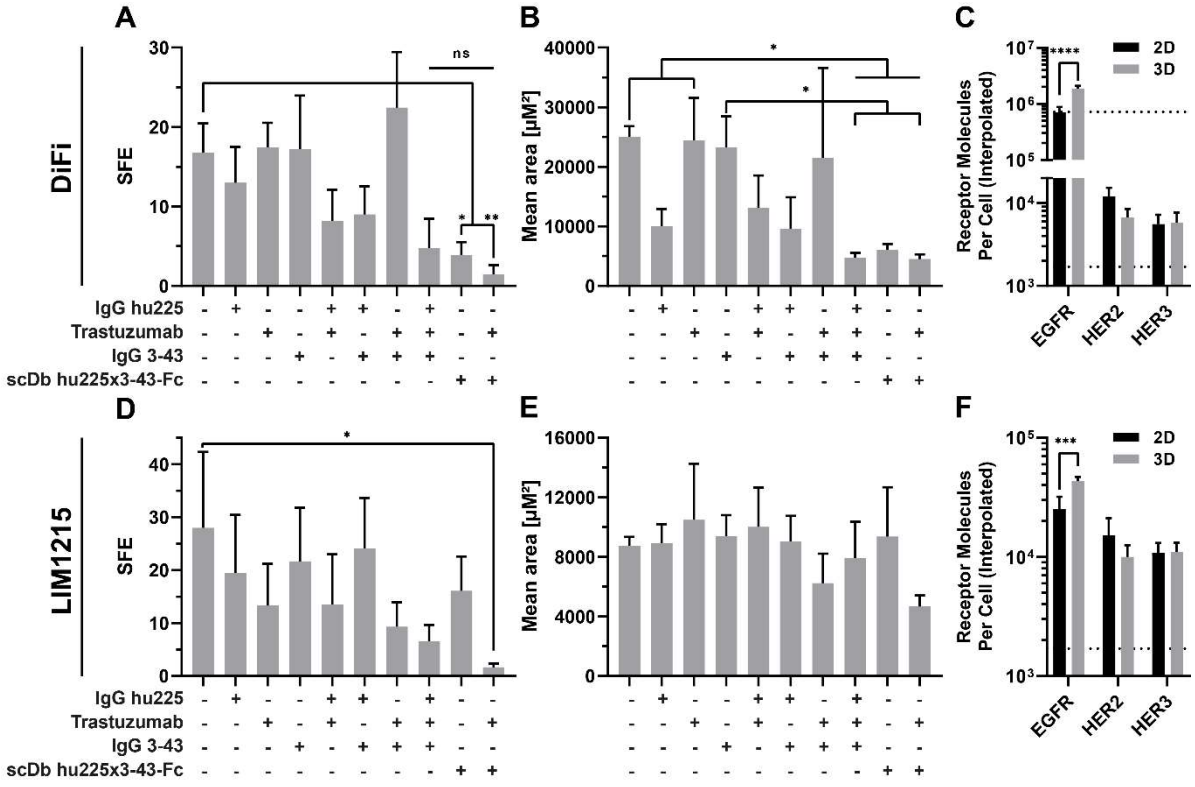

Figure 17: Sphere formation efficiency was strongly reduced upon triple targeting of EGFR, HER2 and HER3. A, B, D, E DiFi (**A, B**) and LIM1215 (**D, E**) cells were grown in pHEMA coated plates for 5 days. Antibodies (50 nM of IgG hu225, Trastuzumab, IgG 3-43, scDb hu225x3 43-Fc, or combination of two or three antibodies) were added immediately after seeding. Sphere forming efficiency (SFE; spheres formed per 1000 seeded cells) and sphere area (see Suppl. Fig 5) were determined from microscope images with ImageJ (n=3, mean ± SD). Data was analyzed by one-way ANOVA and Tukey's test for multiple comparison. P ≤ 0.05 (*), P ≤ 0.01 (**), P ≤ 0.001 (***), P ≤ 0.0001 (****), n.s. (not significant). **C, F** DiFi (**C**) and LIM1215 (**F**) cells were grown in 2D in T75 flasks in RPMI + 10 % FCS. For 3D cells were grown in pHEMA coated 10 cm dishes for 5 days. Cells were stained with primary antibodies (mouse) targeting EGFR, HER2, or HER3. Quantitative analysis was performed using the QIFIKIT (n=3, mean ± SD). Data was analyzed by one-way ANOVA and Tukey's test for multiple comparison. P ≤ 0.05 (*), P ≤ 0.01 (**), P ≤ 0.001 (***), P ≤ 0.0001 (****), n.s. (not significant). Dotted lines indicate upper and lower detection limit.

Additionally, the influence of the triple-targeted treatments on the stem cell frequency in an extreme limiting dilution assay (ELDA) was analyzed (Table 8). Primary oncospheres of DiFi and LIM1215 cells were treated for 5 days either with scDb-Fc + Trastuzumab, or the combination of IgG hu225, Trastuzumab and IgG 3-43. Then, the spheres were collected, singularized and re-seeded into the ELDA (1, 10, or 100 cells per well). After 9 days, wells containing spheres were counted and the stem cell frequency was estimated as described by Hu and Smyth (Hu and Smyth 2009). Of note, while no difference was observed between both treatments in LIM1215 cells, the combination of scDb-Fc and Trastuzumab significantly

reduced the stem cell frequency in DiFi cells, compared to combination of IgG hu225, Trastuzumab and IgG 3-43 (2.33 ± 0.58 vs. 10.0 ± 2.0; w/o antibody control: 13 ± 5.29) when 10 cells per well were seeded.

Table 8: ELDA assay. Cells from colonosphere assays were seeded into 20 wells per dilution step and the number of wells with spheres was counted manually under the microscope. Data represent relative estimated cell number (n=3, mean ± SD). Data was analyzed by one-way ANOVA and Tukey's test for multiple comparison. P ≤ 0.05 (*), P ≤ 0.01 (**), P ≤ 0.001 (***), P ≤ 0.0001 (****), n.s. (not significant).

Cell line	Cell number per well	w/o antibody	IgG hu225 + Trastuzumab + IgG 3-43		scDb hu225x3-43-Fc +Trastuzumab	
DiFi	1	2 ± 2.65	2 ± 1		1 ± 1	
	10	13 ± 5.29	10 ± 2	*	2.33 ± 0.58	
	100	20 ± 0	20 ± 0		4.33 ± 7.51	
LIM1215	1	0.67 ± 0.58	1.67 ± 1.16		0.67 ± 1.16	ns
	10	5 ± 3	11 ± 7		13.33 ± 6.43	
	100	20 ± 0	20 ± 0		20 ± 0	

CD133 is a pentaspan transmembrane glycoprotein that has been suggested to mark cancer stem cells in various tumor types (Glumac and LeBeau 2018). CD133 positive colon cancer cells were described to be able to initiate tumor formation, when transplanted subcutaneously, or into renal capsule of immunodeficient mice (O'Brien et al. 2007; Ricci-Vitiani et al. 2007). Furthermore, CD133 expression predicts poor survival in colorectal cancer patients (Horst et al. 2009). To confirm the reduction of cancer cells with stem-cell like properties the surface expression of CD133 of cells grown in 3D in serum-free HRG-supplemented medium was compared to cells grown in 2D under basal cell culture conditions (Figure 18A). DiFi spheres expressed significantly higher amounts of CD133 on their cell surface, compared to cells grown under basal 2D culture conditions (2D: 5429 vs. 3D: 13485). Surface CD133 expression of LIM1215 spheres was below the detection limit when analyzed by flow cytometry. However, more sensitive analyses by qRT-PCR revealed an approximately 2-fold increase of CD133 mRNA expression in 3D, compared to basal 2D conditions (Figure 18B). The increased expression of CD133 indicated enrichment of stem-cell like cells during sphere formation. Taken together, the combination of scDb-Fc and Trastuzumab potently inhibited SFE and showed a benefit over the combination of IgG hu225, Trastuzumab and IgG 3-43 in ELDA assays.

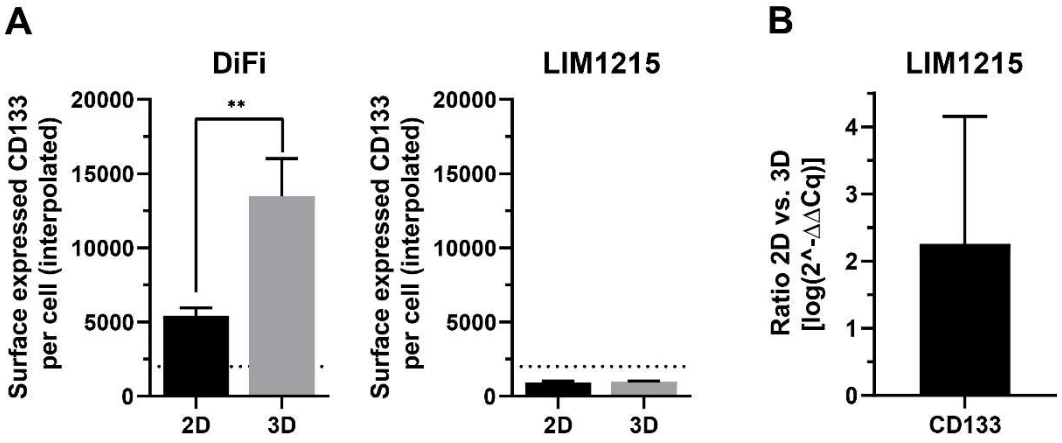

Figure 18: Expression of the cancer stem cell marker CD133 in DiFi and LIM1215 cells. A DiFi and LIM1215 cells were grown in 2D in T75 flasks in RPMI + 10 % FCS. For 3D cells were grown in pHEMA coated 10 cm dishes for 5 days. Cells were stained with primary antibodies (mouse) targeting CD133. Quantitative analysis was performed using the QIFIKIT (n=3, mean ± SD). Data were analyzed by t-Test. P ≤ 0.05 (*), P ≤ 0.01 (**), P ≤ 0.001 (***), P ≤ 0.0001 (****), n.s. (not significant). Dotted line indicates lower detection limit (2000 molecules per cell). **B** Stem cell marker CD133 analysis via qRT-PCR. Cells were cultured as described in **A** (n=3, mean ± SD).

4.4.4 Primary CRC organoids as model for drug testing

Patient derived organoids (PDO) are bridging the gap between the easy to handle cell lines and complex patient-derived xenografts (PDX) (Drost and Clevers 2018). PDOs are derived from primary cancer tissue and grown *ex-vivo* in 3D culture. CRC PDOs were reported to have well conserved cellular and biological pathways, compared to the primary tissue and are well suited for predicting response to targeted treatments in patients (Vlachogiannis et al. 2018; Schütte et al. 2017). Here, four PDO cultures established from CRC tumors expressing wild-type K-Ras, as based on genomic exon sequencing (for details see 2.12), were analyzed on proliferation upon HER-family targeted antibody treatment or treatment with a small molecule tyrosine kinase inhibitor.

Organoids are cultivated in a defined, serum-free medium that typically contains the growth factors EGF and/or bFGF (Schütte et al. 2017). First it was investigated whether the substitution of EGF and bFGF by HRG can maintain the properties of the PDOs in relation to morphology, growth rate and whole-genome gene expression. These properties were analyzed exemplarily for one PDO (PDO1), where no changes in morphology or growth rate (fold change of area per hour) were observed (EGF: 0.023 1/h vs. HRG: 0.024 1/h) (Figure 19A, B). For the whole-genome gene expression analysis a fold change >2 and Bonferroni-adjusted p-value <0.05 was set (Figure 19C). In total, reduced gene expression was observed only for two genes, DKK4 (dickkopf WNT signaling pathway inhibitor 4) and SLC14A1 (solute carrier family 14 member

1). Further analysis of the data using the false discovery rate (FDR) method of Benjamini and Hochberg leaves no significant difference in expression for any gene (Benjamini and Hochberg 1995). This provides strong evidence that HRG can substitute for EGF/bFGF, maintaining the characteristics of the primary organoid culture.

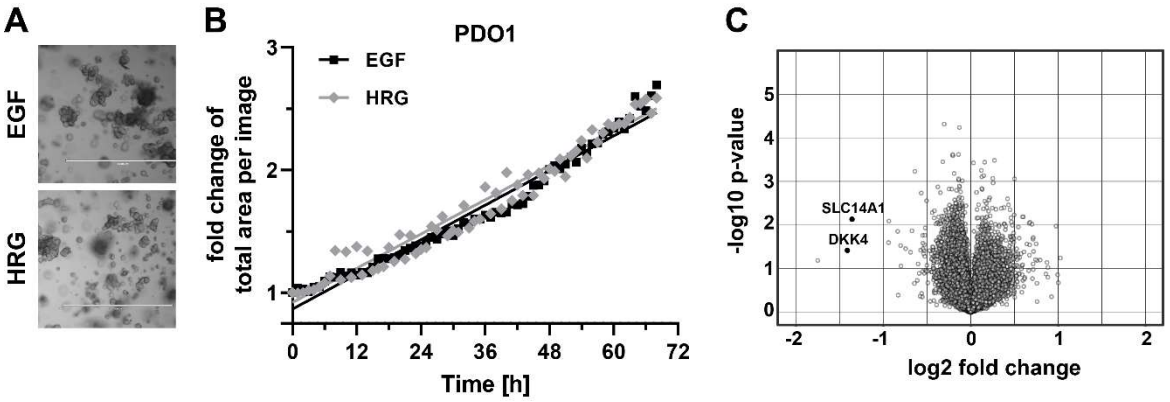

Figure 19: HRG sustains PDO growth in 3D culture. **A** Microscopy images of PDO1 organoids grown under standard conditions (EGF/bFGF) or HRG conditions. **B** Growth of PDO1 under EGF or HRG conditions was analyzed using the multispheroid analysis mode of the Incucyte S3. The occupied area at 0 h of the organoids was set as 1. Data represent mean of fold change of total area per image (EGF/bFGF n=1; HRG n=3). Simple linear regression was performed using GraphPad Prism 7 for comparison of growth rate. **C** Volcano plot of changes in the whole-genome gene expression profiles of PDO1 cells grown in EGF/bFGF or HRG supplemented medium. Two significantly differentially expressed mRNAs with fold change >2 and Bonferroni-adjusted p-value <0.05 were detected. Labeled dots indicate the two down-regulated genes (SLC14A1 and DKK4). Whole-genome gene expression profiling was conducted by Nicole Janssen.

In a next step, the proliferation of four *KRAS*-wt CRC PDOs was analyzed, which were grown in HRG-supplemented medium and treated with antibodies targeting EGFR, HER2 and/or HER3. As a control the EGFR, HER2 and HER4 inhibiting small molecule Afatinib was added (Figure 20). Treatment with IgG hu225 had no or only little effect in all four PDOs (PDO1: 89.3 ± 13.5 %, PDO2: 101.1 ± 10.2 %, PDO3: 90.7 ± 8.1 %, PDO4: 103.1 ± 8.9 %, w/o antibody control: 100 %). In all four PDOs, the dual targeting of EGFR and HER3 led to stronger inhibition of proliferation, compared to IgG hu225 alone. For PDO1 and PDO3 a stronger inhibition of proliferation was observed for the scDb-Fc, compared to IgG hu225 + IgG 3-43 (PDO1: 64.8 ± 11.9 % vs. 79.3 ± 12.6 %; PDO3: 33.7 ± 12.6 % vs. 56.0 ± 15.7 %). Both triple-targeted treatments showed potent inhibition in all four PDOs, with tendency to stronger inhibition for scDb-Fc + Trastuzumab, compared to combination of IgG hu225, Trastuzumab and IgG 3-43 (PDO1: 41.7 ± 4.0 % vs. 46.6 ± 7.6 %; PDO2: 32.4 ± 3.0 % vs. 39.0 ± 4.8 %; PDO3: 12.2 ± 5.2 % vs. 19.0 ± 7.2 %; PDO4: 50.9 ± 24.5 % vs. 65.0 ± 18.4 %). Of note, afatinib treatment showed strong inhibitory effects on the proliferation of PDO1 and PDO3, while no or only minor inhibition was observed for PDO2 and PDO4 (PDO1: 19.5 ± 16.9 %, PDO2:

83.6 ± 27.8 %, PDO3: 7.8 ± 1.4 %, PDO4: 91.0 ± 6.4 %). Taken together, triple-targeted treatment with antibodies showed strong and consistent inhibition of proliferation in all four PDOs.

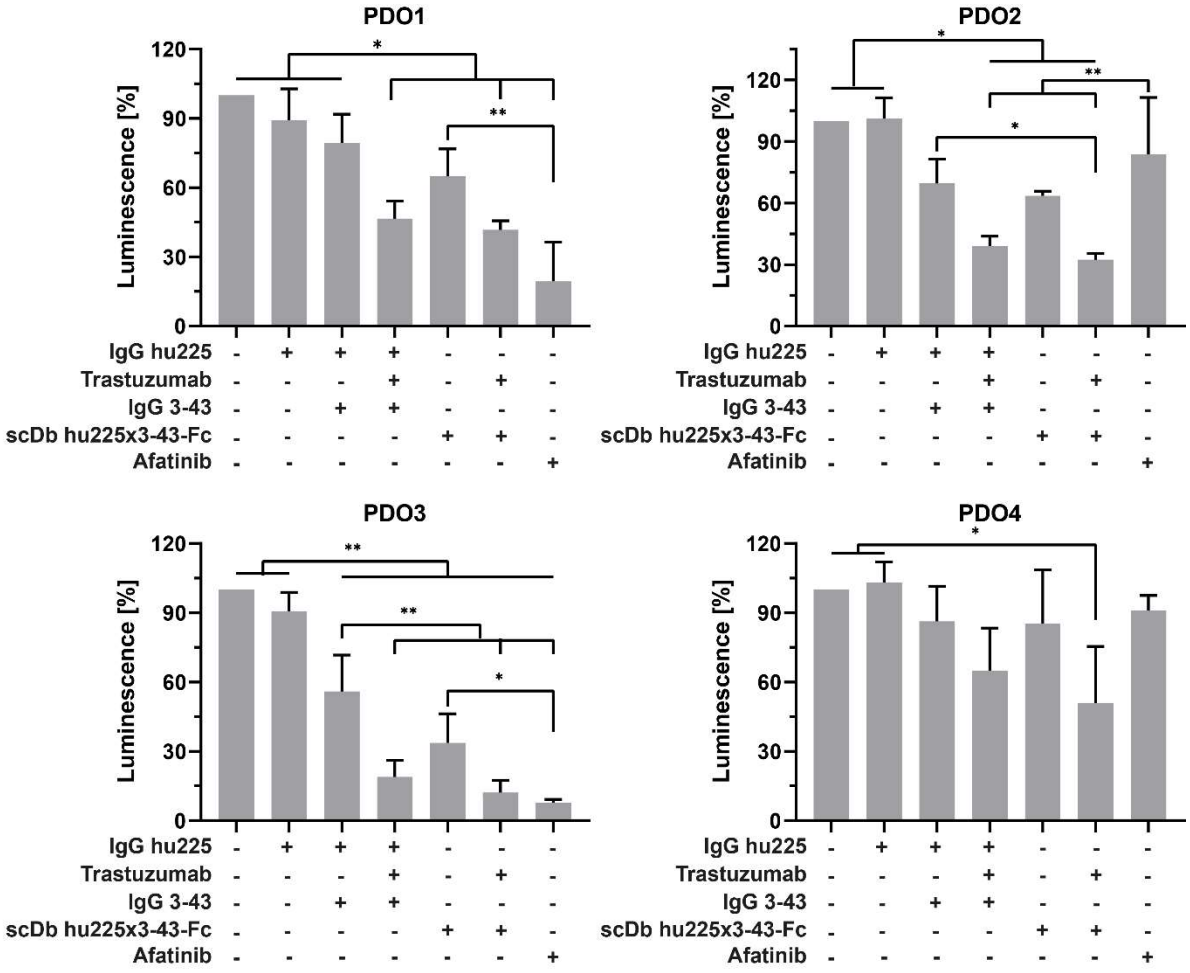

Figure 20: Growth analysis of CRC organoids treated with EGFR-, HER2- and HER3-targeting antibodies: Inhibition of proliferation of four CRC organoids (PDO1 - PDO4) after 3 days of incubation. Cells were treated with 50 nM antibodies (IgG hu225, Trastuzumab, IgG 3-43, scDb hu225x3-43-Fc, or combination of two or three antibodies) or 500 nM Afatinib. Cell viability was analyzed by luminescence measurement with CellTiter-Glo® 3D (n=3, mean ± SD). Data was analyzed by one-way ANOVA and Tukey's test for multiple comparison. P ≤ 0.05 (*), P ≤ 0.01 (**), P ≤ 0.001 (***), P ≤ 0.0001 (****), n.s. (not significant).

5 Discussion

Bispecific antibodies have become more relevant in the last decade, which reflects in the total number of antibody therapeutics entering clinical study per year. In 2010 bispecific antibodies comprised less than 10 % and in 2018 the number had risen to 25 % (Reichert 2020). In this study, a bispecific and tetravalent scDb-Fc targeting EGFR and HER3 was developed. Binding properties and affinity were similar to the parental antibodies IgG hu225 and IgG 3-43. Additionally, pharmacokinetic analysis revealed IgG-like half-life and drug exposure. In several HER-family expressing cancer cell lines, the scDb-Fc demonstrated inhibition of receptor activation and downstream signaling, which was associated with the inhibition of proliferation and migration. Furthermore, the scDb-Fc inhibited the growth of cells with stem-cell like properties, as seen in sphere formation assays of TNBC and CRC cell lines and was additionally confirmed *in vivo* in an orthotopic TNBC xenograft model. In two CRC cell lines, the combination of the bispecific antibody with the HER2-targeting antibody Trastuzumab resulted in even more potent inhibition of receptor signaling and associated biological response. Finally, the triple-targeted treatment demonstrated consistent inhibition of proliferation of four patient-derived primary organoid cultures.

5.1 Bispecific antibodies targeting EGFR and HER3

For the generation of the bispecific EGFR- and HER3-targeting antibody used in this study, the scDb-Fc format was chosen. The scDb-Fc comprises the binding moieties of the humanized Cetuximab (IgG hu225), as well as the fully human IgG 3-43. This format allows for the formation of an IgG-like bispecific and tetravalent antibody, overcoming the light chain and heavy chain problem of other bispecific IgG-like antibody formats (Brinkmann and Kontermann 2017). In total, two scDb molecules and six scDb-Fc molecules with varying linker lengths were analyzed for their purity and integrity, as well as homogeneity. Production yields varied between 0.7 mg and 46.8 mg per liter of HEK293-6E culture supernatant and were thus in the expected range of a laboratory scale production. For all eight molecules an additional peak with an approximately 2-fold higher apparent mass was observed, indicating formation of non-covalently formed dimers (Völkel et al. 2001). Consequently, preparative FPLC-SEC purification was used for dimer removal. In an earlier study, linker extension of a HER2- and HER3-targeting scDb-Fc molecule dramatically improved the production yield and binding to recombinant receptor (Rau 2017). Change of linker lengths within the EGFR- and HER3-targeting scDb-Fc, compared to the classical scDb-Fc format, did not result in beneficial changes of yield or homogeneity. However, elongation of linker 4 from 5 to 10 aa, as well as exchange of the variable domains of the two moieties in relation to the plasmid arrangement,

led to dramatic decrease of production yield. Alterations in linker length and rigidity influence both immunogenicity and conformational dynamics, thus finding the most suitable linker is crucial in the process of antibody engineering (Klein et al. 2014). Furthermore, differences in linker length can impact antibody internalization, as described for two DVD-Ig molecules (Gu et al. 2015). Here, differences in linker length led to conformational changes upon binding to the cell surface, which triggered enhanced internalization. Because in this study, none of the linker modifications had a significant beneficial effect on production yield or homogeneity, the classical scDb-Fc format was used for all further experiments (5, 15, 5 and 5 amino acids for linker 1, 2, 3 and 4, respectively) (Alt et al. 1999; Völkel et al. 2001).

Kinetic measurements by QCM of the scDb-Fc to recombinant receptors revealed an approximately 2-fold weaker affinity to EGFR and HER3, compared to the parental antibodies (Schmitt et al. 2017). Cell binding revealed strong binding with EC_{50} values similar to those of the parental antibodies. Nevertheless, despite decreased affinity and similar cell binding properties, the scDb-Fc was equal or superior to its parental antibodies at inhibiting receptor activation (phosphorylation of EGFR and HER3) and subsequent downstream signaling (phosphorylation of Akt and Erk1/2) in MCF7 and FaDu cells upon stimulation with EGF, HRG or the combination of both ligands. Comparison of a tetravalent EGFR and HER3-targeting DVD-Ig to the combination of monospecific antibodies, as well as to a bivalent form (Half DVD-Ig) revealed stronger antiproliferative effects as well as stronger activation of apoptosis, which was attributed to avidity effects (Gu et al. 2015). Similar avidity effects were also observed for the tetravalent scDb hu225x3-43-Fc. Direct comparison with the combination of parental antibodies demonstrated ~7- or ~10-fold lower IC_{50} values for the scDb-Fc in a proliferation assay with FaDu cells under unstimulated or HRG-stimulated conditions, respectively. Depending on target expression ratios, primary binding to a highly expressed target can shift the affinity to the second target toward a higher affinity interaction (Rhoden et al. 2016). Further, the ability of simultaneous binding of both targets is obligate for bispecific avidity effects, which were shown for the scDb-Fc by ELISA. High levels of EGFR, compared to HER3 (143,500 vs. 2,884, ratio: ~50:1) on FaDu cells most likely allows for initial binding to EGFR and then to HER3 with higher avidity than observed in binding and affinity analyses. This could explain the enhanced inhibition of phosphorylation of HER3 in downstream signaling analysis, as well as the up to ~10-fold lower IC_{50} values in proliferation assays of the scDb-Fc compared to the combination of the parental antibodies.

Invasion or directed migration of tumor cells is one of the hallmarks of cancer and a prerequisite for the formation of metastasis (Gerashchenko et al. 2019; Hanahan and Weinberg 2011). Compared to treatment with single parental antibodies, the scDb-Fc as well as the combination of IgG hu225 and IgG 3-43 demonstrated significant reduction of cell migration. Both receptors, EGFR and HER3, were described to increase motility upon activation, and thus inhibition of motility by the single treatments was expected (Xue et al. 2006; Smirnova et al. 2012; Yarden and Sliwkowski 2001). However, a crucial interplay between the HER2/HER3/PI3K and EGFR/HER2/PLC-γ1 signaling pathways in breast cancer cell migration and dissemination, as well as in esophageal epithelial cell invasion was described (Fichter et al. 2017; Balz et al. 2012). This interplay could explain the insufficient inhibition by the single treatments. However, the analysis of proliferation of FaDu cells embedded in a 3D matrix revealed similar inhibitory effects of scDb-Fc, compared to IgG hu225 alone, indicating dominant EGFR signaling under these conditions. This translated into long-lasting tumor growth inhibition in a FaDu xenograft model, where the scDb-Fc performed comparably to IgG hu225. Analysis of the serum protein concentration after the first and last treatment revealed accumulation of IgG hu225, IgG 3-43 and the scDb-Fc, with highest accumulation observed for IgG hu225. Cross-reactivity of the 3-43 binding moiety with mouse HER3, which results in internalization of the antibodies in non-tumor tissue, could be an explanation for the lower accumulation of IgG 3-43 and scDb-Fc (Schmitt et al. 2017; Rosestedt et al. 2019). In contrast, the hu225 moiety is not cross-reactive with mouse EGFR (Hoeben et al. 2011). Additional important aspects are pharmacokinetic properties such as half-life or drug exposure. The number of applications and the dose of a therapeutic antibody depends directly on its half-life (Kontermann 2011). For the scDb-Fc, IgG-like pharmacokinetic properties, similar to IgG 3-43, where observed in CD1 mice, making it suitable as a therapeutic.

5.2 Targeting EGFR and HER3 in TNBC

TNBC is associated with poor prognosis and linked to high morbidity (Perou et al. 2000; Foulkes et al. 2010). Although EGFR expression is abundant in up to ~80 % of TNBC patients, no EGFR-targeted therapy was approved to date (Baselga et al. 2013; Finn et al. 2009; Carey et al. 2012). Cetuximab alone, or in combination with platin-derivates showed only modest efficacy with response rates of ~10 % or ~20 % (Baselga et al. 2013; Carey et al. 2012). In TNBC patients treated with Lapatinib, an EGFR- and HER2-inhibiting small molecule, a negative trend was observed for progression free survival (Finn et al. 2009). As one possible explanation, *in vitro* studies described stabilization of an asymmetric orientation, forcing a head-to-head kinase interaction instead of head-to-tail, leading to the promotion of heterodimerization of HER2 and HER3 (Claus et al. 2018; Roskoski 2014). This orientation boosted proliferation of breast cancer

cell lines under HRG stimulation. Although TNBC is defined as HER2-negative (IHC result is 0 or 1+), studies indicate TNBC subgroups with moderate expression and alterations between hormone receptor and HER2 status can occur throughout tumor progression, as described for relapsed breast cancer (Lindström et al. 2012; Ho-Pun-Cheung et al. 2020). EGFR inhibition was described to activate resistance formation via HER3 upregulation in TNBC, whereby HER3 upregulation is highly associated with worse overall survival (Fracol et al. 2017; Bae et al. 2013; Ogden et al. 2017; Tao et al. 2014). Further, HRG, the ligand of HER3, was shown to induce the formation of breast cancer stem cells (Jeong et al. 2014). Treatment with Seribantumab, a HER3-targeting antibody, in combination with paclitaxel did not result in any benefit in a phase II trial for TNBC patients (Holmes et al. 05012015). However, bispecific targeting of EGFR and HER3 with Duligotuzumab enhanced PI3K inhibition by small molecules in preclinical studies *in vitro* and *in vivo* (Tao et al. 2014). Although a lot of effort was put into finding a targeted therapy for TNBC patients, until now only four targeted treatments are approved: Tecentriq® (anti-PD-L1, Atezolizumab) in combination with nab-Paclitaxel, Keytruda® (anti-PD-1, Pembrolizumab) combined with chemotherapy as neoadjuvant treatment, and continued as a single agent as adjuvant treatment, Lynparza® (PARP-inhibitor, Olaparib) and Trodelvy® (anti-Trop-2-SN-38, sacituzumab govitecan-hziy) (Pérez-García et al. 2020; Matthews Hew and Zuberi 2019; FDA 2020; FDA 2021). Thus, TNBC is still a disease with a high unmet need for new targeted therapeutic approaches.

In this study, TNBC treatment with the EGFR- and HER3-targeting bispecific scDb-Fc demonstrated similar inhibition of proliferation compared to IgG hu225 or the combination of IgG hu225 and IgG 3-43. Under HRG-stimulated conditions the combination of the parental antibodies and the scDb-Fc showed stronger effects on the inhibition of proliferation of MDA-MB-468 cells in comparison to single treatments with IgG hu225 or IgG 3-43. These enhanced inhibitory effects were also demonstrated in an orthotopic xenograft model, where the bispecific antibody showed strongest reduction of tumor burden. Tao and coworkers analyzed by IHC the abundance of EGFR and HER3 in TNBC patient samples, before and after treatment with Panitumumab or Cetuximab (Tao et al. 2014). EGFR abundance was decreased and HER3 abundance was increased in 25 of 42 analyzed samples after treatment. Additionally, increased dimerization of EGFR and HER3 was observed in FRET analysis. Furthermore, combined HER3-EGFR protein expression, but not individual HER3 or EGFR protein expression, was described to be an independent predictive marker for worse overall survival and distant metastasis-free survival (Ogden et al. 2017). This link between EGFR and HER3 abundance in TNBC gives one explanation for the strong beneficial effects on tumor growth inhibition by the dual targeting with the bispecific scDb-Fc, especially *in vivo*.

Generally, apart from differentiated tumor cells, cells with stem cell-like characteristics contribute to the heterogeneity of tumors (Chaffer and Weinberg 2015; Meacham and Morrison 2013). Stem cells remain in a quiescent state but can divide in an asymmetric way and are capable of undergoing EMT, and triggering invasion and metastasis (Visvader and Lindeman 2012; Cho and Kim 2020). Stem cells were shown to be responsible for resistance formation and tumor recurrence, both predominant characteristics of TNBC (Tsai et al. 2015; O'Conor et al. 2018). Treatment approaches for cancer patients usually aim at killing the bulk population of a tumor, and classical TNBC chemotherapeutics, like taxanes, were demonstrated to increase TNBC stem cell prevalence, thereby driving tumor relapse and recurrence (Creighton et al. 2009; Li et al. 2008b). Notably, EGFR-targeting therapies showed either no enrichment or even a reduction of CSC's in breast cancer cell lines and patient-derived biopsies (Li et al. 2008b; Tanei et al. 2016). In this thesis, the scDb-Fc inhibited sphere formation of MDA-MB-468 and HCC1806 TNBC cell lines in serum-free suspension culture supplemented with HRG. This sphere formation assay is routinely used for the assessment of stem cell activity and self-renewal capacity of cancer cells (Shaw et al. 2012). Additionally, ALDH measurements revealed reduced numbers of stem-cell like cells and ELDA assays demonstrated strongly reduced stem cell frequency when cells were treated with scDb-Fc. Remarkably, these strong effects on TNBC stem cells were also visible in the TNBC xenograft model, where the $ALDH^{high}$ population was reduced by IgG 3-43 and the scDb-Fc, but not by the other antibody treatments. Consistent with the literature a reduction of stem-cell like cells in sphere formation assay by EGFR targeting, and additionally a stronger decrease upon bispecific EGFR and HER3 targeting was observed. Hence, the scDb-Fc is of great potential as a therapeutic approach for TNBC tumors, regarding holistic TNBC tumor growth inhibition.

5.3 Triple-targeted treatment of HER-family in CRC

The EGFR-targeting antibody Cetuximab was first approved in 2004, and Panitumumab, another EGFR-targeting antibody, in 2006, both for the treatment of metastatic CRC. While patients where mainly selected by the expression of EGFR, IHC clinical studies revealed a major impact on therapy success by downstream effector mutations. Mutations in *KRAS* exons 2, 3 and 4, *NRAS*, *BRAF* and *PIK3CA,* and non-functional *PTEN* predict primary resistance to anti-EGFR therapies, of which one or more was found in ~50% of patients, limiting the number of patients that could benefit from an EGFR-targeting therapy (Benjamin 2016; Lièvre et al. 2006; Chang et al. 2016; Therkildsen et al. 2014). In line with TNBC, HER3 and its ligand HRG were described to induce resistance to EGFR-targeted therapies in CRC.

In this study, treatment of the CRC cancer cell line DiFi with the scDb-Fc revealed strong inhibition of proliferation in 2D and 3D assays, independent of HRG-stimulation. Interestingly, treatment of HRG-stimulated LIM1215 cells with antibodies targeting EGFR, HER3 or both receptors, respectively, was ineffective. Furthermore, dual targeting of EGFR and HER3 had no beneficial effect, compared to single treatment with IgG hu225 alone. This could be explained by the expression profile of the LIM1215 cells, which have comparable levels of EGFR, HER2 and HER3 (22,249 vs. 16,452 vs. 12,273), allowing for bypassing mechanisms by HER2. However, this expression pattern was determined under standard culture conditions, which are different from the conditions present in the proliferation assay. Western blot analysis of FaDu cells grown and treated under proliferation assay conditions, revealed increased HER2 levels in the presence of HRG and when treated with the combination of IgG hu225 and IgG 3-43, or the scDb-Fc, respectively. Of note, phosphorylation of HER2 was inhibited by the scDb-Fc, but not by the combination of IgG hu225 and IgG 3-43. This compensatory mechanism could explain the increased inhibition of proliferation by combining the scDb-Fc with the HER2-specifc Trastuzumab in LIM1215 cells and should therefore be further assessed.

Primary expression as well as *de novo* expression of HER2 were described as resistance mechanisms in CRC patients and CRC PDX models treated with Cetuximab (Yonesaka et al. 2011; Bertotti et al. 2011; Belli et al. 2019). This led to the idea of triple targeting of EGFR, HER2 and HER3 with the antibodies IgG hu225, Trastuzumab and IgG 3-43, or scDb-Fc in combination with Trastuzumab, respectively. The triple-targeted treatment with scDb-Fc and Trastuzumab significantly inhibited HRG-stimulated proliferation of LIM1215 cells. This strong inhibition of proliferation by the triple-targeted treatment could be explained by the blockade of bypassing proliferative signaling by the HER2:HER4 dimer, which is also activated by HRG (Fujiwara et al. 2014; Tzahar et al. 1996; Kennedy et al. 2019; Mota et al. 2017; Weiß et al. 1997). However, this inhibition of the proliferation was not observed for the triple treatment with the combination of IgG hu225, Trastuzumab and IgG 3-43, which could be explained by the lower IC_{50} value of the scDb-Fc compared to the combination of the parental antibodies, IgG hu225 and IgG 3-43 in a proliferation assay with FaDu cells under HRG-stimulated conditions. Furthermore, blockade of EGFR, HER2 and HER4 with an antibody mixture of IgG hu225, Trastuzumab and the HER4-targeting IgG 3U9U did not inhibit proliferation (data not shown), indicating the importance of HER3 signaling. However, downstream signaling analysis in LIM1215 cells revealed only a non-significant tendency toward stronger inhibition of phosphorylated Akt signals by the combination of the bispecific scDb-Fc and Trastuzumab. Akt regulates cell growth, contributes to cell proliferation, mediates cell survival, and inhibition of phosphorylation of Akt activates expression of HER3 (Chakrabarty et al. 2011; Bosch-Vilaro et

al. 2017). Considering the high plasticity of the HER-family expression and feedback mechanisms, which can be activated by blockade of the receptors, different time points should be analyzed to further assess the difference between the triple treatment with single monoclonal antibodies versus the combination of scDb-Fc with Trastuzumab in the context of signaling inhibition (Fichter et al. 2014; Sergina et al. 2007; Ritter et al. 2007; Kjær et al. 2016).

The healthy epithelium of the intestinal tract underlies continuous self-renewal of stem cells in the crypts, which give rise to progenitors (transit amplifying cells), which then undergo additional cell division prior to terminal differentiation and maturation (Noah et al. 2011). In the development and progression of CRC two hypothesis are discussed (Munro et al. 2018): One explains the tumorigenesis as a bottom-up process, in which mutations of crypt-based stem cells account for the tumor formation (Cole and McKalen 1963; Lane and Lev 1963). The second hypothesis describes the tumorigenesis as a top-down process, where altered cells in the superficial portions of the mucosae form new crypts, replacing the preexisting healthy ones (Shih et al. 2001). Both models, no matter which will hold true, emphasize the importance of cancer stem cells in CRC. Therefore, the EGFR-, HER2- and/or HER3-targeting antibody combinations were tested on the sphere formation of DiFi and LIM1215 cells. In both cell lines, the combination of the scDb-Fc and Trastuzumab showed the strongest inhibitory effects. Furthermore, in DiFi cells, the scDb-Fc significantly reduced secondary sphere formation as determined by ELDA assays. Compared to 2D culture, DiFi and LIM1215 cells grown as spheres expressed higher protein or mRNA levels of the stem cell marker CD133. CD133 is a well-documented CRC cancer stem cell marker, and CD133 positive cells are capable of forming tumors in mice, they remain undifferentiated when cultured in serum-free media and become more aggressive over the span of generations (Munro et al. 2018). Furthermore, CD133 positive cells were described to be resistant to chemo and radiation therapy (Zhou et al. 2017; Todaro et al. 2007; Kostovski et al. 2020). Although one single marker is not sufficient to ultimately select for colorectal cancer stem cells, this emphasizes the importance of a holistic targeting of bulk and stem cells to achieve long-lasting anti-tumor effects, preventing tumor relapse (Woodward and Sulman 2008).

CRC patient derived organoids (PDOs) are primary cultures derived from individual patients, which can be maintained long-term, cryopreserved and xenografted into immunocompromised mice and re-derived as organoids (Dart 2019; Drost and Clevers 2018). PDOs contain a self-renewing stem cell population which can differentiate into multiple cell types that can recapitulate the morphology and the genetic landscapes of donor tumors, making this cultures of primary tumor cells highly suitable as a therapeutic testing model, bridging the gap between 2D culture and xenograft models (Sato et al. 2011; Drost and Clevers 2018; Fan et al. 2019;

Schütte et al. 2017; Ooft et al. 2019). In this thesis, four *KRAS-wt* CRC PDOs were used to analyze whether triple-targeted treatments are also effective in this primary cultures. Before proliferation analysis of CRC PDOs were performed, substitution of EGF and bFGF by HRG was analyzed. EGF is used to trigger proliferation of healthy intestinal organoids, whereas CRC PDOs are not necessarily dependent on the addition of growth factor ligands (Sato et al. 2011). However, as seen for LIM1215 cells, HRG stimulation fully rescued proliferation when treated with the scDb-Fc. Hence, analysis of inhibition of proliferation was performed with PDOs cultured in HRG-supplemented medium. The substitution had no effect on PDO morphology or growth rate. In contrast, it was reported that mammary organoids cultured in medium with a substitution of EGF by HRG increased cell viability and the size of the organoids (Jardé et al. 2016). Furthermore, whole genome expression analysis revealed only two significantly differentially expressed genes, *DKK4* and *SLC14A1*. The DKK4 protein has an antagonistic activity on the Wnt/β-catenin pathway and its role in cancer is ambiguous (Cai et al. 2018). While downregulation of DKK4 expression was described in hepatocellular carcinoma, the overexpression was described in other cancer types, e.g. CRC (Cai et al. 2018). Liang et al. described upregulated expression of DKK4 in CRC cell lines and CRC primary tissue as a positive prognostic marker for survival, due to its property as a negative feedback regulator of the Wnt/β-catenin pathway (Liang et al. 2022). *SLCA14A1* encodes for type-B urea transporter (UT-B), which allows for the passive movement of urea across cell membrane. Altered expression of UT-B is associated with urothelial cancer (Hou et al. 2017). Furthermore, *SLC14A1* was identified in an intestinal stem cell signature and reported to be associated with poor clinical outcome in CRC (Alajez 2016). However, these two changes in expression were not significant after FDR method by Benjamini and Hochberg, indicating that HRG can be used to substitute EGF and bFGF (Benjamini and Hochberg 1995). In summary, CRC PDOs can be cultured in HRG-supplemented medium and are suitable for the analysis of proliferation inhibition. In future, cancer PDOs comprising matching stromal and immune cells, called "Organoid 2.0", will allow for more closer recapitulation of the properties and complex interactions found in a patients tumor (Dart 2019; Neal et al. 2018).

For the proliferation analysis in CRC PDOs, as an additional control, the small molecule Afatinib was used. Afatinib irreversibly inhibits EGFR, HER2 and HER4 kinase activity and is approved for the treatment of lung cancer patients (NSCLC, SCCL) (Li et al. 2008a). For both triple targeted treatments, either the combination of IgG hu225, Trastuzumab and IgG 3-43, or scDb-Fc + Trastuzumab similar inhibition of proliferation was observed, with the combination of scDb-Fc and Trastuzumab always showing slightly stronger effects. Interestingly, Afatinib treatment was ineffective in two out of four PDOs, while triple targeted antibody treatments

inhibited the proliferation of all four PDOs. Of note, Afatinib showed inferior effects in a clinical trial in PFS and OS compared to Cetuximab (Hickish et al. 2014). Jacobsen et al. observed for Sym013, a mixture of six antibodies targeting EGFR, HER2 and HER3 (two monospecific antibodies targeting each receptor), broad efficacious inhibition of proliferation in cell lines carrying mutations in a range of clinically relevant oncogenes, including *TP53* and *KRAS* and amplified or mutated *EGFR* and *ERBB2* genes (Jacobsen et al. 2015). In another preclinical study the same triple-targeted antibody approach was superior in inhibiting proliferation and tumor growth of breast cancer xenograft models, compared to Trastuzumab/Lapatinib (TL), Trastuzumab/Pertuzumab (TP), or T-DM1 (Schwarz et al. 2017). Thus, the triple-targeting of EGFR, HER2 and HER3 provide broader efficacy than dual- or mono-targeting of receptors of the HER-family, thus representing a better strategy to deal with primary and acquired resistances and as such may be a viable therapy option for HER-family dependent tumors.

In summary the inhibition of proliferation and the tumor-growth by the EGFR- and HER3-targeting bispecific antibody alone, and even more by the triple targeted (+ anti-HER2) approach were strong and long lasting. However, translation into the clinic will need a risk-benefit assessment. Treatment with the bispecific antibody Duligotuzumab alone or in combination with chemotherapy resulted in milder skin rash, compared to Cetuximab alone, or in combination with chemotherapy. However, more GI toxicity, susceptibility for infections and diarrhea was observed in the same study in Duligotuzumab treated patients (Fayette et al. 2016; Hill et al. 2018). On the contrary, the treatment with the combination of the HER3-targeting antibody Seribantumab and Cetuximab, revealed comparable toxicities to Cetuximab alone (Cleary et al. 2017). The safety and tolerability profile of the triple targeted antibody mixture Sym013 was determined in a phase I clinical trial and unfortunately did not warrant further development (Berlin et al. 2022). Disorders of the skin and the gastrointestinal tract were observed in 81 %, and 75 % of the patients, including dermatitis/rash, stomatitis, and diarrhea, while only very limited responses were achieved (one partial response and 12 patients with stable disease of 32 enrolled patients). These side effects are commonly observed in patients treated with single agent HER-family targeting antibodies, as well as TKIs (Li et al. 2022; Sodergren et al. 2016; Mishra et al. 2018). Undoubtfully, further studies on toxicity and tolerability for the herein described combination of scDb-Fc with Trastuzumab as described here will be necessary to assure safe administration in patients.

5.4 Conclusion and outlook

In this study, the EGFR- and HER3-targeting bispecific and tetravalent scDb hu225x3-43-Fc demonstrated strong binding to the respective recombinant receptors, as well as to HER-family

members expressing cell lines. Compared to the combination of the parental antibodies (IgG hu225 + IgG 3-43) the scDb-Fc showed comparable or enhanced inhibitory activity regarding receptor activation and signaling, migration, proliferation, and anti-tumor activity in HNSCC and TNBC xenograft mouse models. Furthermore, stem like characteristics of cancer cells were inhibited *in vitro* and in the case of TNBC also *in vivo.* Considering that cancer stem cells are the main drivers of drug resistance, metastasis, relapse and recurrence, this underlines the potential of the scDb-Fc as an effective cancer therapeutic (Cho and Kim 2020; Shibata and Hoque 2019). Further improvement of the scDb-Fc could be achieved by engineering of the γ1-Fc region, improving effector functions such as antibody-dependent cell-mediated cytotoxicity (ADCC), thereby leading to even stronger anti-tumor effects. The parental IgG 3-43 carries two mutations (S239D/I332E) in the Fc region that were demonstrated to increase Fc receptor binding, thereby enhancing ADCC (Horton et al. 2008; Schmitt et al. 2017). These mutations could easily be applied to the scDb-Fc enhancing its Fc-mediated effector functions. Overall, the anti-tumor activity of the scDb-Fc observed *in vitro* and *in vivo* warrant further studies in TNBC as well as other tumor entities.

Although, the HER-family members are well established as tumor targets, many pitfalls of targeted therapies are known. The dynamic expression of the HER-family members upon treatment that lead to the bypassing of targeted therapy is a major issue. To overcome these compensatory mechanisms, the combination of the scDb-Fc with the HER2-targeting antibody Trastuzumab was investigated for CRC cell lines and PDOs. The triple targeting of EGFR, HER2 and HER3 demonstrated strong inhibition of signaling, proliferation, and sphere formation of stem-cell like cancer cells. Furthermore, the antibody approach targeting EGFR, HER2 and HER3 was effective at inhibiting the proliferation of all four CRC PDOs tested in this study. In contrast, the small molecule Afatinib inhibited proliferation only in two out of four PDOs. Afatinib targets EGFR, HER2 and HER4, but not HER3. Since the role of HER4 and more precisely the role of the different isoforms of HER4 are not well established, targeting of HER3 appears more reasonable. However, as seen for Sym013, translation into the clinic of the triple-targeting approach failed so far. This was due to safety and tolerability issues, likely caused by the additive on-target off-tumor side effects which are typically observed for single target HER-family inhibitors, but also by the enhanced CDC and strong ADCC observed for this antibody mixture. Hence, for the triple-targeted approach with the bispecific scDb-Fc in combination with Trastuzumab an appropriate *in vitro* and *in vivo* toxicology assessment will be crucial. Combinations of antibody variants with reduced effector function of the scDb-Fc, Trastuzumab or both could improve safety and tolerability, however, most likely with the cost of reduced efficacy at the same time. Adverse events as a result of targeted antibody treatments can differ

depending on epitope specificity, affinity, geometry and valency, parameters which evidently influence neutralizing and therapeutic activity of monospecific and bispecific antibodies (Xu et al. 2013; Harms et al. 2014). Hence, the safety of the scDb-Fc in combination with Trastuzumab could differ significantly from Sym013, leaving hope that the triple-targeted approach could be translated promisingly into the clinic.

Frequent expression of the different HER-family members on different types of cancers, the well-studied requirement of homo- and heterodimerization as well as good accessibility make the HER receptors highly suitable for antibody-based treatment approaches. Furthermore, HER-family targeted treatments are now approved for more than 20 years, allowing for access to a wide range of knowledge about primary and *de novo* resistance mechanisms. This indicates that it is the right time to develop new strategies targeting this receptor tyrosine kinase family, for example, as described in this study with a new bispecific scDb-Fc, alone or in combination with Trastuzumab. In conclusion, the dual targeting approach for HER-family members with scDb-Fc, as well as the triple-targeting approach additionally combining Trastuzumab, demonstrated robust inhibition of cancer cell proliferation. Furthermore, both approaches demonstrated inhibition of growth of cancer stem cells. Consequently, the holistic approach of inhibiting the growth of the bulk population and the cancer stem cells should translate into long-lasting anti-tumor effects, avoiding drug-resistance, recurrence and metastasis.

6 Publication bibliography

Alajez, Nehad M. (2016): Large-Scale Analysis of Gene Expression Data Reveals a Novel Gene Expression Signature Associated with Colorectal Cancer Distant Recurrence. In *PloS one* 11 (12), e0167455. DOI: 10.1371/journal.pone.0167455.

Alt, Margitta; Müller, Rolf; Kontermann, Roland E. (1999): Novel tetravalent and bispecific IgG-like antibody molecules combining single-chain diabodies with the immunoglobulin γ1 Fc or CH3 region. In *FEBS letters* 454 (1-2), pp. 90–94. DOI: 10.1016/S0014-5793(99)00782-6.

Amin, Dhara N.; Campbell, Marcia R.; Moasser, Mark M. (2010): The role of HER3, the unpretentious member of the HER family, in cancer biology and cancer therapeutics. In *Seminars in cell & developmental biology* 21 (9), pp. 944–950. DOI: 10.1016/j.semcdb.2010.08.007.

Arnli, Magnus Bossum; Meta, Rahmina; Lydersen, Stian; Torp, Sverre Helge (2019): HER3 and HER4 are highly expressed in human meningiomas. In *Pathology - Research and Practice*, p. 152551. DOI: 10.1016/j.prp.2019.152551.

Arnold, Melina; Sierra, Mónica S.; Laversanne, Mathieu; Soerjomataram, Isabelle; Jemal, Ahmedin; Bray, Freddie (2017): Global patterns and trends in colorectal cancer incidence and mortality. In *Gut* 66 (4), pp. 683–691. DOI: 10.1136/gutjnl-2015-310912.

Atlas, Ella; Cardillo, Marina; Mehmi, Inderjit; Zahedkargaran, Hengameh; Tang, Careen; Lupu, Ruth (2003): Heregulin is sufficient for the promotion of tumorigenicity and metastasis of breast cancer cells in vivo. In *Molecular cancer research : MCR* 1 (3), pp. 165–175.

Babar, Tania; Blomberg, Christopher; Hoffner, Eileen; Yan, Xinhua (2014): Anti-HER2 cancer therapy and cardiotoxicity. In *Current pharmaceutical design* 20 (30), pp. 4911–4919. DOI: 10.2174/1381612820666140604145037.

Bae, Soo Youn; La Choi, Yoon; Kim, Sangmin; Kim, Minkuk; Kim, Jiyoung; Jung, Seung Pil et al. (2013): HER3 status by immunohistochemistry is correlated with poor prognosis in hormone receptor-negative breast cancer patients. In *Breast cancer research and treatment* 139 (3), pp. 741–750. DOI: 10.1007/s10549-013-2570-6.

Balz, Lydia M.; Bartkowiak, Kai; Andreas, Antje; Pantel, Klaus; Niggemann, Bernd; Zänker, Kurt S. et al. (2012): The interplay of HER2/HER3/PI3K and EGFR/HER2/PLC-γ1 signalling in breast cancer cell migration and dissemination. In *The Journal of pathology* 227 (2), pp. 234–244. DOI: 10.1002/path.3991.

Bang, Y. J.; Giaccone, G.; Im, S. A.; Oh, D. Y.; Bauer, T. M.; Nordstrom, J. L. et al. (2017): First-in-human phase 1 study of margetuximab (MGAH22), an Fc-modified chimeric monoclonal antibody, in patients with HER2-positive advanced solid tumors. In *Annals of oncology : official journal of the European Society for Medical Oncology* 28 (4), pp. 855–861. DOI: 10.1093/annonc/mdx002.

Baselga, J.; Norton, L.; Albanell, J.; Kim, Y. M.; Mendelsohn, J. (1998): Recombinant humanized anti-HER2 antibody (Herceptin) enhances the antitumor activity of paclitaxel and doxorubicin against HER2/neu overexpressing human breast cancer xenografts. In *Cancer research* 58 (13), pp. 2825–2831.

Baselga, José; Gómez, Patricia; Greil, Richard; Braga, Sofia; Climent, Miguel A.; Wardley, Andrew M. et al. (2013): Randomized phase II study of the anti-epidermal growth factor receptor monoclonal antibody cetuximab with cisplatin versus cisplatin alone in patients with metastatic triple-negative breast cancer. In *JCO* 31 (20), pp. 2586–2592. DOI: 10.1200/JCO.2012.46.2408.

Batzer, A. G.; Rotin, D.; Ureña, J. M.; Skolnik, E. Y.; Schlessinger, J. (1994): Hierarchy of binding sites for Grb2 and Shc on the epidermal growth factor receptor. In *Molecular and cellular biology* 14 (8), pp. 5192–5201.

Belli, Valentina; Matrone, Nunzia; Napolitano, Stefania; Migliardi, Giorgia; Cottino, Francesca; Bertotti, Andrea et al. (2019): Combined blockade of MEK and PI3KCA as an effective antitumor strategy in HER2 gene amplified human colorectal cancer models. In *Journal of experimental & clinical cancer research : CR* 38 (1), p. 236. DOI: 10.1186/s13046-019-1230-z.

Benedict, Chris A.; MacKrell, Albert J.; Anderson, W.French (1997): Determination of the binding affinity of an anti-CD34 single-chain antibody using a novel, flow cytometry based assay. In *Journal of immunological methods* 201 (2), pp. 223–231. DOI: 10.1016/s0022-1759(96)00227-x.

Benjamin, Laura E. (2016): Commentary on "KRAS Mutation Status Is Predictive of Response to Cetuximab Therapy in Colorectal Cancer". In *Cancer research* 76 (15), pp. 4309–4310. DOI: 10.1158/0008-5472.CAN-16-1871.

Benjamini, Yoav; Hochberg, Yosef (1995): Controlling the False Discovery Rate: A Practical and Powerful Approach to Multiple Testing. In *Journal of the Royal Statistical Society: Series B (Methodological)* 57 (1), pp. 289–300. DOI: 10.1111/j.2517-6161.1995.tb02031.x.

Berlin, Jordan; Tolcher, Anthony W.; Ding, Cliff; Whisenant, Jennifer G.; Horak, Ivan D.; Wood, Debra L. et al. (2022): First-in-human trial exploring safety, antitumor activity, and

pharmacokinetics of Sym013, a recombinant pan-HER antibody mixture, in advanced epithelial malignancies. In *Investigational new drugs* 40 (3), pp. 586–595. DOI: 10.1007/s10637-022-01217-7.

Bertotti, Andrea; Migliardi, Giorgia; Galimi, Francesco; Sassi, Francesco; Torti, Davide; Isella, Claudio et al. (2011): A molecularly annotated platform of patient-derived xenografts ("xenopatients") identifies HER2 as an effective therapeutic target in cetuximab-resistant colorectal cancer. In *Cancer Discov* 1 (6), pp. 508–523. DOI: 10.1158/2159-8290.CD-11-0109.

Black, Laurel E.; Longo, Jody F.; Carroll, Steven L. (2019): Mechanisms of Receptor Tyrosine-Protein Kinase ErbB-3 (ERBB3) Action in Human Neoplasia. In *The American journal of pathology* 189 (10), pp. 1898–1912. DOI: 10.1016/j.ajpath.2019.06.008.

Bon, Giulia; Loria, Rossella; Amoreo, Carla Azzurra; Verdina, Alessandra; Sperduti, Isabella; Mastrofrancesco, Arianna et al. (2016): Dual targeting of HER3 and MEK may overcome HER3-dependent drug-resistance of colon cancers. In *Oncotarget*. DOI: 10.18632/oncotarget.11400.

Bonner, James A.; Harari, Paul M.; Giralt, Jordi; Azarnia, Nozar; Shin, Dong M.; Cohen, Roger B. et al. (2006): Radiotherapy plus cetuximab for squamous-cell carcinoma of the head and neck. In *The New England journal of medicine* 354 (6), pp. 567–578. DOI: 10.1056/NEJMoa053422.

Bosch-Vilaro, Albert; Jacobs, Bart; Pomella, Valentina; Abbasi Asbagh, Layka; Kirkland, Richard; Michel, Joe et al. (2017): Feedback activation of HER3 attenuates response to EGFR inhibitors in colon cancer cells. In *Oncotarget* 8 (3), pp. 4277–4288. DOI: 10.18632/oncotarget.13834.

Braig, Friederike; Brandt, Anna; Goebeler, Mariele; Tony, Hans-Peter; Kurze, Anna-Katharina; Nollau, Peter et al. (2017): Resistance to anti-CD19/CD3 BiTE in acute lymphoblastic leukemia may be mediated by disrupted CD19 membrane trafficking. In *Blood* 129 (1), pp. 100–104. DOI: 10.1182/blood-2016-05-718395.

Brand, Toni M.; Hartmann, Stefan; Bhola, Neil E.; Peyser, Noah D.; Li, Hua; Zeng, Yan et al. (2017): Human Papillomavirus Regulates HER3 Expression in Head and Neck Cancer: Implications for Targeted HER3 Therapy in HPV+ Patients. In *Clinical cancer research : an official journal of the American Association for Cancer Research* 23 (12), pp. 3072–3083. DOI: 10.1158/1078-0432.CCR-16-2203.

Brandl, Christian; Haas, Cornelia; d'Argouges, Sandrine; Fisch, Tanja; Kufer, Peter; Brischwein, Klaus et al. (2007): The effect of dexamethasone on polyclonal T cell activation and redirected target cell lysis as induced by a CD19/CD3-bispecific single-chain antibody construct. In

Cancer immunology, immunotherapy : CII 56 (10), pp. 1551–1563. DOI: 10.1007/s00262-007-0298-z.

Bray, Freddie; Ferlay, Jacques; Soerjomataram, Isabelle; Siegel, Rebecca L.; Torre, Lindsey A.; Jemal, Ahmedin (2018): Global cancer statistics 2018: GLOBOCAN estimates of incidence and mortality worldwide for 36 cancers in 185 countries. In *CA: a cancer journal for clinicians* 68 (6), pp. 394–424. DOI: 10.3322/caac.21492.

Brinkmann, Ulrich; Kontermann, Roland E. (2017): The making of bispecific antibodies. In *mAbs* 9 (2), pp. 182–212. DOI: 10.1080/19420862.2016.1268307.

Brinkmann, Ulrich; Kontermann, Roland E. (2021): Bispecific antibodies. In *Science (New York, N.Y.)* 372 (6545), pp. 916–917. DOI: 10.1126/science.abg1209.

Britsch, Stefan (2007): The Neuregulin-I/ErbB Signaling System in Development and Disease. Berlin, Heidelberg: Springer Berlin Heidelberg (190).

Cai, Xinjia; Yao, Zhigang; Li, Long; Huang, Junhui (2018): Role of DKK4 in Tumorigenesis and Tumor Progression. In *International journal of biological sciences* 14 (6), pp. 616–621. DOI: 10.7150/ijbs.24329.

Carey, Lisa A.; Rugo, Hope S.; Marcom, P. Kelly; Mayer, Erica L.; Esteva, Francisco J.; Ma, Cynthia X. et al. (2012): TBCRC 001: randomized phase II study of cetuximab in combination with carboplatin in stage IV triple-negative breast cancer. In *JCO* 30 (21), pp. 2615–2623. DOI: 10.1200/JCO.2010.34.5579.

Carpenter, C. L.; Duckworth, B. C.; Auger, K. R.; Cohen, B.; Schaffhausen, B. S.; Cantley, L. C. (1990): Purification and characterization of phosphoinositide 3-kinase from rat liver. In *The Journal of biological chemistry* 265 (32), pp. 19704–19711.

Carter, P.; Presta, L.; Gorman, C. M.; Ridgway, J. B.; Henner, D.; Wong, W. L. et al. (1992): Humanization of an anti-p185HER2 antibody for human cancer therapy. In *Proceedings of the National Academy of Sciences of the United States of America* 89 (10), pp. 4285–4289. DOI: 10.1073/pnas.89.10.4285.

Caruso, Catherine (2019): ZW25 Effective in HER2-Positive Cancers. In *Cancer Discov* 9 (1), p. 8. DOI: 10.1158/2159-8290.CD-NB2018-162.

Chaffer, Christine L.; Weinberg, Robert A. (2015): How does multistep tumorigenesis really proceed? In *Cancer Discov* 5 (1), pp. 22–24. DOI: 10.1158/2159-8290.CD-14-0788.

Chakrabarty, Anindita; Sánchez, Violeta; Kuba, María G.; Rinehart, Cammie; Arteaga, Carlos L. (2011): Feedback upregulation of HER3 (ErbB3) expression and activity attenuates antitumor

effect of PI3K inhibitors. In *Proceedings of the National Academy of Sciences of the United States of America* 109 (8), pp. 2718–2723. DOI: 10.1073/pnas.1018001108.

Chang, Matthew T.; Asthana, Saurabh; Gao, Sizhi Paul; Lee, Byron H.; Chapman, Jocelyn S.; Kandoth, Cyriac et al. (2015): Identifying recurrent mutations in cancer reveals widespread lineage diversity and mutational specificity. In *Nature biotechnology* 34 (2), pp. 155–163. DOI: 10.1038/nbt.3391.

Chang, Yu-Yao; Lin, Pei-Ching; Lin, Hung-Hsin; Lin, Jen-Kou; CHEN, WEI-SHONE; Jiang, Jeng-Kai et al. (2016): Mutation spectra of RAS gene family in colorectal cancer. In *American journal of surgery* 212 (3), 537-544.e3. DOI: 10.1016/j.amjsurg.2016.02.013.

Chenoweth, Alicia; Crescioli, Silvia (2022): Antibody therapeutics product data. Edited by Antibody Society. Available online at https://www.antibodysociety.org/antibody-therapeutics-product-data/, checked on 11/12/2022.

Cheong, Kwang Ho; Lee, Seung Hyun; Lin, Powei; Lee, Byoul; Hwang, Jae Woong (2016): ANTI-EGFR/ANTI-HER2 BISPECIFIC ANTIBODIES WITH ANTI-EGFR DARPINS. Available online at https://patents.google.com/patent/US9499622B2/en.

Cho, Yena; Kim, Yong Kee (2020): Cancer Stem Cells as a Potential Target to Overcome Multidrug Resistance. In *Front. Oncol.* 10, Article 764. DOI: 10.3389/fonc.2020.00764.

Choi, Byoungsan; Cha, Minkwon; Eun, Gee Sung; Lee, Dae Hee; Lee, Seul; Ehsan, Muhammad et al. (2020): Single-molecule functional anatomy of endogenous HER2-HER3 heterodimers. In *eLife* 9. DOI: 10.7554/eLife.53934.

Citri, Ami; Yarden, Yosef (2006): EGF-ERBB signalling: towards the systems level. In *Nature reviews. Molecular cell biology* 7 (7), pp. 505–516. DOI: 10.1038/nrm1962.

Claus, Jeroen; Patel, Gargi; Autore, Flavia; Colomba, Audrey; Weitsman, Gregory; Soliman, Tanya N. et al. (2018): Inhibitor-induced HER2-HER3 heterodimerisation promotes proliferation through a novel dimer interface. In *eLife* 7. DOI: 10.7554/eLife.32271.

Cleary, James M.; McRee, Autumn J.; Shapiro, Geoffrey I.; Tolaney, Sara M.; O'Neil, Bert H.; Kearns, Jeffrey D. et al. (2017): A phase 1 study combining the HER3 antibody seribantumab (MM-121) and cetuximab with and without irinotecan. In *Investigational new drugs* 35 (1), pp. 68–78. DOI: 10.1007/s10637-016-0399-7.

Cohen, B. D.; Kiener, P. A.; Green, J. M.; Foy, L.; Fell, H. P.; Zhang, K. (1996): The relationship between human epidermal growth-like factor receptor expression and cellular transformation in NIH3T3 cells. In *The Journal of biological chemistry* 271 (48), pp. 30897–30903. DOI: 10.1074/jbc.271.48.30897.

Cohen, Ezra E. W.; Bell, R. Bryan; Bifulco, Carlo B.; Burtness, Barbara; Gillison, Maura L.; Harrington, Kevin J. et al. (2019): The Society for Immunotherapy of Cancer consensus statement on immunotherapy for the treatment of squamous cell carcinoma of the head and neck (HNSCC). In *Journal for immunotherapy of cancer* 7 (1), p. 184. DOI: 10.1186/s40425-019-0662-5.

Cohen, Roger B. (2003): Epidermal growth factor receptor as a therapeutic target in colorectal cancer. In *Clinical colorectal cancer* 2 (4), pp. 246–251. DOI: 10.3816/CCC.2003.n.006.

Cole, Jack W.; McKalen, Anne (1963): Studies on the morphogenesis of adenomatous polyps in the human colon. In *Cancer* 16 (8), pp. 998–1002. DOI: 10.1002/1097-0142(196308)16:8<998::AID-CNCR2820160806>3.0.CO;2-C.

Conradi, Lena-Christin; Spitzner, Melanie; Metzger, Anna-Lena; Kisly, Merle; Middel, Peter; Bohnenberger, Hanibal et al. (2019): Combined targeting of HER-2 and HER-3 represents a promising therapeutic strategy in colorectal cancer. In *BMC cancer* 19 (1), p. 880. DOI: 10.1186/s12885-019-6051-0.

Conradi, Lena-Christin; Styczen, Hanna; Sprenger, Thilo; Wolff, Hendrik A.; Rödel, Claus; Nietert, Manuel et al. (2013): Frequency of HER-2 positivity in rectal cancer and prognosis. In *The American journal of surgical pathology* 37 (4), pp. 522–531. DOI: 10.1097/PAS.0b013e318272ff4d.

Conte, PierFranco; Schneeweiss, Andreas; Loibl, Sibylle; Mamounas, Eleftherios P.; Minckwitz, Gunter von; Mano, Max S. et al. (2020): Patient-reported outcomes from KATHERINE: A phase 3 study of adjuvant trastuzumab emtansine versus trastuzumab in patients with residual invasive disease after neoadjuvant therapy for human epidermal growth factor receptor 2-positive breast cancer. In *Cancer*. DOI: 10.1002/cncr.32873.

Costa, Ricardo L. B.; Czerniecki, Brian J. (2020): Clinical development of immunotherapies for HER2+ breast cancer: a review of HER2-directed monoclonal antibodies and beyond. In *NPJ breast cancer* 6, p. 10. DOI: 10.1038/s41523-020-0153-3.

Creighton, Chad J.; Li, Xiaoxian; Landis, Melissa; Dixon, J. Michael; Neumeister, Veronique M.; Sjolund, Ashley et al. (2009): Residual breast cancers after conventional therapy display mesenchymal as well as tumor-initiating features. In *Proceedings of the National Academy of Sciences of the United States of America* 106 (33), pp. 13820–13825. DOI: 10.1073/pnas.0905718106.

Dart, Anna (2019): Organoid 2.0. In *Nat Rev Cancer* 19 (3), pp. 126–127. DOI: 10.1038/s41568-019-0108-x.

Davis, Jonathan H.; Aperlo, Christel; Li, Yue; Kurosawa, Emmi; Lan, Yan; Lo, Kin-Ming; Huston, James S. (2010): SEEDbodies: fusion proteins based on strand-exchange engineered domain (SEED) CH3 heterodimers in an Fc analogue platform for asymmetric binders or immunofusions and bispecific antibodies. In *Protein engineering, design & selection : PEDS* 23 (4), pp. 195–202. DOI: 10.1093/protein/gzp094.

Denlinger, Crystal Shereen; Alsina Maqueda, Maria; Watkins, David J.; Sym, Sun Jin; Bendell, Johanna C.; Park, Se Hoon et al. (2016): Randomized phase 2 study of paclitaxel (PTX), trastuzumab (T) with or without MM-111 in HER2 expressing gastroesophageal cancers (GEC). In *JCO* 34 (15_suppl), p. 4043. DOI: 10.1200/JCO.2016.34.15_suppl.4043.

Dent, Rebecca; Trudeau, Maureen; Pritchard, Kathleen I.; Hanna, Wedad M.; Kahn, Harriet K.; Sawka, Carol A. et al. (2007): Triple-negative breast cancer: clinical features and patterns of recurrence. In *Clinical cancer research : an official journal of the American Association for Cancer Research* 13 (15 Pt 1), pp. 4429–4434. DOI: 10.1158/1078-0432.CCR-06-3045.

Drebin, J. A.; Link, V. C.; Stern, D. F.; Weinberg, R. A.; Greene, M. I. (1986): Development of monoclonal antibodies reactive with the product of the neu oncogene. In *Symposium on Fundamental Cancer Research* 38, pp. 277–289.

Drost, Jarno; Clevers, Hans (2018): Organoids in cancer research. In *Nat Rev Cancer* 18 (7), pp. 407–418. DOI: 10.1038/s41568-018-0007-6.

Duvvuri, Umamaheswar; George, Jonathan; Kim, Seungwon; Alvarado, Diego; Neumeister, Veronique M.; Chenna, Ahmed et al. (2019): Molecular and Clinical Activity of CDX-3379, an Anti-ErbB3 Monoclonal Antibody, in Head and Neck Squamous Cell Carcinoma Patients. In *Clinical cancer research : an official journal of the American Association for Cancer Research* 25 (19), pp. 5752–5758. DOI: 10.1158/1078-0432.CCR-18-3453.

El-Deiry, Wafik S.; Vijayvergia, Namrata; Xiu, Joanne; Scicchitano, Angelique; Lim, Bora; Yee, Nelson S. et al. (2015): Molecular profiling of 6,892 colorectal cancer samples suggests different possible treatment options specific to metastatic sites. In *Cancer biology & therapy* 16 (12), pp. 1726–1737. DOI: 10.1080/15384047.2015.1113356.

Elenius, K.; Corfas, G.; Paul, S.; Choi, C. J.; Rio, C.; Plowman, G. D.; Klagsbrun, M. (1997): A novel juxtamembrane domain isoform of HER4/ErbB4. Isoform-specific tissue distribution and differential processing in response to phorbol ester. In *The Journal of biological chemistry* 272 (42), pp. 26761–26768. DOI: 10.1074/jbc.272.42.26761.

Erben, Larissa; He, Ming-Xiao; Laeremans, Annelies; Park, Emily; Buonanno, Andres (2018): A Novel Ultrasensitive In Situ Hybridization Approach to Detect Short Sequences and Splice

Variants with Cellular Resolution. In *Molecular neurobiology* 55 (7), pp. 6169–6181. DOI: 10.1007/s12035-017-0834-6.

Erickson, S. L.; O'Shea, K. S.; Ghaboosi, N.; Loverro, L.; Frantz, G.; Bauer, M. et al. (1997): ErbB3 is required for normal cerebellar and cardiac development: a comparison with ErbB2- and heregulin-deficient mice. In *Development (Cambridge, England)* 124 (24), pp. 4999–5011.

Fan, Han; Demirci, Utkan; Chen, Pu (2019): Emerging organoid models: leaping forward in cancer research. In *Journal of hematology & oncology* 12 (1), p. 142. DOI: 10.1186/s13045-019-0832-4.

Fayette, Jérôme; Wirth, Lori; Oprean, Cristina; Udrea, Anghel; Jimeno, Antonio; Rischin, Danny et al. (2016): Randomized Phase II Study of Duligotuzumab (MEHD7945A) vs. Cetuximab in Squamous Cell Carcinoma of the Head and Neck (MEHGAN Study). In *Frontiers in oncology* 6, p. 232. DOI: 10.3389/fonc.2016.00232.

FDA (2021): FDA approves pembrolizumab for high-risk early-stage triple-negative breast cancer. Edited by Food and Drug Administration.

FDA 2020: FDA Approves New Therapy for Triple Negative Breast Cancer That Has Spread, Not Responded to Other Treatments, Food and Drug Administration. Available online at https://www.fda.gov/news-events/press-announcements/fda-approves-new-therapy-triple-negative-breast-cancer-has-spread-not-responded-other-treatments, checked on 6/2/2020.

Fernández-Real, José Manuel; Menendez, Javier A.; Frühbeck, Gema; Moreno-Navarrete, José María; Vazquez-Martín, Alejandro; Ricart, Wifredo (2010): Serum HER-2 concentration is associated with insulin resistance and decreases after weight loss. In *Nutrition & metabolism* 7, p. 14. DOI: 10.1186/1743-7075-7-14.

Fichter, Christiane Daniela; Przypadlo, Camilla Maria; Buck, Achim; Herbener, Nicola; Riedel, Bianca; Schäfer, Luisa et al. (2017): A new model system identifies epidermal growth factor receptor-human epidermal growth factor receptor 2 (HER2) and HER2-human epidermal growth factor receptor 3 heterodimers as potent inducers of oesophageal epithelial cell invasion. In *The Journal of pathology* 243 (4), pp. 481–495. DOI: 10.1002/path.4987.

Fichter, Christiane Daniela; Timme, Sylvia; Braun, Julia Alexandra; Gudernatsch, Verena; Schöpflin, Anja; Bogatyreva, Lioudmilla et al. (2014): EGFR, HER2 and HER3 dimerization patterns guide targeted inhibition in two histotypes of esophageal cancer. In *International journal of cancer* 135 (7), pp. 1517–1530. DOI: 10.1002/ijc.28771.

Finn, Richard S.; Press, Michael F.; Dering, Judy; Arbushites, Michael; Koehler, Maria; Oliva, Cristina et al. (2009): Estrogen receptor, progesterone receptor, human epidermal growth

factor receptor 2 (HER2), and epidermal growth factor receptor expression and benefit from lapatinib in a randomized trial of paclitaxel with lapatinib or placebo as first-line treatment in HER2-negative or unknown metastatic breast cancer. In *JCO* 27 (24), pp. 3908–3915. DOI: 10.1200/JCO.2008.18.1925.

Foulkes, William D.; Smith, Ian E.; Reis-Filho, Jorge S. (2010): Triple-negative breast cancer. In *The New England journal of medicine* 363 (20), pp. 1938–1948. DOI: 10.1056/NEJMra1001389.

Fracol, Megan; Datta, Jashodeep; Lowenfeld, Lea; Xu, Shuwen; Zhang, Paul J.; Fisher, Carla S.; Czerniecki, Brian J. (2017): Loss of Anti-HER-3 CD4+ T-Helper Type 1 Immunity Occurs in Breast Tumorigenesis and is Negatively Associated with Outcomes. In *Annals of surgical oncology* 24 (2), pp. 407–417. DOI: 10.1245/s10434-016-5584-6.

Fremd, Carlo; Jaeger, Dirk; Schneeweiss, Andreas (2018): Targeted and immuno-biology driven treatment strategies for triple-negative breast cancer: current knowledge and future perspectives. In *Expert review of anticancer therapy*, pp. 1–14. DOI: 10.1080/14737140.2019.1537785.

Fuchs, I.; Vorsteher, N.; Bühler, H.; Evers, K.; Sehouli, J.; Schaller, G.; Kümmel, S. (2007): The prognostic significance of human epidermal growth factor receptor correlations in squamous cell cervical carcinoma. In *Anticancer research* 27 (2), pp. 959–963.

Fudenberg, H. H.; Drews, Genevieve; Nisonoff, A. (1964): SEROLOGIC DEMONSTRATION OF DUAL SPECIFICITY OF RABBIT BIVALENT HYBRID ANTIBODY. In *The Journal of Experimental Medicine* 119 (1), pp. 151–166.

Fujiwara, Saori; Hung, Mutsuko; Yamamoto-Ibusuk, Chi-Ming; Yamamoto, Yutaka; Yamamoto, Satoko; Tomiguchi, Mai et al. (2014): The localization of HER4 intracellular domain and expression of its alternately-spliced isoforms have prognostic significance in ER+ HER2- breast cancer. In *Oncotarget* 5 (11), pp. 3919–3930. DOI: 10.18632/oncotarget.2002.

Gandullo-Sánchez, Lucía; Ocaña, Alberto; Pandiella, Atanasio (2022): HER3 in cancer: from the bench to the bedside. In *Journal of experimental & clinical cancer research : CR* 41 (1), p. 310. DOI: 10.1186/s13046-022-02515-x.

Garrett, Thomas P.J.; McKern, Neil M.; Lou, Meizhen; Elleman, Thomas C.; Adams, Timothy E.; Lovrecz, George O. et al. (2003): The Crystal Structure of a Truncated ErbB2 Ectodomain Reveals an Active Conformation, Poised to Interact with Other ErbB Receptors. In *Molecular cell* 11 (2), pp. 495–505. DOI: 10.1016/s1097-2765(03)00048-0.

Gassmann, M.; Casagranda, F.; Orioli, D.; Simon, H.; Lai, C.; Klein, R.; Lemke, G. (1995): Aberrant neural and cardiac development in mice lacking the ErbB4 neuregulin receptor. In *Nature* 378 (6555), pp. 390–394. DOI: 10.1038/378390a0.

Gerashchenko, Tatiana S.; Novikov, Nikita M.; Krakhmal, Nadezhda V.; Zolotaryova, Sofia Y.; Zavyalova, Marina V.; Cherdyntseva, Nadezhda V. et al. (2019): Markers of Cancer Cell Invasion: Are They Good Enough? In *Journal of clinical medicine* 8 (8). DOI: 10.3390/jcm8081092.

Geuijen, Cecile A. W.; Nardis, Camilla de; Maussang, David; Rovers, Eric; Gallenne, Tristan; Hendriks, Linda J. A. et al. (2018): Unbiased Combinatorial Screening Identifies a Bispecific IgG1 that Potently Inhibits HER3 Signaling via HER2-Guided Ligand Blockade. In *Cancer cell* 33 (5), 922-936.e10. DOI: 10.1016/j.ccell.2018.04.003.

Glumac, Paige M.; LeBeau, Aaron M. (2018): The role of CD133 in cancer: a concise review. In *Clinical and translational medicine* 7 (1), p. 18. DOI: 10.1186/s40169-018-0198-1.

Goebeler, Maria-Elisabeth; Bargou, Ralf C. (2020): T cell-engaging therapies - BiTEs and beyond. In *Nature reviews. Clinical oncology*. DOI: 10.1038/s41571-020-0347-5.

Golay, Josée; Choblet, Sylvie; Iwaszkiewicz, Justyna; Cérutti, Pierre; Ozil, Annick; Loisel, Séverine et al. (2016): Design and Validation of a Novel Generic Platform for the Production of Tetravalent IgG1-like Bispecific Antibodies. In *Journal of immunology (Baltimore, Md. : 1950)* 196 (7), pp. 3199–3211. DOI: 10.4049/jimmunol.1501592.

Goldhirsch, A.; Winer, E. P.; Coates, A. S.; Gelber, R. D.; Piccart-Gebhart, M.; Thürlimann, B.; Senn, H-J (2013): Personalizing the treatment of women with early breast cancer: highlights of the St Gallen International Expert Consensus on the Primary Therapy of Early Breast Cancer 2013. In *Annals of oncology : official journal of the European Society for Medical Oncology* 24 (9), pp. 2206–2223. DOI: 10.1093/annonc/mdt303.

Goldstein, N. I.; Prewett, M.; Zuklys, K.; Rockwell, P.; Mendelsohn, J. (1995): Biological efficacy of a chimeric antibody to the epidermal growth factor receptor in a human tumor xenograft model. In *Clinical cancer research : an official journal of the American Association for Cancer Research* 1 (11), pp. 1311–1318.

Gonçalves, Homero; Guerra, Maximiliano Ribeiro; Duarte Cintra, Jane Rocha; Fayer, Vívian Assis; Brum, Igor Vilela; Bustamante Teixeira, Maria Teresa (2018): Survival Study of Triple-Negative and Non-Triple-Negative Breast Cancer in a Brazilian Cohort. In *Clinical Medicine Insights. Oncology* 12, 1179554918790563. DOI: 10.1177/1179554918790563.

Gu, Jinming; Yang, Jinsong; Chang, Qing; Liu, Zhihong; Ghayur, Tariq; Gu, Jijie (2015): Identification of Anti-EGFR and Anti-ErbB3 Dual Variable Domains Immunoglobulin (DVD-Ig) Proteins with Unique Activities. In *PloS one* 10 (5), e0124135. DOI: 10.1371/journal.pone.0124135.

Hamblett, Kevin J.; Hammond, Phil W.; Barnscher, Stuart D.; Fung, Vincent K.; Davies, Rupert H.; Wickman, Grant R. et al. (07012018): Abstract 3914: ZW49, a HER2-targeted biparatopic antibody-drug conjugate for the treatment of HER2-expressing cancers. In : Experimental and Molecular Therapeutics. Proceedings: AACR Annual Meeting 2018; April 14-18, 2018; Chicago, IL: American Association for Cancer Research, p. 3914.

Hamilton, Erika Paige; Patel, Manish R.; Pegram, Mark D.; Tan, Antoinette R.; Storniolo, Anna Maria; Li, John et al. (2016): A Phase 1 study to evaluate the safety, pharmacokinetics, immunogenicity, and antitumor activity of MEDI4276 in patients with select HER2-expressing advanced solid tumors. In *JCO* 34 (15_suppl), TPS632-TPS632. DOI: 10.1200/JCO.2016.34.15_suppl.TPS632.

Hammerman, Peter S.; Hayes, D. Neil; Grandis, Jennifer R. (2015): Therapeutic insights from genomic studies of head and neck squamous cell carcinomas. In *Cancer Discov* 5 (3), pp. 239–244. DOI: 10.1158/2159-8290.CD-14-1205.

Hanahan, Douglas; Weinberg, Robert A. (2011): Hallmarks of cancer: the next generation. In *Cell* 144 (5), pp. 646–674. DOI: 10.1016/j.cell.2011.02.013.

Haratani, Koji; Yonesaka, Kimio; Takamura, Shiki; Maenishi, Osamu; Kato, Ryoji; Takegawa, Naoki et al. (2019): U3-1402 sensitizes HER3-expressing tumors to PD-1 blockade by immune activation. In *The Journal of clinical investigation* 130 (1), pp. 374–388. DOI: 10.1172/JCI126598.

Harms, Brian D.; Kearns, Jeffrey D.; Iadevaia, Sergio; Lugovskoy, Alexey A. (2014): Understanding the role of cross-arm binding efficiency in the activity of monoclonal and multispecific therapeutic antibodies. In *Methods (San Diego, Calif.)* 65 (1), pp. 95–104. DOI: 10.1016/j.ymeth.2013.07.017.

Hashimoto, Yuuri; Koyama, Kumiko; Kamai, Yasuki; Hirotani, Kenji; Ogitani, Yusuke; Zembutsu, Akiko et al. (2019): A Novel HER3-Targeting Antibody-Drug Conjugate, U3-1402, Exhibits Potent Therapeutic Efficacy through the Delivery of Cytotoxic Payload by Efficient Internalization. In *Clinical cancer research : an official journal of the American Association for Cancer Research*. DOI: 10.1158/1078-0432.CCR-19-1745.

Hellyer, N. J.; Cheng, K.; Koland, J. G. (1998): ErbB3 (HER3) interaction with the p85 regulatory subunit of phosphoinositide 3-kinase. In *The Biochemical journal* 333 (Pt 3), pp. 757–763. DOI: 10.1042/bj3330757.

Helsten, Teresa L.; Lo, Shelly S.; Yau, Christina; Kalinsky, Kevin; Elias, Anthony D.; Wallace, Anne M. et al. (02152020): Abstract P3-11-02: Evaluation of patritumab/paclitaxel/trastuzumab over standard paclitaxel/trastuzumab in early stage, high-risk HER2 positive breast cancer: Results from the neoadjuvant I-SPY 2 trial. In : Poster Session Abstracts. Abstracts: 2019 San Antonio Breast Cancer Symposium; December 10-14, 2019; San Antonio, Texas: American Association for Cancer Research, P3-11-02-P3-11-02.

Herbst, Roy S.; Kies, Merrill S. (2003): Gefitinib: current and future status in cancer therapy. In *Clinical advances in hematology & oncology : H&O* 1 (8), pp. 466–472.

Hickish, Tamas; Cassidy, Jim; Propper, David; Chau, Ian; Falk, Stephen; Ford, Hugo et al. (2014): A randomised, open-label phase II trial of afatinib versus cetuximab in patients with metastatic colorectal cancer. In *European journal of cancer (Oxford, England : 1990)* 50 (18), pp. 3136–3144. DOI: 10.1016/j.ejca.2014.08.008.

Hill, Andrew G.; Findlay, Michael P.; Burge, Matthew E.; Jackson, Christopher; Alfonso, Pilar Garcia; Samuel, Leslie et al. (2018): Phase II Study of the Dual EGFR/HER3 Inhibitor Duligotuzumab (MEHD7945A) versus Cetuximab in Combination with FOLFIRI in Second-Line RAS Wild-Type Metastatic Colorectal Cancer. In *Clinical cancer research : an official journal of the American Association for Cancer Research* 24 (10), pp. 2276–2284. DOI: 10.1158/1078-0432.CCR-17-0646.

Hinohara, Kunihiko; Kobayashi, Seiichiro; Kanauchi, Hajime; Shimizu, Seiichiro; Nishioka, Kotoe; Tsuji, Ei-ichi et al. (2012): ErbB receptor tyrosine kinase/NF-κB signaling controls mammosphere formation in human breast cancer. In *Proceedings of the National Academy of Sciences of the United States of America* 109 (17), pp. 6584–6589. DOI: 10.1073/pnas.1113271109.

Hoeben, Bianca A. W.; Molkenboer-Kuenen, Janneke D. M.; Oyen, Wim J. G.; Peeters, Wenny J. M.; Kaanders, Johannes H. A. M.; Bussink, Johan; Boerman, Otto C. (2011): Radiolabeled cetuximab: dose optimization for epidermal growth factor receptor imaging in a head-and-neck squamous cell carcinoma model. In *International journal of cancer* 129 (4), pp. 870–878. DOI: 10.1002/ijc.25727.

Hollmén, M.; Määttä, J. A.; Bald, L.; Sliwkowski, M. X.; Elenius, K. (2009): Suppression of breast cancer cell growth by a monoclonal antibody targeting cleavable ErbB4 isoforms. In *Oncogene* 28 (10), pp. 1309–1319. DOI: 10.1038/onc.2008.481.

Hollmén, Maija; Liu, Ping; Kurppa, Kari; Wildiers, Hans; Reinvall, Irene; Vandorpe, Thijs et al. (2012): Proteolytic processing of ErbB4 in breast cancer. In *PloS one* 7 (6), e39413. DOI: 10.1371/journal.pone.0039413.

Holmes, Frankie A.; McIntyre, Kristi J.; Krop, Ian E.; Osborne, Cynthia R.; Smith II, John W.; Modiano, Manuel R. et al. (05012015): Abstract P3-11-03: A randomized, phase 2 trial of preoperative MM-121 with paclitaxel in triple negative (TN) and hormone receptor (HR) positive, HER2-negative breast cancer. In : Poster Session Abstracts. Thirty-Seventh Annual CTRC-AACR San Antonio Breast Cancer Symposium; December 9-13, 2014; San Antonio, TX: American Association for Cancer Research, P3-11-03-P3-11-03.

Honer, Jonas (2016): Multivalent and bispecific antibodies targeting ErbB family members. Stuttgart. Master Thesis.

Ho-Pun-Cheung, Alexandre; Bazin, Hervé; Boissière-Michot, Florence; Mollevi, Caroline; Simony-Lafontaine, Joëlle; Landas, Emeline et al. (2020): Quantification of HER1, HER2 and HER3 by time-resolved Förster resonance energy transfer in FFPE triple-negative breast cancer samples. In *British journal of cancer* 122 (3), pp. 397–404. DOI: 10.1038/s41416-019-0670-8.

Horst, David; Kriegl, Lydia; Engel, Jutta; Kirchner, Thomas; Jung, Andreas (2009): Prognostic significance of the cancer stem cell markers CD133, CD44, and CD166 in colorectal cancer. In *Cancer investigation* 27 (8), pp. 844–850. DOI: 10.1080/07357900902744502.

Horton, Holly M.; Bernett, Matthew J.; Pong, Erik; Peipp, Matthias; Karki, Sher; Chu, Seung Y. et al. (2008): Potent in vitro and in vivo activity of an Fc-engineered anti-CD19 monoclonal antibody against lymphoma and leukemia. In *Cancer research* 68 (19), pp. 8049–8057. DOI: 10.1158/0008-5472.CAN-08-2268.

Hou, R.; Kong, X.; Yang, B.; Xie, Y.; Chen, G. (2017): SLC14A1: a novel target for human urothelial cancer. In *Clinical & translational oncology : official publication of the Federation of Spanish Oncology Societies and of the National Cancer Institute of Mexico* 19 (12), pp. 1438–1446. DOI: 10.1007/s12094-017-1693-3.

Hu, Yifang; Smyth, Gordon K. (2009): ELDA: extreme limiting dilution analysis for comparing depleted and enriched populations in stem cell and other assays. In *Journal of immunological methods* 347 (1-2), pp. 70–78. DOI: 10.1016/j.jim.2009.06.008.

Huang, Sijia; Li, Feng; Liu, Huifang; Ye, Pei; Fan, Xiaochuan; Yuan, Xinqiu et al. (2018): Structural and functional characterization of MBS301, an afucosylated bispecific anti-HER2 antibody. In *mAbs* 10 (6), pp. 864–875. DOI: 10.1080/19420862.2018.1486946.

Hynes, Nancy E.; Lane, Heidi A. (2005): ERBB receptors and cancer: the complexity of targeted inhibitors. In *Nat Rev Cancer* 5 (5), pp. 341–354. DOI: 10.1038/nrc1609.

Hynes, Nancy E.; MacDonald, Gwen (2009): ErbB receptors and signaling pathways in cancer. In *Current opinion in cell biology* 21 (2), pp. 177–184. DOI: 10.1016/j.ceb.2008.12.010.

Jacob, Wolfgang; James, Ian; Hasmann, Max; Weisser, Martin (2018): Clinical development of HER3-targeting monoclonal antibodies: Perils and progress. In *Cancer treatment reviews* 68, pp. 111–123. DOI: 10.1016/j.ctrv.2018.06.011.

Jacobsen, Helle J.; Poulsen, Thomas T.; Dahlman, Anna; Kjær, Ida; Koefoed, Klaus; Sen, Jette W. et al. (2015): Pan-HER, an Antibody Mixture Simultaneously Targeting EGFR, HER2, and HER3, Effectively Overcomes Tumor Heterogeneity and Plasticity. In *Clinical cancer research : an official journal of the American Association for Cancer Research* 21 (18), pp. 4110–4122. DOI: 10.1158/1078-0432.CCR-14-3312.

Jaiswal, Bijay S.; Kljavin, Noelyn M.; Stawiski, Eric W.; Chan, Emily; Parikh, Chaitali; Durinck, Steffen et al. (2013): Oncogenic ERBB3 mutations in human cancers. In *Cancer cell* 23 (5), pp. 603–617. DOI: 10.1016/j.ccr.2013.04.012.

Janne, Pasi A.; Baik, Christina S.; Su, Wu-Chou; Johnson, Melissa Lynne; Hayashi, Hidetoshi; Nishio, Makoto et al. (2021): Efficacy and safety of patritumab deruxtecan (HER3-DXd) in EGFR inhibitor-resistant, EGFR -mutated (EGFR m) non-small cell lung cancer (NSCLC). In *JCO* 39 (15_suppl), p. 9007. DOI: 10.1200/JCO.2021.39.15_suppl.9007.

Jardé, Thierry; Lloyd-Lewis, Bethan; Thomas, Mairian; Kendrick, Howard; Melchor, Lorenzo; Bougaret, Lauriane et al. (2016): Wnt and Neuregulin1/ErbB signalling extends 3D culture of hormone responsive mammary organoids. In *Nature communications* 7, p. 13207. DOI: 10.1038/ncomms13207.

Jeong, Hoiseon; Kim, Jinkyoung; Lee, Youngseok; Seo, Jae Hong; Hong, Sung Ran; Kim, Aeree (2014): Neuregulin-1 induces cancer stem cell characteristics in breast cancer cell lines. In *Oncology reports* 32 (3), pp. 1218–1224. DOI: 10.3892/or.2014.3330.

Jian, Wen; Wei, Chun-Mei; Guan, Jia-Hui; Mo, Chang-Hua; Xu, Yu-Tao; Zheng, Wen-Bo et al. (2020): Association between serum HER2/ErbB2 levels and coronary artery disease: a case-control study. In *Journal of translational medicine* 18 (1), p. 124. DOI: 10.1186/s12967-020-02292-1.

Jones, Frank E. (2008): HER4 intracellular domain (4ICD) activity in the developing mammary gland and breast cancer. In *Journal of mammary gland biology and neoplasia* 13 (2), pp. 247–258. DOI: 10.1007/s10911-008-9076-6.

Kang, Jeffrey C.; Poovassery, Jayakumar S.; Bansal, Pankaj; You, Sungyong; Manjarres, Isabel M.; Ober, Raimund J.; Ward, E. Sally (2013): Engineering multivalent antibodies to target heregulin-induced HER3 signaling in breast cancer cells. In *mAbs* 6 (2), pp. 340–353. DOI: 10.4161/mabs.27658.

Kaplon, Hélène; Chenoweth, Alicia; Crescioli, Silvia; Reichert, Janice M. (2022): Antibodies to watch in 2022. In *mAbs* 14 (1), p. 2014296. DOI: 10.1080/19420862.2021.2014296.

Kennedy, Sean P.; Han, Jeremy Z. R.; Portman, Neil; Nobis, Max; Hastings, Jordan F.; Murphy, Kendelle J. et al. (2019): Targeting promiscuous heterodimerization overcomes innate resistance to ERBB2 dimerization inhibitors in breast cancer. In *Breast cancer research : BCR* 21 (1), p. 43. DOI: 10.1186/s13058-019-1127-y.

Kim, Ji-Yeon; Jung, Hae Hyun; Do, In-Gu; Bae, SooYoun; Lee, Se Kyung; Kim, Seok Won et al. (2016): Prognostic value of ERBB4 expression in patients with triple negative breast cancer. In *BMC cancer* 16, p. 138. DOI: 10.1186/s12885-016-2195-3.

Kitazawa, Takehisa; Igawa, Tomoyuki; Sampei, Zenjiro; Muto, Atsushi; Kojima, Tetsuo; Soeda, Tetsuhiro et al. (2012): A bispecific antibody to factors IXa and X restores factor VIII hemostatic activity in a hemophilia A model. In *Nature medicine* 18 (10), pp. 1570–1574. DOI: 10.1038/nm.2942.

Kitazawa, Takehisa; Shima, Midori (2020): Emicizumab, a humanized bispecific antibody to coagulation factors IXa and X with a factor VIIIa-cofactor activity. In *International journal of hematology* 111 (1), pp. 20–30. DOI: 10.1007/s12185-018-2545-9.

Kjær, Ida; Lindsted, Trine; Fröhlich, Camilla; Olsen, Jesper Velgaard; Horak, Ivan David; Kragh, Michael; Pedersen, Mikkel Wandahl (2016): Cetuximab Resistance in Squamous Carcinomas of the Upper Aerodigestive Tract Is Driven by Receptor Tyrosine Kinase Plasticity: Potential for mAb Mixtures. In *Molecular cancer therapeutics* 15 (7), pp. 1614–1626. DOI: 10.1158/1535-7163.MCT-15-0565.

Klein, Christian; Schaefer, Wolfgang; Regula, Joerg T.; Dumontet, Charles; Brinkmann, Ulrich; Bacac, Marina; Umaña, Pablo (2019): Engineering therapeutic bispecific antibodies using CrossMab technology. In *Methods (San Diego, Calif.)* 154, pp. 21–31. DOI: 10.1016/j.ymeth.2018.11.008.

Klein, Joshua S.; Jiang, Siduo; Galimidi, Rachel P.; Keeffe, Jennifer R.; Bjorkman, Pamela J. (2014): Design and characterization of structured protein linkers with differing flexibilities. In *Protein engineering, design & selection : PEDS* 27 (10), pp. 325–330. DOI: 10.1093/protein/gzu043.

Koganemaru, Shigehiro; Kuboki, Yasutoshi; Koga, Yoshikatsu; Kojima, Takashi; Yamauchi, Mayumi; Maeda, Naoyuki et al. (2019): U3-1402, a Novel HER3-Targeting Antibody-Drug Conjugate, for the Treatment of Colorectal Cancer. In *Molecular cancer therapeutics* 18 (11), pp. 2043–2050. DOI: 10.1158/1535-7163.MCT-19-0452.

Köhler, G.; Milstein, C. (1975): Continuous cultures of fused cells secreting antibody of predefined specificity. In *Nature* 256 (5517), pp. 495–497. DOI: 10.1038/256495a0.

Kontermann, Roland E. (2011): Strategies for extended serum half-life of protein therapeutics. In *Current opinion in biotechnology* 22 (6), pp. 868–876. DOI: 10.1016/j.copbio.2011.06.012.

Kostovski, Ognen; Antovic, Svetozar; Trajkovski, Gjorgji; Kostovska, Irena; Jovanovic, Rubens; Jankulovski, Nikola (2020): High expression of CD133 - stem cell marker for prediction of clinically agressive type of colorectal cancer. In *Polski przeglad chirurgiczny* 92 (3), pp. 9–14. DOI: 10.5604/01.3001.0014.0999.

Kramer, Nina; Walzl, Angelika; Unger, Christine; Rosner, Margit; Krupitza, Georg; Hengstschläger, Markus; Dolznig, Helmut (2013): In vitro cell migration and invasion assays. In *Mutation research* 752 (1), pp. 10–24. DOI: 10.1016/j.mrrev.2012.08.001.

Krane, I. M.; Leder, P. (1996): NDF/heregulin induces persistence of terminal end buds and adenocarcinomas in the mammary glands of transgenic mice. In *Oncogene* 12 (8), pp. 1781–1788.

Kraus, M. H.; Issing, W.; Miki, T.; Popescu, N. C.; Aaronson, S. A. (1989): Isolation and characterization of ERBB3, a third member of the ERBB/epidermal growth factor receptor family: evidence for overexpression in a subset of human mammary tumors. In *Proceedings of the National Academy of Sciences of the United States of America* 86 (23), pp. 9193–9197. DOI: 10.1073/pnas.86.23.9193.

Kruser, Tim J.; Wheeler, Deric L. (2010): Mechanisms of resistance to HER family targeting antibodies. In *Experimental cell research* 316 (7), pp. 1083–1100. DOI: 10.1016/j.yexcr.2010.01.009.

Labrijn, Aran F.; Janmaat, Maarten L.; Reichert, Janice M.; Parren, Paul W. H. I. (2019): Bispecific antibodies: a mechanistic review of the pipeline. In *Nature reviews. Drug discovery* 18 (8), pp. 585–608. DOI: 10.1038/s41573-019-0028-1.

LaFleur, David W.; Abramyan, Donara; Kanakaraj, Palanisamy; Smith, Rodger G.; Shah, Rutul R.; Wang, Geping et al. (2013): Monoclonal antibody therapeutics with up to five specificities: functional enhancement through fusion of target-specific peptides. In *mAbs* 5 (2), pp. 208–218. DOI: 10.4161/mabs.23043.

Lane, Nathan; Lev, Robert (1963): Observations on the origin of adenomatous epithelium of the colon.Serial section studies of minute polyps in familial polyposis. In *Cancer* 16 (6), pp. 751–764. DOI: 10.1002/1097-0142(196306)16:6<751::AID-CNCR2820160610>3.0.CO;2-0.

Langhans, Sigrid A. (2018): Three-Dimensional in Vitro Cell Culture Models in Drug Discovery and Drug Repositioning. In *Frontiers in pharmacology* 9, p. 6. DOI: 10.3389/fphar.2018.00006.

Lanotte, Romain; Garambois, Véronique; Gaborit, Nadège; Larbouret, Christel; Musnier, Astrid; Martineau, Pierre et al. (2019): Biasing HER4 Tyrosine Kinase Signaling with Antibodies: Induction of Cell Death by Antibody-Dependent HER4 Intracellular Domain Trafficking.

Lédel, F.; Hallström, M.; Ragnhammar, P.; Öhrling, K.; Edler, D. (2014): HER3 expression in patients with primary colorectal cancer and corresponding lymph node metastases related to clinical outcome. In *European Journal of Cancer* 50 (3), pp. 656–662. DOI: 10.1016/j.ejca.2013.11.008.

Lédel, Frida; Stenstedt, Kristina; Hallström, Marja; Ragnhammar, Peter; Edler, David (2015): HER3 expression in primary colorectal cancer including corresponding metastases in lymph node and liver. In *Acta oncologica (Stockholm, Sweden)* 54 (4), pp. 480–486. DOI: 10.3109/0284186X.2014.983654.

Lee, Cleo Yi-Fang; Lin, Yuan; Bratman, Scott V.; Feng, Weiguo; Kuo, Angera H.; Scheeren, Ferenc A. et al. (2014): Neuregulin autocrine signaling promotes self-renewal of breast tumor-initiating cells by triggering HER2/HER3 activation. In *Cancer research* 74 (1), pp. 341–352. DOI: 10.1158/0008-5472.CAN-13-1055.

Lee, Hahn-Jun; Jung, Kwang-Mook; Huang, Yang Z.; Bennett, Lori B.; Lee, Joanne S.; Mei, Lin; Kim, Tae-Wan (2002): Presenilin-dependent gamma-secretase-like intramembrane cleavage of ErbB4. In *The Journal of biological chemistry* 277 (8), pp. 6318–6323. DOI: 10.1074/jbc.M110371200.

Lee, Sangwon; Greenlee, Etienne B.; Amick, Joseph R.; Ligon, Gwenda F.; Lillquist, Jay S.; Natoli, Edward J. et al. (2015): Inhibition of ErbB3 by a monoclonal antibody that locks the extracellular domain in an inactive configuration. In *Proceedings of the National Academy of Sciences of the United States of America* 112 (43), pp. 13225–13230. DOI: 10.1073/pnas.1518361112.

Leto, Simonetta M.; Sassi, Francesco; Catalano, Irene; Torri, Valter; Migliardi, Giorgia; Zanella, Eugenia R. et al. (2015): Sustained Inhibition of HER3 and EGFR Is Necessary to Induce Regression of HER2-Amplified Gastrointestinal Carcinomas. In *Clinical cancer research : an*

official journal of the American Association for Cancer Research 21 (24), pp. 5519–5531. DOI: 10.1158/1078-0432.CCR-14-3066.

Leto, Simonetta M.; Trusolino, Livio (2014): Primary and acquired resistance to EGFR-targeted therapies in colorectal cancer. Impact on future treatment strategies. In *Journal of molecular medicine (Berlin, Germany)* 92 (7), pp. 709–722. DOI: 10.1007/s00109-014-1161-2.

Levva, Sofia; Kotoula, Vassiliki; Kostopoulos, Ioannis; Manousou, Kyriaki; Papadimitriou, Christos; Papadopoulou, Kyriaki et al. (2017): Prognostic Evaluation of Epidermal Growth Factor Receptor (EGFR) Genotype and Phenotype Parameters in Triple-negative Breast Cancers. In *Cancer genomics & proteomics* 14 (3), pp. 181–195. DOI: 10.21873/cgp.20030.

Lewis Phillips, Gail D.; Li, Guangmin; Dugger, Debra L.; Crocker, Lisa M.; Parsons, Kathryn L.; Mai, Elaine et al. (2008): Targeting HER2-positive breast cancer with trastuzumab-DM1, an antibody-cytotoxic drug conjugate. In *Cancer research* 68 (22), pp. 9280–9290. DOI: 10.1158/0008-5472.CAN-08-1776.

Li, D.; Ambrogio, L.; Shimamura, T.; Kubo, S.; Takahashi, M.; Chirieac, L. R. et al. (2008a): BIBW2992, an irreversible EGFR/HER2 inhibitor highly effective in preclinical lung cancer models. In *Oncogene* 27 (34), pp. 4702–4711. DOI: 10.1038/onc.2008.109.

Li, Xiaoxian; Lewis, Michael T.; Huang, Jian; Gutierrez, Carolina; Osborne, C. Kent; Wu, Meng-Fen et al. (2008b): Intrinsic resistance of tumorigenic breast cancer cells to chemotherapy. In *Journal of the National Cancer Institute* 100 (9), pp. 672–679. DOI: 10.1093/jnci/djn123.

Li, Yanping; Fu, Ruoqiu; Jiang, Tingting; Duan, Dongyu; Wu, Yuanlin; Li, Chen et al. (2022): Mechanism of Lethal Skin Toxicities Induced by Epidermal Growth Factor Receptor Inhibitors and Related Treatment Strategies. In *Front. Oncol.* 12, p. 804212. DOI: 10.3389/fonc.2022.804212.

Liang, Junrong; Sun, Lina; Li, Yujun; Liu, Wanning; Li, Danxiu; Chen, Ping et al. (2022): Wnt signaling modulator DKK4 inhibits colorectal cancer metastasis through an AKT/Wnt/β-catenin negative feedback pathway. In *The Journal of biological chemistry* 298 (11), p. 102545. DOI: 10.1016/j.jbc.2022.102545.

Liedtke, Cornelia; Mazouni, Chafika; Hess, Kenneth R.; André, Fabrice; Tordai, Attila; Mejia, Jaime A. et al. (2008): Response to neoadjuvant therapy and long-term survival in patients with triple-negative breast cancer. In *JCO* 26 (8), pp. 1275–1281. DOI: 10.1200/JCO.2007.14.4147.

Lièvre, Astrid; Bachet, Jean-Baptiste; Le Corre, Delphine; Boige, Valérie; Landi, Bruno; Emile, Jean-François et al. (2006): KRAS mutation status is predictive of response to cetuximab

therapy in colorectal cancer. In *Cancer research* 66 (8), pp. 3992–3995. DOI: 10.1158/0008-5472.CAN-06-0191.

Lindström, Linda Sofie; Karlsson, Eva; Wilking, Ulla M.; Johansson, Ulla; Hartman, Johan; Lidbrink, Elisabet Kerstin et al. (2012): Clinically used breast cancer markers such as estrogen receptor, progesterone receptor, and human epidermal growth factor receptor 2 are unstable throughout tumor progression. In *JCO* 30 (21), pp. 2601–2608. DOI: 10.1200/JCO.2011.37.2482.

Lopez-Albaitero, Andres; Xu, Hong; Guo, Hongfen; Wang, Linlin; Wu, Zhihao; Tran, Hoa et al. (2017): Overcoming resistance to HER2-targeted therapy with a novel HER2/CD3 bispecific antibody. In *Oncoimmunology* 6 (3), e1267891. DOI: 10.1080/2162402X.2016.1267891.

LoRusso, Patricia; Jänne, Pasi A.; Oliveira, Moacyr; Rizvi, Naiyer; Malburg, Lisa; Keedy, Vicki et al. (2013): Phase I study of U3-1287, a fully human anti-HER3 monoclonal antibody, in patients with advanced solid tumors. In *Clinical cancer research : an official journal of the American Association for Cancer Research* 19 (11), pp. 3078–3087. DOI: 10.1158/1078-0432.CCR-12-3051.

Lucas, Lauren M.; Dwivedi, Vipasha; Senfeld, Jared I.; Cullum, Richard L.; Mill, Christopher P.; Piazza, J. Tyler et al. (2022): The Yin and Yang of ERBB4: Tumor Suppressor and Oncoprotein. In *Pharmacological reviews* 74 (1), pp. 18–47. DOI: 10.1124/pharmrev.121.000381.

Luetteke, Noreen C.; Qiu, Ting Hu; Peiffer, Robert L.; Oliver, Paula; Smithies, Oliver; Lee, David C. (1993): TGFα deficiency results in hair follicle and eye abnormalities in targeted and waved-1 mice. In *Cell* 73 (2), pp. 263–278. DOI: 10.1016/0092-8674(93)90228-I.

Määttä, Jorma A.; Sundvall, Maria; Junttila, Teemu T.; Peri, Liisa; Laine, V. Jukka O.; Isola, Jorma et al. (2006): Proteolytic cleavage and phosphorylation of a tumor-associated ErbB4 isoform promote ligand-independent survival and cancer cell growth. In *Molecular biology of the cell* 17 (1), pp. 67–79. DOI: 10.1091/mbc.E05–05–0402.

Machleidt, Anna; Buchholz, Stefan; Diermeier-Daucher, Simone; Zeman, Florian; Ortmann, Olaf; Brockhoff, Gero (2013): The prognostic value of Her4 receptor isoform expression in triple-negative and Her2 positive breast cancer patients. In *BMC cancer* 13, p. 437. DOI: 10.1186/1471-2407-13-437.

Malm, Magdalena; Frejd, Fredrik Y.; Ståhl, Stefan; Löfblom, John (2016): Targeting HER3 using mono- and bispecific antibodies or alternative scaffolds. In *mAbs* 8 (7), pp. 1195–1209. DOI: 10.1080/19420862.2016.1212147.

Matthews Hew, Trevanne; Zuberi, Lara (2019): PARP Inhibitor Olaparib Use in a BRCA1-Positive Patient With Metastatic Triple-Negative Breast Cancer, Without the Initial Use of Platinum-Based Chemotherapy, Showing Significant Rapid Near Resolution of Large Liver Metastasis While Patient Experienced Gout-Like Symptoms. In *Journal of investigative medicine high impact case reports* 7, 2324709619864989. DOI: 10.1177/2324709619864989.

Mazor, Yariv; Oganesyan, Vaheh; Yang, Chunning; Hansen, Anna; Wang, Jihong; Liu, Hongji et al. (2015): Improving target cell specificity using a novel monovalent bispecific IgG design. In *mAbs* 7 (2), pp. 377–389. DOI: 10.1080/19420862.2015.1007816.

McDermott, Jessica D.; Bowles, Daniel W. (2019): Epidemiology of Head and Neck Squamous Cell Carcinomas: Impact on Staging and Prevention Strategies. In *Current treatment options in oncology* 20 (5), p. 43. DOI: 10.1007/s11864-019-0650-5.

Meacham, Corbin E.; Morrison, Sean J. (2013): Tumour heterogeneity and cancer cell plasticity. In *Nature* 501 (7467), pp. 328–337. DOI: 10.1038/nature12624.

Mendelsohn, J.; Baselga, J. (2000): The EGF receptor family as targets for cancer therapy. In *Oncogene* 19 (56), pp. 6550–6565. DOI: 10.1038/sj.onc.1204082.

Meric-Bernstam, Funda; Hurwitz, Herbert; Raghav, Kanwal Pratap Singh; McWilliams, Robert R.; Fakih, Marwan; VanderWalde, Ari et al. (2019): Pertuzumab plus trastuzumab for HER2-amplified metastatic colorectal cancer (MyPathway): an updated report from a multicentre, open-label, phase 2a, multiple basket study. In *The Lancet. Oncology* 20 (4), pp. 518–530. DOI: 10.1016/S1470-2045(18)30904-5.

Miettinen, P. J.; Berger, J. E.; Meneses, J.; Phung, Y.; Pedersen, R. A.; Werb, Z.; Derynck, R. (1995): Epithelial immaturity and multiorgan failure in mice lacking epidermal growth factor receptor. In *Nature* 376 (6538), pp. 337–341. DOI: 10.1038/376337a0.

Milstein, C.; Cuello, A. C. (1983): Hybrid hybridomas and their use in immunohistochemistry. In *Nature* 305 (5934), pp. 537–540. DOI: 10.1038/305537a0.

Minckwitz, Gunter von; Huang, Chiun-Sheng; Mano, Max S.; Loibl, Sibylle; Mamounas, Eleftherios P.; Untch, Michael et al. (2019): Trastuzumab Emtansine for Residual Invasive HER2-Positive Breast Cancer. In *The New England journal of medicine* 380 (7), pp. 617–628. DOI: 10.1056/NEJMoa1814017.

Mishra, Rosalin; Patel, Hima; Alanazi, Samar; Yuan, Long; Garrett, Joan T. (2018): HER3 signaling and targeted therapy in cancer. In *Oncology reviews* 12 (1), p. 355. DOI: 10.4081/oncol.2018.355.

Morante, Zaida; La Cruz Ku, Gabriel Antonio de; Enriquez, Daniel; Saavedra, Antonella; Luján, Maria; Luque, Renato et al. (2018): Post-recurrence survival in triple negative breast cancer. In *JCO* 36 (15_suppl), e13120-e13120. DOI: 10.1200/JCO.2018.36.15_suppl.e13120.

Mota, Jose Mauricio; Collier, Katharine Ann; Barros Costa, Ricardo Lima; Taxter, Timothy; Kalyan, Aparna; Leite, Caio A. et al. (2017): A comprehensive review of heregulins, HER3, and HER4 as potential therapeutic targets in cancer. In *Oncotarget* 8 (51), pp. 89284–89306. DOI: 10.18632/oncotarget.18467.

Müller-Brüsselbach, Sabine; Korn, Tina; Völkel, Tina; Müller, Rolf; Kontermann, Roland (1999): Enzyme recruitment and tumor cell killing in vitro by a secreted bispecific single-chain diabody. In *Tumor Targeting* 4, pp. 115–123.

Munro, Matthew J.; Wickremesekera, Susrutha K.; Peng, Lifeng; Tan, Swee T.; Itinteang, Tinte (2018): Cancer stem cells in colorectal cancer: a review. In *Journal of clinical pathology* 71 (2), pp. 110–116. DOI: 10.1136/jclinpath-2017-204739.

Nakai, Katsuya; Hung, Mien-Chie; Yamaguchi, Hirohito (2016): A perspective on anti-EGFR therapies targeting triple-negative breast cancer. In *American Journal of Cancer Research* 6 (8), pp. 1609–1623.

Nakajima, Hiroki; Ishikawa, Yuko; Furuya, Mio; Sano, Takaaki; Ohno, Yoshihiro; Horiguchi, Jun; Oyama, Tetsunari (2014): Protein expression, gene amplification, and mutational analysis of EGFR in triple-negative breast cancer. In *Breast cancer (Tokyo, Japan)* 21 (1), pp. 66–74. DOI: 10.1007/s12282-012-0354-1.

Nakamura, Y.; Okamoto, W.; Kato, T.; Hasegawa, H.; Kato, K.; Iwasa, S. et al. (2019): TRIUMPH: Primary efficacy of a phase II trial of trastuzumab (T) and pertuzumab (P) in patients (pts) with metastatic colorectal cancer (mCRC) with HER2 (ERBB2) amplification (amp) in tumour tissue or circulating tumour DNA (ctDNA): A GOZILA sub-study. In *Annals of Oncology* 30, v199-v200. DOI: 10.1093/annonc/mdz246.004.

Neal, James T.; Li, Xingnan; Zhu, Junjie; Giangarra, Valeria; Grzeskowiak, Caitlin L.; Ju, Jihang et al. (2018): Organoid Modeling of the Tumor Immune Microenvironment. In *Cell* 175 (7), 1972-1988.e16. DOI: 10.1016/j.cell.2018.11.021.

Nisonoff, A.; Wissler, F. C.; Lipman, L. N. (1960): Properties of the major component of a peptic digest of rabbit antibody. In *Science (New York, N.Y.)* 132 (3441), pp. 1770–1771. DOI: 10.1126/science.132.3441.1770.

Noah, Taeko K.; Donahue, Bridgitte; Shroyer, Noah F. (2011): Intestinal development and differentiation. In *Experimental cell research* 317 (19), pp. 2702–2710. DOI: 10.1016/j.yexcr.2011.09.006.

O'Brien, Catherine A.; Pollett, Aaron; Gallinger, Steven; Dick, John E. (2007): A human colon cancer cell capable of initiating tumour growth in immunodeficient mice. In *Nature* 445 (7123), pp. 106–110. DOI: 10.1038/nature05372.

O'Conor, Christopher J.; Chen, Tiffany; González, Iván; Cao, Dengfeng; Peng, Yan (2018): Cancer stem cells in triple-negative breast cancer: a potential target and prognostic marker. In *Biomarkers in medicine* 12 (7), pp. 813–820. DOI: 10.2217/bmm-2017-0398.

Ogden, Angela; Bhattarai, Shristi; Green, Andrew R.; Aleskandarany, Mohammed A.; Rakha, Emad A.; Ellis, Ian O. et al. (2017): HER3-EGFR score to predict clinical outcomes in triple-negative breast cancer. In *JCO* 35 (15_suppl), p. 11612. DOI: 10.1200/JCO.2017.35.15_suppl.11612.

Oh, Do-Youn; Bang, Yung-Jue (2020): HER2-targeted therapies - a role beyond breast cancer. In *Nature reviews. Clinical oncology* 17 (1), pp. 33–48. DOI: 10.1038/s41571-019-0268-3.

Olayioye, M. A.; Neve, R. M.; Lane, H. A.; Hynes, N. E. (2000): The ErbB signaling network: receptor heterodimerization in development and cancer. In *The EMBO journal* 19 (13), pp. 3159–3167. DOI: 10.1093/emboj/19.13.3159.

Oliveras-Ferraros, Cristina; Massaguer Vall-Llovera, Anna; Vazquez-Martin, Alejandro; Salip, Dolors Carrion; Queralt, Bernardo; Cufí, Silvia et al. (2012): Transcriptional upregulation of HER2 expression in the absence of HER2 gene amplification results in cetuximab resistance that is reversed by trastuzumab treatment. In *Oncology reports* 27 (6), pp. 1887–1892. DOI: 10.3892/or.2012.1732.

Ooft, Salo N.; Weeber, Fleur; Dijkstra, Krijn K.; McLean, Chelsea M.; Kaing, Sovann; van Werkhoven, Erik et al. (2019): Patient-derived organoids can predict response to chemotherapy in metastatic colorectal cancer patients. In *Science translational medicine* 11 (513). DOI: 10.1126/scitranslmed.aay2574.

Park, Heae Surng; Jang, Min Hye; Kim, Eun Joo; Kim, Hyun Jeong; Lee, Hee Jin; Kim, Yu Jung et al. (2014): High EGFR gene copy number predicts poor outcome in triple-negative breast cancer. In *Modern pathology : an official journal of the United States and Canadian Academy of Pathology, Inc* 27 (9), pp. 1212–1222. DOI: 10.1038/modpathol.2013.251.

Pauw, Ines de; Lardon, Filip; van den Bossche, Jolien; Baysal, Hasan; Pauwels, Patrick; Peeters, Marc et al. (2019): Overcoming Intrinsic and Acquired Cetuximab Resistance in RAS Wild-Type

Colorectal Cancer: An In Vitro Study on the Expression of HER Receptors and the Potential of Afatinib. In *Cancers* 11 (1). DOI: 10.3390/cancers11010098.

Paz-Arez, Luis; Serwatowski, Piotr; Szczęsna, Aleksandra; Pawel, Joachim von; Toschi, Luca; Tibor, Csőszi et al. (2017): P3.02b-045 Patritumab plus Erlotinib in EGFR Wild-Type Advanced Non–Small Cell Lung Cancer (NSCLC): Part a Results of HER3-Lung Study. In *Journal of Thoracic Oncology* 12 (1), S1214-S1215. DOI: 10.1016/j.jtho.2016.11.1712.

Pegram, Mark D.; Miles, David; Tsui, C. Kimberly; Zong, Yu (2020): HER2-Overexpressing/Amplified Breast Cancer as a Testing Ground for Antibody-Drug Conjugate Drug Development in Solid Tumors. In *Clinical cancer research : an official journal of the American Association for Cancer Research* 26 (4), pp. 775–786. DOI: 10.1158/1078-0432.CCR-18-1976.

Penuel, Elicia; Akita, Robert W.; Sliwkowski, Mark X. (2002): Identification of a region within the ErbB2/HER2 intracellular domain that is necessary for ligand-independent association. In *The Journal of biological chemistry* 277 (32), pp. 28468–28473. DOI: 10.1074/jbc.M202510200.

Pérez-García, José; Soberino, Jesús; Racca, Fabricio; Gion, María; Stradella, Agostina; Cortés, Javier (2020): Atezolizumab in the treatment of metastatic triple-negative breast cancer. In *Expert opinion on biological therapy*, pp. 1–9. DOI: 10.1080/14712598.2020.1769063.

Perou, C. M.; Sørlie, T.; Eisen, M. B.; van de Rijn, M.; Jeffrey, S. S.; Rees, C. A. et al. (2000): Molecular portraits of human breast tumours. In *Nature* 406 (6797), pp. 747–752. DOI: 10.1038/35021093.

Piulats, Jose M.; Kondo, Jumpei; Endo, Hiroko; Ono, Hiromasa; Hagihara, Takeshi; Okuyama, Hiroaki et al. (2018): Promotion of malignant phenotype after disruption of the three-dimensional structure of cultured spheroids from colorectal cancer. In *Oncotarget* 9 (22), pp. 15968–15983. DOI: 10.18632/oncotarget.24641.

Plowman, G. D.; Culouscou, J. M.; Whitney, G. S.; Green, J. M.; Carlton, G. W.; Foy, L. et al. (1993): Ligand-specific activation of HER4/p180erbB4, a fourth member of the epidermal growth factor receptor family. In *Proceedings of the National Academy of Sciences of the United States of America* 90 (5), pp. 1746–1750.

Plowman, G. D.; Whitney, G. S.; Neubauer, M. G.; Green, J. M.; McDonald, V. L.; Todaro, G. J.; Shoyab, M. (1990): Molecular cloning and expression of an additional epidermal growth factor receptor-related gene. In *Proceedings of the National Academy of Sciences of the United States of America* 87 (13), pp. 4905–4909. DOI: 10.1073/pnas.87.13.4905.

Porter, R. R. (1958): Separation and isolation of fractions of rabbit gamma-globulin containing the antibody and antigenic combining sites. In *Nature* 182 (4636), pp. 670–671. DOI: 10.1038/182670a0.

Rau, Alexander (2017): Bispecific scDb-Fc antibodies targeting ErbB family members. Stuttgart.

Rau, Alexander; Janssen, Nicole; Kühl, Lennart; Sell, Thomas; Kalmykova, Svetlana; Mürdter, Thomas E. et al. (2022): Triple Targeting of HER Receptors Overcomes Heregulin-mediated Resistance to EGFR Blockade in Colorectal Cancer. In *Molecular cancer therapeutics* 21 (5), pp. 799–809. DOI: 10.1158/1535-7163.MCT-21-0818.

Rau, Alexander; Lieb, Wolfgang S.; Seifert, Oliver; Honer, Jonas; Birnstock, Dennis; Richter, Fabian et al. (2020): Inhibition of tumor cell growth and cancer stem cell expansion by a bispecific antibody targeting EGFR and HER3. In *Molecular cancer therapeutics*. DOI: 10.1158/1535-7163.MCT-19-1095.

Reichert, Janice M. (2020): Bispecific antibodies come to the fore. https://www.antibodysociety.org. Available online at https://www.antibodysociety.org/bispecific-antibodies/, updated on 2/11/2020, checked on 5/12/2020.

Rhoden, John J.; Dyas, Gregory L.; Wroblewski, Victor J. (2016): A Modeling and Experimental Investigation of the Effects of Antigen Density, Binding Affinity, and Antigen Expression Ratio on Bispecific Antibody Binding to Cell Surface Targets. In *The Journal of biological chemistry* 291 (21), pp. 11337–11347. DOI: 10.1074/jbc.M116.714287.

Ricci-Vitiani, Lucia; Lombardi, Dario G.; Pilozzi, Emanuela; Biffoni, Mauro; Todaro, Matilde; Peschle, Cesare; Maria, Ruggero de (2007): Identification and expansion of human colon-cancer-initiating cells. In *Nature* 445 (7123), pp. 111–115. DOI: 10.1038/nature05384.

Ridgway, J. B.; Presta, L. G.; Carter, P. (1996): 'Knobs-into-holes' engineering of antibody CH3 domains for heavy chain heterodimerization. In *Protein engineering* 9 (7), pp. 617–621. DOI: 10.1093/protein/9.7.617.

Riesenberg, R.; Buchner, A.; Pohla, H.; Lindhofer, H. (2001): Lysis of prostate carcinoma cells by trifunctional bispecific antibodies (alpha EpCAM x alpha CD3). In *The journal of histochemistry and cytochemistry : official journal of the Histochemistry Society* 49 (7), pp. 911–917. DOI: 10.1177/002215540104900711.

Riethmüller, Gert (2012): Symmetry breaking: bispecific antibodies, the beginnings, and 50 years on. In *Cancer Immunity* 12.

Rio, C.; Buxbaum, J. D.; Peschon, J. J.; Corfas, G. (2000): Tumor necrosis factor-alpha-converting enzyme is required for cleavage of erbB4/HER4. In *The Journal of biological chemistry* 275 (14), pp. 10379–10387. DOI: 10.1074/jbc.275.14.10379.

Ritter, Christoph A.; Perez-Torres, Marianela; Rinehart, Cammie; Guix, Marta; Dugger, Teresa; Engelman, Jeffrey A.; Arteaga, Carlos L. (2007): Human breast cancer cells selected for resistance to trastuzumab in vivo overexpress epidermal growth factor receptor and ErbB ligands and remain dependent on the ErbB receptor network. In *Clinical cancer research : an official journal of the American Association for Cancer Research* 13 (16), pp. 4909–4919. DOI: 10.1158/1078-0432.CCR-07-0701.

Robinson, M. K.; Hodge, K. M.; Horak, E.; Sundberg, A. L.; Russeva, M.; Shaller, C. C. et al. (2008): Targeting ErbB2 and ErbB3 with a bispecific single-chain Fv enhances targeting selectivity and induces a therapeutic effect in vitro. In *British journal of cancer* 99 (9), pp. 1415–1425. DOI: 10.1038/sj.bjc.6604700.

Rocha-Lima, Caio M.; Soares, Heloisa P.; Raez, Luis E.; Singal, Rakesh (2007): EGFR targeting of solid tumors. In *Cancer control : journal of the Moffitt Cancer Center* 14 (3), pp. 295–304. DOI: 10.1177/107327480701400313.

Rose, Suzanne (2019): MCLA-128 Fights NRG1 Fusion-Positive Cancers. In *Cancer Discov* 9 (12), p. 1636. DOI: 10.1158/2159-8290.CD-NB2019-128.

Rosestedt, Maria; Andersson, Ken G.; Rinne, Sara S.; Leitao, Charles Dahlsson; Mitran, Bogdan; Vorobyeva, Anzhelika et al. (2019): Improved contrast of affibody-mediated imaging of HER3 expression in mouse xenograft model through co-injection of a trivalent affibody for in vivo blocking of hepatic uptake. In *Scientific reports* 9 (1), p. 6779. DOI: 10.1038/s41598-019-43145-2.

Roskoski, Robert (2014): The ErbB/HER family of protein-tyrosine kinases and cancer. In *Pharmacological research* 79, pp. 34–74. DOI: 10.1016/j.phrs.2013.11.002.

Roskoski, Robert (2019): Small molecule inhibitors targeting the EGFR/ErbB family of protein-tyrosine kinases in human cancers. In *Pharmacological research* 139, pp. 395–411. DOI: 10.1016/j.phrs.2018.11.014.

Rugo, Hope S.; Im, Seock-Ah; Wright, Gail Lynn Shaw; Escriva-de-Romani, Santiago; DeLaurentiis, Michelino; Cortes, Javier et al. (2019): SOPHIA primary analysis: A phase 3 (P3) study of margetuximab (M) + chemotherapy (C) versus trastuzumab (T) + C in patients (pts) with HER2+ metastatic (met) breast cancer (MBC) after prior anti-HER2 therapies (Tx). In *JCO* 37 (15_suppl), p. 1000. DOI: 10.1200/JCO.2019.37.15_suppl.1000.

Sabatier, Renaud; Lopez, Marc; Guille, Arnaud; Billon, Emilien; Carbuccia, Nadine; Garnier, Séverine et al. (2019): High Response to Cetuximab in a Patient With EGFR -Amplified Heavily Pretreated Metastatic Triple-Negative Breast Cancer. In *JCO Precision Oncology* (3), pp. 1–8. DOI: 10.1200/PO.18.00310.

Sachs, Norman; Ligt, Joep de; Kopper, Oded; Gogola, Ewa; Bounova, Gergana; Weeber, Fleur et al. (2018): A Living Biobank of Breast Cancer Organoids Captures Disease Heterogeneity. In *Cell* 172 (1-2), 373-386.e10. DOI: 10.1016/j.cell.2017.11.010.

Sartor, Carolyn I.; Zhou, Hong; Kozlowska, Ewa; Guttridge, Katherine; Kawata, Evelyn; Caskey, Laura et al. (2001): HER4 Mediates Ligand-Dependent Antiproliferative and Differentiation Responses in Human Breast Cancer Cells. In *Molecular and cellular biology* 21 (13), pp. 4265–4275. DOI: 10.1128/MCB.21.13.4265-4275.2001.

Sartore-Bianchi, Andrea; Trusolino, Livio; Martino, Cosimo; Bencardino, Katia; Lonardi, Sara; Bergamo, Francesca et al. (2016): Dual-targeted therapy with trastuzumab and lapatinib in treatment-refractory, KRAS codon 12/13 wild-type, HER2-positive metastatic colorectal cancer (HERACLES): a proof-of-concept, multicentre, open-label, phase 2 trial. In *The Lancet Oncology* 17 (6), pp. 738–746. DOI: 10.1016/S1470-2045(16)00150-9.

Sato, Toshiro; Stange, Daniel E.; Ferrante, Marc; Vries, Robert G. J.; van Es, Johan H.; van den Brink, Stieneke et al. (2011): Long-term expansion of epithelial organoids from human colon, adenoma, adenocarcinoma, and Barrett's epithelium. In *Gastroenterology* 141 (5), pp. 1762–1772. DOI: 10.1053/j.gastro.2011.07.050.

Schaefer, Gabriele; Haber, Lauric; Crocker, Lisa M.; Shia, Steven; Shao, Lily; Dowbenko, Donald et al. (2011a): A two-in-one antibody against HER3 and EGFR has superior inhibitory activity compared with monospecific antibodies. In *Cancer cell* 20 (4), pp. 472–486. DOI: 10.1016/j.ccr.2011.09.003.

Schaefer, Wolfgang; Regula, Jörg T.; Bähner, Monika; Schanzer, Jürgen; Croasdale, Rebecca; Dürr, Harald et al. (2011b): Immunoglobulin domain crossover as a generic approach for the production of bispecific IgG antibodies. In *Proceedings of the National Academy of Sciences of the United States of America* 108 (27), pp. 11187–11192. DOI: 10.1073/pnas.1019002108.

Schechter, A. L.; Stern, D. F.; Vaidyanathan, L.; Decker, S. J.; Drebin, J. A.; Greene, M. I.; Weinberg, R. A. (1984): The neu oncogene: an erb-B-related gene encoding a 185,000-Mr tumour antigen. In *Nature* 312 (5994), pp. 513–516. DOI: 10.1038/312513a0.

Schlessinger, Joseph (2000): Cell Signaling by Receptor Tyrosine Kinases. In *Cell* 103 (2), pp. 211–225. DOI: 10.1016/S0092-8674(00)00114-8.

Schmitt, Lisa C.; Rau, Alexander; Seifert, Oliver; Honer, Jonas; Hutt, Meike; Schmid, Simone et al. (2017): Inhibition of HER3 activation and tumor growth with a human antibody binding to a conserved epitope formed by domain III and IV. In *mAbs* 9 (5), pp. 831–843. DOI: 10.1080/19420862.2017.1319023.

Schütte, Moritz; Risch, Thomas; Abdavi-Azar, Nilofar; Boehnke, Karsten; Schumacher, Dirk; Keil, Marlen et al. (2017): Molecular dissection of colorectal cancer in pre-clinical models identifies biomarkers predicting sensitivity to EGFR inhibitors. In *Nature communications* 8, p. 14262. DOI: 10.1038/ncomms14262.

Schuurman, J.; van Ree, R.; Perdok, G. J.; van Doorn, H. R.; Tan, K. Y.; Aalberse, R. C. (1999): Normal human immunoglobulin G4 is bispecific: it has two different antigen-combining sites. In *Immunology* 97 (4), pp. 693–698. DOI: 10.1046/j.1365-2567.1999.00845.x.

Schwarz, Luis J.; Hutchinson, Katherine E.; Rexer, Brent N.; Estrada, Mónica Valeria; Gonzalez Ericsson, Paula I.; Sanders, Melinda E. et al. (2017): An ERBB1-3 Neutralizing Antibody Mixture With High Activity Against Drug-Resistant HER2+ Breast Cancers With ERBB Ligand Overexpression. In *Journal of the National Cancer Institute* 109 (11). DOI: 10.1093/jnci/djx065.

Seifert, Oliver; Rau, Alexander; Beha, Nadine; Richter, Fabian; Kontermann, Roland E. (2019): Diabody-Ig: a novel platform for the generation of multivalent and multispecific antibody molecules. In *mAbs*, pp. 1–11. DOI: 10.1080/19420862.2019.1603024.

Seo, An Na; Kwak, Yoonjin; Kim, Duck-Woo; Kang, Sung-Bum; Choe, Gheeyoung; Kim, Woo Ho; Lee, Hye Seung (2014): HER2 status in colorectal cancer: its clinical significance and the relationship between HER2 gene amplification and expression. In *PloS one* 9 (5), e98528. DOI: 10.1371/journal.pone.0098528.

Sergina, Natalia V.; Rausch, Megan; Wang, Donghui; Blair, Jimmy; Hann, Byron; Shokat, Kevan M.; Moasser, Mark M. (2007): Escape from HER-family tyrosine kinase inhibitor therapy by the kinase-inactive HER3. In *Nature* 445 (7126), pp. 437–441. DOI: 10.1038/nature05474.

Shaw, Frances L.; Harrison, Hannah; Spence, Katherine; Ablett, Matthew P.; Simões, Bruno M.; Farnie, Gillian; Clarke, Robert B. (2012): A detailed mammosphere assay protocol for the quantification of breast stem cell activity. In *Journal of mammary gland biology and neoplasia* 17 (2), pp. 111–117. DOI: 10.1007/s10911-012-9255-3.

Shepard, H. M.; Lewis, G. D.; Sarup, J. C.; Fendly, B. M.; Maneval, D.; Mordenti, J. et al. (1991): Monoclonal antibody therapy of human cancer: taking the HER2 protooncogene to the clinic. In *Journal of clinical immunology* 11 (3), pp. 117–127. DOI: 10.1007/bf00918679.

Shi, Fumin; Telesco, Shannon E.; Liu, Yingting; Radhakrishnan, Ravi; Lemmon, Mark A. (2010): ErbB3/HER3 intracellular domain is competent to bind ATP and catalyze autophosphorylation. In *Proceedings of the National Academy of Sciences of the United States of America* 107 (17), pp. 7692–7697. DOI: 10.1073/pnas.1002753107.

Shibata, Masahiro; Hoque, Mohammad Obaidul (2019): Targeting Cancer Stem Cells: A Strategy for Effective Eradication of Cancer. In *Cancers* 11 (5). DOI: 10.3390/cancers11050732.

Shih, I. M.; Wang, T. L.; Traverso, G.; Romans, K.; Hamilton, S. R.; Ben-Sasson, S. et al. (2001): Top-down morphogenesis of colorectal tumors. In *Proceedings of the National Academy of Sciences of the United States of America* 98 (5), pp. 2640–2645. DOI: 10.1073/pnas.051629398.

Skegro, Darko; Stutz, Cian; Ollier, Romain; Svensson, Emelie; Wassmann, Paul; Bourquin, Florence et al. (2017): Immunoglobulin domain interface exchange as a platform technology for the generation of Fc heterodimers and bispecific antibodies. In *The Journal of biological chemistry* 292 (23), pp. 9745–9759. DOI: 10.1074/jbc.M117.782433.

Slamon, D. J.; Clark, G. M.; Wong, S. G.; Levin, W. J.; Ullrich, A.; McGuire, W. L. (1987): Human breast cancer: correlation of relapse and survival with amplification of the HER-2/neu oncogene. In *Science (New York, N.Y.)* 235 (4785), pp. 177–182. DOI: 10.1126/science.3798106.

Sliwkowski, M. X.; Lofgren, J. A.; Lewis, G. D.; Hotaling, T. E.; Fendly, B. M.; Fox, J. A. (1999): Nonclinical studies addressing the mechanism of action of trastuzumab (Herceptin). In *Seminars in oncology* 26 (4 Suppl 12), pp. 60–70.

Smirnova, T.; Zhou, Z. N.; Flinn, R. J.; Wyckoff, J.; Boimel, P. J.; Pozzuto, M. et al. (2012): Phosphoinositide 3-kinase signaling is critical for ErbB3-driven breast cancer cell motility and metastasis. In *Oncogene* 31 (6), pp. 706–715. DOI: 10.1038/onc.2011.275.

Smith, I. E. (2001): Efficacy and safety of Herceptin in women with metastatic breast cancer: results from pivotal clinical studies. In *Anti-cancer drugs* 12 Suppl 4, S3-10. DOI: 10.1097/00001813-200112004-00002.

Sodergren, Samantha C.; Copson, Ellen; White, Alice; Efficace, Fabio; Sprangers, Mirjam; Fitzsimmons, Deborah et al. (2016): Systematic Review of the Side Effects Associated With Anti-HER2-Targeted Therapies Used in the Treatment of Breast Cancer, on Behalf of the EORTC Quality of Life Group. In *Targeted oncology* 11 (3), pp. 277–292. DOI: 10.1007/s11523-015-0409-2.

Staerz, U. D.; Kanagawa, O.; Bevan, M. J. (1985): Hybrid antibodies can target sites for attack by T cells. In *Nature* 314 (6012), pp. 628–631. DOI: 10.1038/314628a0.

Stahler, Arndt; Heinemann, Volker; Neumann, Jens; Crispin, Alexander; Schalhorn, Andreas; Stintzing, Sebastian et al. (2017): Prevalence and influence on outcome of HER2/neu, HER3 and NRG1 expression in patients with metastatic colorectal cancer. In *Anti-cancer drugs*. DOI: 10.1097/CAD.0000000000000510.

Strickler, J. H.; Zemla, T.; Ou, F.-S.; Cercek, A.; Wu, C.; Sanchez, F. A. et al. (2019): Trastuzumab and tucatinib for the treatment of HER2 amplified metastatic colorectal cancer (mCRC): Initial results from the MOUNTAINEER trial. In *Annals of Oncology* 30, v200. DOI: 10.1093/annonc/mdz246.005.

Styczen, Hanna; Nagelmeier, Iris; Beissbarth, Tim; Nietert, Manuel; Homayounfar, Kia; Sprenger, Thilo et al. (2015): HER-2 and HER-3 expression in liver metastases of patients with colorectal cancer. In *Oncotarget* 6 (17), pp. 15065–15076.

Taberna, Miren; Torres, Montserrat; Alejo, María; Mena, Marisa; Tous, Sara; Marquez, Sandra et al. (2018): The Use of HPV16-E5, EGFR, and pEGFR as Prognostic Biomarkers for Oropharyngeal Cancer Patients. In *Frontiers in oncology* 8, p. 589. DOI: 10.3389/fonc.2018.00589.

Tanei, Tomonori; Choi, Dong Soon; Rodriguez, Angel A.; Liang, Diana Hwang; Dobrolecki, Lacey; Ghosh, Madhumita et al. (2016): Antitumor activity of Cetuximab in combination with Ixabepilone on triple negative breast cancer stem cells. In *Breast cancer research : BCR* 18 (1), p. 6. DOI: 10.1186/s13058-015-0662-4.

Tao, Jessica J.; Castel, Pau; Radosevic-Robin, Nina; Elkabets, Moshe; Auricchio, Neil; Aceto, Nicola et al. (2014): Antagonism of EGFR and HER3 enhances the response to inhibitors of the PI3K-Akt pathway in triple-negative breast cancer. In *Science signaling* 7 (318), ra29. DOI: 10.1126/scisignal.2005125.

Thakur, Krishan K.; Bordoloi, Devivasha; Kunnumakkara, Ajaikumar B. (2018): Alarming Burden of Triple-Negative Breast Cancer in India. In *Clinical Breast Cancer* 18 (3), e393-e399. DOI: 10.1016/j.clbc.2017.07.013.

Therkildsen, Christina; Bergmann, Troels K.; Henrichsen-Schnack, Tine; Ladelund, Steen; Nilbert, Mef (2014): The predictive value of KRAS, NRAS, BRAF, PIK3CA and PTEN for anti-EGFR treatment in metastatic colorectal cancer: A systematic review and meta-analysis. In *Acta oncologica (Stockholm, Sweden)* 53 (7), pp. 852–864. DOI: 10.3109/0284186X.2014.895036.

Thomas, Rintu; Weihua, Zhang (2019): Rethink of EGFR in Cancer With Its Kinase Independent Function on Board. In *Frontiers in oncology* 9, p. 800. DOI: 10.3389/fonc.2019.00800.

Todaro, Matilde; Alea, Mileidys Perez; Di Stefano, Anna B.; Cammareri, Patrizia; Vermeulen, Louis; Iovino, Flora et al. (2007): Colon cancer stem cells dictate tumor growth and resist cell death by production of interleukin-4. In *Cell stem cell* 1 (4), pp. 389–402. DOI: 10.1016/j.stem.2007.08.001.

Tovey, Sian M.; Witton, Caroline J.; Bartlett, John M. S.; Stanton, Peter D.; Reeves, Jonathan R.; Cooke, Timothy G. (2004): Outcome and human epidermal growth factor receptor (HER) 1-4 status in invasive breast carcinomas with proliferation indices evaluated by bromodeoxyuridine labelling. In *Breast cancer research : BCR* 6 (3), R246-51. DOI: 10.1186/bcr783.

Troiani, Teresa; Napolitano, Stefania; Della Corte, Carminia Maria; Martini, Giulia; Martinelli, Erika; Morgillo, Floriana; Ciardiello, Fortunato (2016): Therapeutic value of EGFR inhibition in CRC and NSCLC: 15 years of clinical evidence. In *ESMO open* 1 (5), e000088. DOI: 10.1136/esmoopen-2016-000088.

Troyer, K. L.; Luetteke, N. C.; Saxon, M. L.; Qiu, T. H.; Xian, C. J.; Lee, D. C. (2001): Growth retardation, duodenal lesions, and aberrant ileum architecture in triple null mice lacking EGF, amphiregulin, and TGF-alpha. In *Gastroenterology* 121 (1), pp. 68–78. DOI: 10.1053/gast.2001.25478.

Tsai, Chung-Hsin; CHIU, JEN-HWEY; YANG, CHU-WEN; WANG, JIR-YOU; TSAI, YI-FANG; TSENG, LING-MING et al. (2015): Molecular characteristics of recurrent triple-negative breast cancer. In *Molecular medicine reports* 12 (5), pp. 7326–7334. DOI: 10.3892/mmr.2015.4360.

Tzahar, E.; Waterman, H.; Chen, X.; Levkowitz, G.; Karunagaran, D.; Lavi, S. et al. (1996): A hierarchical network of interreceptor interactions determines signal transduction by Neu differentiation factor/neuregulin and epidermal growth factor. In *Molecular and cellular biology* 16 (10), pp. 5276–5287.

Ueno, Naoto T.; Zhang, Dongwei (2011): Targeting EGFR in Triple Negative Breast Cancer. In *Journal of Cancer* 2, pp. 324–328.

van Cutsem, Eric; Köhne, Claus-Henning; Hitre, Erika; Zaluski, Jerzy; Chang Chien, Chung-Rong; Makhson, Anatoly et al. (2009): Cetuximab and chemotherapy as initial treatment for metastatic colorectal cancer. In *The New England journal of medicine* 360 (14), pp. 1408–1417. DOI: 10.1056/NEJMoa0805019.

Veikkolainen, Ville; Vaparanta, Katri; Halkilahti, Kalle; Iljin, Kristiina; Sundvall, Maria; Elenius, Klaus (2011): Function of ERBB4 is determined by alternative splicing. In *Cell cycle (Georgetown, Tex.)* 10 (16), pp. 2647–2657. DOI: 10.4161/cc.10.16.17194.

Vermorken, Jan B.; Trigo, José; Hitt, Ricardo; Koralewski, Piotr; Diaz-Rubio, Eduardo; Rolland, Frédéric et al. (2007): Open-label, uncontrolled, multicenter phase II study to evaluate the efficacy and toxicity of cetuximab as a single agent in patients with recurrent and/or metastatic squamous cell carcinoma of the head and neck who failed to respond to platinum-based therapy. In *JCO* 25 (16), pp. 2171–2177. DOI: 10.1200/JCO.2006.06.7447.

Vernieri, Claudio; Milano, Monica; Brambilla, Marta; Mennitto, Alessia; Maggi, Claudia; Cona, Maria Silvia et al. (2019): Resistance mechanisms to anti-HER2 therapies in HER2-positive breast cancer: Current knowledge, new research directions and therapeutic perspectives. In *Critical reviews in oncology/hematology* 139, pp. 53–66. DOI: 10.1016/j.critrevonc.2019.05.001.

Vijayaraghavan, Smruthi; Lipfert, Lorraine; Chevalier, Kristen; Bushey, Barbara S.; Henley, Benjamin; Lenhart, Ryan et al. (2020): Amivantamab (JNJ-61186372), an Fc Enhanced EGFR/cMet Bispecific Antibody, Induces Receptor Downmodulation and Antitumor Activity by Monocyte/Macrophage Trogocytosis. In *Molecular cancer therapeutics* 19 (10), pp. 2044–2056. DOI: 10.1158/1535-7163.MCT-20-0071.

Visvader, Jane E.; Lindeman, Geoffrey J. (2012): Cancer stem cells: current status and evolving complexities. In *Cell stem cell* 10 (6), pp. 717–728. DOI: 10.1016/j.stem.2012.05.007.

Vlachogiannis, Georgios; Hedayat, Somaieh; Vatsiou, Alexandra; Jamin, Yann; Fernández-Mateos, Javier; Khan, Khurum et al. (2018): Patient-derived organoids model treatment response of metastatic gastrointestinal cancers. In *Science (New York, N.Y.)* 359 (6378), pp. 920–926. DOI: 10.1126/science.aao2774.

Völkel, T.; Korn, T.; Bach, M.; Müller, R.; Kontermann, R. E. (2001): Optimized linker sequences for the expression of monomeric and dimeric bispecific single-chain diabodies. In *Protein engineering* 14 (10), pp. 815–823. DOI: 10.1093/protein/14.10.815.

Vries Schultink, Aurelia H. M. de; Bol, Kees; Doornbos, Robert P.; Murat, Anastasia; Wasserman, Ernesto; Dorlo, Thomas P. C. et al. (2020): Population Pharmacokinetics of MCLA-128, a HER2/HER3 Bispecific Monoclonal Antibody, in Patients with Solid Tumors. In *Clinical pharmacokinetics*. DOI: 10.1007/s40262-020-00858-2.

Wang, Lintao; Huang, Zhouqing; Huang, Weijian; Chen, Xuemei; Shan, Peiren; Zhong, Peng et al. (2017): Inhibition of epidermal growth factor receptor attenuates atherosclerosis via

decreasing inflammation and oxidative stress. In *Scientific reports* 8, p. 45917. DOI: 10.1038/srep45917.

Wang, Zhixiang (2017): ErbB Receptors and Cancer. In *Methods in molecular biology (Clifton, N.J.)* 1652, pp. 3–35. DOI: 10.1007/978-1-4939-7219-7_1.

Wei, Hudie; Cai, Haiyan; Jin, Yuhao; Wang, Pilin; Zhang, Qingqing; Lin, Yihui et al. (2017): Structural basis of a novel heterodimeric Fc for bispecific antibody production. In *Oncotarget* 8 (31), pp. 51037–51049. DOI: 10.18632/oncotarget.17558.

Weiß, F. Ulrich; Wallasch, Christian; Campiglio, Manuela; Issing, Wolfgang; Ullrich, Axel (1997): Distinct characteristics of heregulin signals mediated by HER3 or HER4. In *J. Cell. Physiol.* 173 (2), pp. 187–195. DOI: 10.1002/(SICI)1097-4652(199711)173:2<187::AID-JCP19>3.0.CO;2-D.

Wheeler, D. L.; Huang, S.; Kruser, T. J.; Nechrebecki, M. M.; Armstrong, E. A.; Benavente, S. et al. (2008): Mechanisms of acquired resistance to cetuximab: role of HER (ErbB) family members. In *Oncogene* 27 (28), pp. 3944–3956. DOI: 10.1038/onc.2008.19.

Wieduwilt, M. J.; Moasser, M. M. (2008): The epidermal growth factor receptor family: biology driving targeted therapeutics. In *Cellular and molecular life sciences : CMLS* 65 (10), pp. 1566–1584. DOI: 10.1007/s00018-008-7440-8.

Wilson, Timothy R.; Lee, Diana Y.; Berry, Leanne; Shames, David S.; Settleman, Jeff (2011): Neuregulin-1-mediated autocrine signaling underlies sensitivity to HER2 kinase inhibitors in a subset of human cancers. In *Cancer cell* 20 (2), pp. 158–172. DOI: 10.1016/j.ccr.2011.07.011.

Woodward, Wendy A.; Sulman, Erik P. (2008): Cancer stem cells: markers or biomarkers? In *Cancer metastasis reviews* 27 (3), pp. 459–470. DOI: 10.1007/s10555-008-9130-2.

Xu, Lihui; Kohli, Neeraj; Rennard, Rachel; Jiao, Yang; Razlog, Maja; Zhang, Kathy et al. (2013): Rapid optimization and prototyping for therapeutic antibody-like molecules. In *mAbs* 5 (2), pp. 237–254. DOI: 10.4161/mabs.23363.

Xu, Mary Jue; Johnson, Daniel E.; Grandis, Jennifer R. (2017): EGFR-targeted therapies in the post-genomic era. In *Cancer metastasis reviews* 36 (3), pp. 463–473. DOI: 10.1007/s10555-017-9687-8.

Xue, Chengsen; Liang, Fubo; Mahmood, Radma; Vuolo, Magalis; Wyckoff, Jeffrey; Qian, Hong et al. (2006): ErbB3-dependent motility and intravasation in breast cancer metastasis. In *Cancer research* 66 (3), pp. 1418–1426. DOI: 10.1158/0008-5472.CAN-05-0550.

Yarden, Y.; Sliwkowski, M. X. (2001): Untangling the ErbB signalling network. In *Nature reviews. Molecular cell biology* 2 (2), pp. 127–137. DOI: 10.1038/35052073.

Yarden, Yosef; Pines, Gur (2012): The ERBB network: at last, cancer therapy meets systems biology. In *Nat Rev Cancer* 12 (8), pp. 553–563. DOI: 10.1038/nrc3309.

Yonesaka, Kimio; Zejnullahu, Kreshnik; Okamoto, Isamu; Satoh, Taroh; Cappuzzo, Federico; Souglakos, John et al. (2011): Activation of ERBB2 signaling causes resistance to the EGFR-directed therapeutic antibody cetuximab. In *Science translational medicine* 3 (99), 99ra86. DOI: 10.1126/scitranslmed.3002442.

Zhang, K.; Sun, J.; Liu, N.; Wen, D.; Chang, D.; Thomason, A.; Yoshinaga, S. K. (1996): Transformation of NIH 3T3 cells by HER3 or HER4 receptors requires the presence of HER1 or HER2. In *The Journal of biological chemistry* 271 (7), pp. 3884–3890.

Zhang, Qian; Park, Euisun; Kani, Kian; Landgraf, Ralf (2012): Functional isolation of activated and unilaterally phosphorylated heterodimers of ERBB2 and ERBB3 as scaffolds in ligand-dependent signaling. In *Proceedings of the National Academy of Sciences of the United States of America* 109 (33), pp. 13237–13242. DOI: 10.1073/pnas.1200105109.

Zhang, Xiaoqian; Wen, Long; Chen, Shanwen; Zhang, Junling; Ma, Yongchen; Hu, Jianwen et al. (2020): The novel long noncoding RNA CRART16 confers cetuximab resistance in colorectal cancer cells by enhancing ERBB3 expression via miR-371a-5p. In *Cancer Cell Int* 20 (1). DOI: 10.1186/s12935-020-1155-9.

Zhou, Yujuan; Xia, Longzheng; Wang, Heran; Oyang, Linda; Su, Min; Liu, Qiang et al. (2017): Cancer stem cells in progression of colorectal cancer. In *Oncotarget* 9 (70), pp. 33403–33415. DOI: 10.18632/oncotarget.23607.

7 Supplement

7.1 Sequences

7.1.1 #2111 pSecTagAL1-scDb hu225x3-43-Fc

7.1.1.1 DNA sequence

```
>Igκ-leader
atggagacagacacactcctgctatgggtactgctgctctgggttccaggttcc  < 54
M  E  T  D  T  L  L  L  W  V  L  L  L  W  V  P  G  S
         10        20        30        40        50

     <>VHhu225
accggTGAAGTGCAGCTGGTTGAAAGCGGCGGTGGTCTGGTTCAGCCGGGTGGC  < 108
T  G  E  V  Q  L  V  E  S  G  G  G  L  V  Q  P  G  G
      60        70        80        90        100

AGCCTGCGTCTGAGCTGTGCGGCGAGCGGCTTTAGCCTGACCAACTATGGCGTG  < 162
S  L  R  L  S  C  A  A  S  G  F  S  L  T  N  Y  G  V
 110       120       130       140       150       160

CATTGGGTGCGTCAGGCACCGGGCAAAGGCCTGGAATGGCTGGGCGTGATTTGG  < 216
H  W  V  R  Q  A  P  G  K  G  L  E  W  L  G  V  I  W
       170       180       190       200       210

AGCGGCGGCAACACCGATTATAACACCCCGTTTACCAGCCGTTTTACCATTAGC  < 270
S  G  G  N  T  D  Y  N  T  P  F  T  S  R  F  T  I  S
   220       230       240       250       260

CGTGATAACAGCAAAAACACCCTGTATCTGCAGATGAACAGCCTGCGTGCGGAA  < 324
R  D  N  S  K  N  T  L  Y  L  Q  M  N  S  L  R  A  E
         280       290       300       310       320

GATACCGCGGTGTATTATTGCGCGCGTGCGCTGACCTATTATGATTACGAATTT  < 378
D  T  A  V  Y  Y  C  A  R  A  L  T  Y  Y  D  Y  E  F
      330       340       350       360       370

                                        <>Linker 1
GCGTATTGGGGCCAGGGCACCACCGTTACGGTCtcgaGTGGCGGTGGCGGATCG  < 432
A  Y  W  G  Q  G  T  T  V  T  V  S  S  G  G  G  G  S
 380       390       400       410       420       430

>VL HER3-43
CAAGCCGGACTGACACAGCCTCCAGCCGTGTCTGTGGCCCCTGGACAGACAGCC  < 486
Q  A  G  L  T  Q  P  P  A  V  S  V  A  P  G  Q  T  A
       440       450       460       470       480

AGCATCACCTGTGGCCGGGACAACATCGGCAGCAGAAGCGTGCACTGGTATCAG  < 540
S  I  T  C  G  R  D  N  I  G  S  R  S  V  H  W  Y  Q
   490       500       510       520       530

CAGAAACCCGGCCAGGCCCCTGTGCTGGTGGTGTACGACGACAGCGATAGACCT  < 594
Q  K  P  G  Q  A  P  V  L  V  V  Y  D  D  S  D  R  P
         550       560       570       580       590

GCCGGCATCCCCGAGAGATTCAGCGGCAGCAACTACGAGAACACCGCCACCCTG  < 648
A  G  I  P  E  R  F  S  G  S  N  Y  E  N  T  A  T  L
      600       610       620       630       640

ACCATCAGCAGAGTGGAAGCCGGCGACGAGGCCGACTACTACTGTCAAGTGTGG  < 702
```

```
T  I  S  R  V  E  A  G  D  E  A  D  Y  Y  C  Q  V  W
 650        660        670        680        690        700

                                                      <
GGCATCACCAGCGATCACGTGGTGTTTGGCGGAGGCACCAAGCTGACAGTGCTG  < 756
G  I  T  S  D  H  V  V  F  G  G  G  T  K  L  T  V  L
       710        720        730        740        750

>Linker2                                        <>VH HER3-43
GGAGGCGGTGGCaGCGGTGGGGGCGGATCGGGCGGAGGTGGCTCACAAGTGCAG  < 810
G  G  G  G  S  G  G  G  G  S  G  G  G  G  S  Q  V  Q
   760        770        780        790        800

CTGCAGCAGTCTGGCCCTGGCCTCGTGAAGCCTAGCCAGACCCTGAGCCTGACC  < 864
L  Q  Q  S  G  P  G  L  V  K  P  S  Q  T  L  S  L  T
         820        830        840        850        860

TGTGCCATCAGCGGCGATAGCGTGTCCAGCAACAGAGCCGCCTGGAACTGGATC  < 918
C  A  I  S  G  D  S  V  S  S  N  R  A  A  W  N  W  I
     870        880        890        900        910

AGACAGAGCCCCAGCAGAGGCCTGGAATGGCTGGGCCGGACCTACTACCGCAGC  < 972
R  Q  S  P  S  R  G  L  E  W  L  G  R  T  Y  Y  R  S
 920        930        940        950        960        970

AAGTGGTACAACGACTACGCCCAGAGCCTGAAGTCCCGGATCACCATCAACCCC  < 1026
K  W  Y  N  D  Y  A  Q  S  L  K  S  R  I  T  I  N  P
       980        990        1000       1010       1020

GACACCCCCAAGAACCAGTTCTCCCTGCAGCTGAACAGCGTGACCCCCGAGGAT  < 1080
D  T  P  K  N  Q  F  S  L  Q  L  N  S  V  T  P  E  D
   1030       1040       1050       1060       1070

ACCGCCGTGTACTACTGCGCCAGAGATGGACAGCTGGGCCTGGACGCCCTGGAC  < 1134
T  A  V  Y  Y  C  A  R  D  G  Q  L  G  L  D  A  L  D
         1090       1100       1110       1120       1130

                                    <>Linker 3     <>VLhu225|
ATTTGGGGCCAGGGCACAATGGTCACAGTGTCCTCTGGAGGCGGGGgatcCGAT  < 1188
I  W  G  Q  G  T  M  V  T  V  S  S  G  G  G  G  S  D
     1140       1150       1160       1170       1180

ATTCAGCTGACCCAGAGCCCGAGCTTTCTGAGCGCGAGCGTGGGCGATCGTGTT  < 1242
I  Q  L  T  Q  S  P  S  F  L  S  A  S  V  G  D  R  V
 1190       1200       1210       1220       1230       1240

ACCATTACCTGTCGTGCAAGCCAGAGCATTGGCACCAACATTCATTGGTATCAG  < 1296
T  I  T  C  R  A  S  Q  S  I  G  T  N  I  H  W  Y  Q
       1250       1260       1270       1280       1290

                                                      |
CAGAAACCGGGCAAAGCGCCGAAACTGCTGATTAAATATGCGAGCGAAAGCATT  < 1350
Q  K  P  G  K  A  P  K  L  L  I  K  Y  A  S  E  S  I
   1300       1310       1320       1330       1340

AGCGGCGTGCCGAGCCGTTTTAGCGGCAGCGGTAGCGGCACCGAATTTACCCTG  < 1404
S  G  V  P  S  R  F  S  G  S  G  S  G  T  E  F  T  L
         1360       1370       1380       1390       1400

ACCATTAGCAGCCTGCAGCCGGAAGATTTTGCGACCTATTATTGCCAGCAGAAC  < 1458
T  I  S  S  L  Q  P  E  D  F  A  T  Y  Y  C  Q  Q  N
     1410       1420       1430       1440       1450

                                                      <
```

```
AACAACTGGCCGACCACCTTTGGTGCGGGCACCAAACTGGAAATTAAACGTGCg  < 1512
N  N  W  P  T  T  F  G  A  G  T  K  L  E  I  K  R  A
 1460      1470      1480      1490      1500      1510

      >Linker 4     <>Hinge                          |
gccgcaggggggaagcggcggtgacaaaactcacacatgcccaccgtgcccagca  < 1566
A  A  G  G  S  G  G  D  K  T  H  T  C  P  P  C  P  A
       1520      1530      1540      1550      1560

                <>CH2
cctgaactcctgggggggaccgtcagtcttcctcttccccccaaaacccaaggac  < 1620
P  E  L  L  G  G  P  S  V  F  L  F  P  P  K  P  K  D
   1570      1580      1590      1600      1610

accctcatgatctcccggaccccctgaggtcacatgcgtggtggtggacgtgagc  < 1674
T  L  M  I  S  R  T  P  E  V  T  C  V  V  V  D  V  S
         1630      1640      1650      1660      1670

cacgaagaccctgaggtcaagttcaactggtacgtggacggcgtggaggtgcat  < 1728
H  E  D  P  E  V  K  F  N  W  Y  V  D  G  V  E  V  H
     1680      1690      1700      1710      1720

          |
aatgccaagacaaagccgcgggaggagcagtacaacagcacgtaccgtgtggtc  < 1782
N  A  K  T  K  P  R  E  E  Q  Y  N  S  T  Y  R  V  V
 1730      1740      1750      1760      1770      1780

agcgtcctcaccgtcctgcaccaggactggctgaatggcaaggagtacaagtgc  < 1836
S  V  L  T  V  L  H  Q  D  W  L  N  G  K  E  Y  K  C
       1790      1800      1810      1820      1830

aaggtctccaacaaagccctcccagccccatcgagaaaaccatctccaaagcc  < 1890
K  V  S  N  K  A  L  P  A  P  I  E  K  T  I  S  K  A
   1840      1850      1860      1870      1880

  <>CH3
aaagggcagccccgagaaccacaggtgtacaccctgcccccatcccgggatgag  < 1944
K  G  Q  P  R  E  P  Q  V  Y  T  L  P  P  S  R  D  E
         1900      1910      1920      1930      1940

ctgaccaagaaccaggtcagcctgacctgcctggtcaaaggcttctatcccagc  < 1998
L  T  K  N  Q  V  S  L  T  C  L  V  K  G  F  Y  P  S
     1950      1960      1970      1980      1990

gacatcgccgtggagtgggagagcaatgggcagccggagaacaactacaagacc  < 2052
D  I  A  V  E  W  E  S  N  G  Q  P  E  N  N  Y  K  T
 2000      2010      2020      2030      2040      2050

 |
acgcctcccgtgctggactccgacggctccttcttcctctacagcaagctcacc  < 2106
T  P  P  V  L  D  S  D  G  S  F  F  L  Y  S  K  L  T
       2060      2070      2080      2090      2100

gtggacaagagcaggtggcagcaggggaacgtcttctcatgctccgtgatgcat  < 2160
V  D  K  S  R  W  Q  Q  G  N  V  F  S  C  S  V  M  H
   2110      2120      2130      2140      2150

                                                       <
gaggctctgcacaaccactacacgcagaagagcctctccctgtctccgggtaaa  < 2214
E  A  L  H  N  H  Y  T  Q  K  S  L  S  L  S  P  G  K
```

7.1.1.2 Amino acid sequence

VHhu225

EVQLVESGGGLVQPGGSLRLSCAASGFSLTNYGVHWVRQAPGKGLEWLGVIWSGGNTDYNTPFTSRFT
ISRDNSKNTLYLQMNSLRAEDTAVYYCARALTYYDYEFAYWGQGTTVTVSS

VLhu225

DIQLTQSPSFLSASVGDRVTITCRASQSIGTNIHWYQQKPGKAPKLLIKYASESISGVPSRFSGSGSG
TEFTLTISSLQPEDFATYYCQQNNNWPTTFGAGTKLEIKR

VH3-43

QVQLQQSGPGLVKPSQTLSLTCAISGDSVSSNRAAWNWIRQSPSRGLEWLGRTYYRSKWYNDYAQSLK
SRITINPDTPKNQFSLQLNSVTPEDTAVYYCARDGQLGLDALDIWGQGTMVTVSS

VL3-43

QAGLTQPPAVSVAPGQTASITCGRDNIGSRSVHWYQQKPGQAPVLVVYDDSDRPAGIPERFSGSNYEN
TATLTISRVEAGDEADYYCQVWGITSDHVVFGGGTKLTVL

Hinge

DKTHTCPPCPAPELLGG

CH2

PSVFLFPPKPKDTLMISRTPEVTCVVVDVSHEDPEVKFNWYVDGVEVHNAKTKPREEQYNSTYRVVSV
LTVLHQDWLNGKEYKCKVSNKALPAPIEKTISKAK

CH3

GQPREPQVYTLPPSRDELTKNQVSLTCLVKGFYPSDIAVEWESNGQPENNYKTTPPVLDSDGSFFLYS
KLTVDKSRWQQGNVFSCSVMHEALHNHYTQKSLSLSPGK

Complete amino acid Sequence

EVQLVESGGGLVQPGGSLRLSCAASGFSLTNYGVHWVRQAPGKGLEWLGVIWSGGNTDYNTPFTSRFT
ISRDNSKNTLYLQMNSLRAEDTAVYYCARALTYYDYEFAYWGQGTTVTVSS**GGGGS**QAGLTQPPAVSV
APGQTASITCGRDNIGSRSVHWYQQKPGQAPVLVVYDDSDRPAGIPERFSGSNYENTATLTISRVEAG
DEADYYCQVWGITSDHVVFGGGTKLTVLGGGGSGGGGSGGGGSQVQLQQSGPGLVKPSQTLSLTCAIS
GDSVSSNRAAWNWIRQSPSRGLEWLGRTYYRSKWYNDYAQSLKSRITINPDTPKNQFSLQLNSVTPED
TAVYYCARDGQLGLDALDIWGQGTMVTVSSGGGGSDIQLTQSPSFLSASVGDRVTITCRASQSIGTNI
HWYQQKPGKAPKLLIKYASESISGVPSRFSGSGSGTEFTLTISSLQPEDFATYYCQQNNNWPTTFGAG
TKLEIKRAAAGGSGGDKTHTCPPCPAPELLGGPSVFLFPPKPKDTLMISRTPEVTCVVVDVSHEDPEV
KFNWYVDGVEVHNAKTKPREEQYNSTYRVVSVLTVLHQDWLNGKEYKCKVSNKALPAPIEKTISKAKG

QPREPQVYTLPPSRDELTKNQVSLTCLVKGFYPSDIAVEWESNGQPENNYKTTPPVLDSDGSFFLYSK
LTVDKSRWQQGNVFSCSVMHEALHNHYTQKSLSLSPGK

List of Figures

List of Tables

Declaration

I hereby declare that I performed and wrote this thesis independent from further help or other materials than stated.

Eigenständigkeitserklärung

Hiermit erkläre ich, dass die vorgelegte Dissertation von mir persönlich und ohne Zuhilfenahme anderer Unterstützung oder Materialien als den angegebenen durchgeführt und geschrieben wurde.

Alexander Rau Ort, Datum

Danksagung

Liebe Moni und lieber Roland, liebe Doktoreltern! Ich möchte euch für so vieles danken! Als Mork hatte ich das Glück von euch beiden sowohl die Entwicklung von Antikörpern als auch die Erforschung ihrer Wirkung bis ins tiefste Detail zu erlernen. Danke euch für euer Vertrauen, eure immerwährende Unterstützung und euer unendliches Verständnis zu jederzeit! Danke für all die großartigen Momente die ich dank euch am IZI erleben durfte! Es war eine unglaublich schöne und erfüllende Zeit, die ich nicht missen möchte und niemals vergessen werde! Danke auch für die tollen Momente außerhalb der Arbeit!

Herzlichen Dank an **Prof. Dr. Jörn Lausen** für die Übernahme des Zweitgutachtens!

Lieber Oli! Dir muss ich für so vieles danken, dass ich es hier nicht erfassen kann! Danke, dass du mir all deine Antikörper Entwicklungsfertigkeiten gezeigt hast! Danke, für all die kleinen und großen Diskussionen über Wissenschaft und das Leben! Danke, für die Liebe zum Fahrradfahren! Danke, dass du mich immer unterstützt hast, privat, sowie professionell!

Lieber Fabi! Auch dir vielen Dank für alles, was ich von dir Lernen durfte, für die wissenschaftlichen Diskussionen (auch heute noch) und für all die Unterstützung zu Jederzeit!

Liebe Nadine, dir möchte ich einen besonderen Dank aussprechen für deine Unterstützung weit über die Promotion hinaus! Du hast mir den nötigen Schupps und das Vertrauen gegeben diese Arbeit fertig zu stellen! Danke!

Lieber Lennart, ich danke dir für all das, was ich von dir lernen durfte! Danke für deine Unterstützung zu Jederzeit! Danke, dass ich mit dir zusammenarbeiten durfte!

Lieber Oli, lieber Fabi, liebe Nadine und lieber Lennart danke für diese besondere Freundschaft!

Liebe Meike, auch dir vielen Dank für die tolle Zeit, deine Unterstützung und die schönen Momente! Prost Meike!

Lieber Hannes, danke für deine großartige Arbeit, sowie für deine entspannte und doch immer fokussierte Art Dinge anzugehen! Danke auch, dass du mir das Bouldern gezeigt hast!

Lieber Sebastian, danke für die sehr gute und erfolgreiche Zusammenarbeit im TNBC-Projekt!

Liebe Nicole, vielen Dank für all die Skills die du mir rund um die Organoide beigebracht hast! Vielen Dank auch für die unkomplizierte und sehr erfolgreiche Zusammenarbeit!

Liebe Nadine, liebe Doris und liebe Sabine, vielen Dank euch für eure Unterstützung im Labor und besonders danke für all das Wissen, dass ihr mir vermittelt habt!

Liebe Alex und liebe Bea, dank euch für die Unterstützung im Tierstall!

Lieber Jonas und liebe Lisa, danke euch für das Einarbeiten und die Einführung ins Labor.

Ich möchte allen **„Kontermännern", „Honkies" und „Olayioyes"** für die tolle Zeit danken! Ein besonderer Dank geht an den **Zonk**, der mich lehrte eine offene Fehlerkultur auszuleben.

Liebe Gabi, danke dir, dass du das IZI in seiner besonderen, freundlichen und auch immer lustigen Art am Laufen hältst!

Danke an **alle am IZI** die diese Zeit so wunderbar gemacht haben, dass ich mich immer wieder gerne zurückerinnere!

Hier möchte ich meiner lieben Familie Danken! Danke **Mama, Papa, Oma, Opa, Julia, Enrico, Stani, Marie-Claire und Mila**, dass ihr immer an mich geglaubt habt und mich immer unterstützt habt, wo immer ihr nur konntet! Auch euch **Benny und Freya** möchte ich für eure immerwährende Unterstützung danken! Du, **Freya**, hast mir immer den Rücken freigehalten und hast einen großen Teil dazu beigetragen diese Arbeit zu ermöglichen. Danke auch an meine Freunde aus Mülle, **Mathieu und Josi, Robin und Heike, Simeon und Annahita, Besart und Sarah, Kotz und Natalie, und Labi**, die mich seit Jahrzenten begleiten und unterstützen!

Nun möchte ich der wichtigsten Person in meinem Leben danken, dir **Sabrina, meine geliebte Ehefrau, mein Engele!** Du wolltest, dass ich studiere, du hast mich die ganze Zeit dazu ermutigt weiterzumachen und auch du hast mich ermutigt die Promotion zu machen! Du hast gesagt, solange wir uns haben, schaffen wir alles! Ich bin unendlich dankbar für die Zeit, die wir hatten, auch wenn sie viel zu kurz war! Deine Liebe, deine Stärke und deine immer positive Art waren, was ich so sehr an dir liebte! Ich hoffe ich werde deine Werte weitertragen können! Du bist mein Engele für immer! Ich bin mir sicher, da wo du jetzt bist, ist es heller!

Curriculum vitae

Alexander Rau

Work Experience

06/2022 – present

Scientist Protein Engineering in the Protein Engineering department
Anaveon AG, Basel, Switzerland

- Design, modify and characterize protein constructs, including antibodies, cytokines and complex antibody-fusion proteins.
- Work with CROs to initiate and coordinate gene synthesis and protein production efforts.
- Develop, qualify and perform bioanalytical assays including characterization by SDS-PAGE, SE-HPLC-MALS, DSF, and AC-SINS.
- Binding and affinity characterization by ELISA, flow cytometry and SPR (T200).

07/2020 – 05/2022

Senior Investigator in the Antibody Engineering department as part of the Display Technologies team
Ichnos Sciences, Lausanne, Switzerland

- Characterization of antigen package and toolbox implementation.
- Screen naïve and immune library phage display and immune NGS outputs by flow cytometry and SPR.
- Cloning, expression, and purification of scFv, Fab, IgG and multispecific antibody molecules in medium to high-throughput (96-well to 100 ml scale) in bacterial and mammalian cells.
- Characterization of potential lead candidates by SDS-PAGE, SE-HPLC, DSF, and AC-SINS.
- Binding and affinity characterization by ELISA, flow cytometry, BLI (OCTET RED96e) and SPR (T200 and 8k+).
- Documentation, analysis, and proactive presentation of obtained data in project team meetings and at laboratory group meetings.

03/2017 – 04/2020

PhD Student in the field of Antibody Engineering and Tumor Cell Biology
University of Stuttgart, Groups of
Prof. Dr. Roland Kontermann (Biomedical Engineering) and
Prof. Dr. Monilola Olayioye (Molecular Tumor Cell Biology)

“Bi- and trispecific targeting of HER/ErbB family members in solid tumors.”

- Development of bi- and trispecifc antibody treatments for colorectal cancer (CRC), triple-negative breast cancer (TNBC), and gastric cancer (GC).
- Cloning, production, purification, and formulation of mono- and bispecific antibodies.
- Characterization of antibodies using ELISA, flow cytometry, QCM, proliferation assay, apoptosis assay, migration assays, cytotoxicity assays, and intracellular signaling analysis by Western Blot.
- Analyzing antibody-based treatments in patient-derived CRC organoids, oncosphere, and 3D cell culture models.
- Pharmacokinetic studies in immunocompetent mice and pharmacodynamic studies in mouse xenograft tumor models.

01/2016 – 03/2017

Master thesis in the field of antibody engineering
University of Stuttgart, Institute for Cell Biology and Immunology, Group of Prof. Dr. Roland Kontermann (Biomedical Engineering)

“Bispecific scDb-Fc antibodies targeting ErbB family members”

- Cloning, production, and functional analysis of mono- and bispecific antibodies, using ELISA, flow cytometry, proliferation assays, and intracellular signaling analysis by Western Blot.

08/2014 – 12/2015

Student Lab Assistant
Fraunhofer IPA, Stuttgart,
Laboratory automation and biomanufacturing engineering

- In-depth knowledge in cell culture methods of cell lines and primary cells.
- Isolation of primary keratinocytes from prepuce skin.
- Establishing new methods for hydrogel and single cell application.
- Technology and patent research for the development of a new bioreactor system.

04/2014 – 07/2014

Bachelor thesis in the field of single cell handling.
Fraunhofer IPA, Stuttgart,
Laboratory automation and biomanufacturing engineering

"A new dosing method to produce 3D tissue models using the *I-DOT* technology."

- Proof of concept studies using the *I-DOT* technology for production of 3D angiogenesis and cancer spheroid models.

Award: Finalist of the "Lab Science Award 2016, Veronika und Hugo Bohny Stiftung", Rapperswil-Jona, Switzerland.

Education

03/2017 – 05/2020	**PhD Student** University of Stuttgart (date of thesis defense to be announced) Groups of Prof. Dr. Roland Kontermann (Biomedical Engineering) and Prof. Dr. Monilola Olayioye (Molecular Tumor Cell Biology)
10/2014 – 03/2017	**Master of Science Technical Biology** University of Stuttgart, (final grade: 1.1) Courses included: Antibody Engineering, Advanced Biocatalysis, DNA Biochemistry and Molecular Epigenetics, and General Genetics of Microorganisms Honor: Scholarship holder of the "Deutschlandstipendium".
10/2011 – 09/2014	**Bachelor of Science Technical Biology** University of Stuttgart, (final grade: 2.0) Courses included: Cytology and Immunology I, Special Microbiology and Microbial Biotechnology, and Process Engineering

Conference contributions, trainings, and workshops

10/2018	European Antibody Congress 2018 (Basel) – Poster presentation
07/2017 – 08/2017	Training for the handling of laboratory animals at DKFZ (Heidelberg) (GV-SOLAS, FELASA-B)

Skills

Software	Protean 3D (DNASTAR), GraphPad Prism, Geneious, Biacore Insight, Serial Cloner, FlowJo, MACSQuantify (Miltenyi Biotec), Microsoft Word, Excel, PowerPoint
Language	German (native), English (fluent), Russian (conversant), intermediate Latin certificate

Publications

ORCID-ID: https://orcid.org/0000-0001-6810-2714

02/2022	**Rau A,** et al.**,** *Triple targeting of HER receptors overcomes heregulin-mediated resistance to EGFR blockade in colorectal cancer.*
03/2021	**Rau A,** et al.**,** *A bivalent, bispecific Dab-Fc antibody molecule for dual targeting of HER2 and HER3.* mAbs. 2021 March
07/2020	**Rau A**, Lieb WS, et al., *Inhibition of tumor cell growth and cancer stem cell expansion by a bispecific antibody targeting EGFR and HER3.* Molecular cancer therapeutics. 2020 July
04/2019	Seifert O, **Rau A**, et al., *Diabody-Ig: a novel platform for the generation of multivalent and multispecific antibody molecules.* mAbs. 2019 April
04/2017	Schmitt LC, **Rau A**, et al., *Inhibition of HER3 activation and tumor growth with a human antibody binding to a conserved epitope formed by domain III and IV.* mAbs. 2017 April

Basel, November 27th, 2022

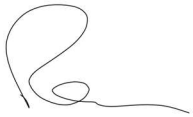

Alexander Rau